British Geological Survey

Hydrological modelling for Panay and Pampanga, Philippines 1979 - 2089

Environmental Change, Adaptation & Resilience Programme

Open Report OR/22/057

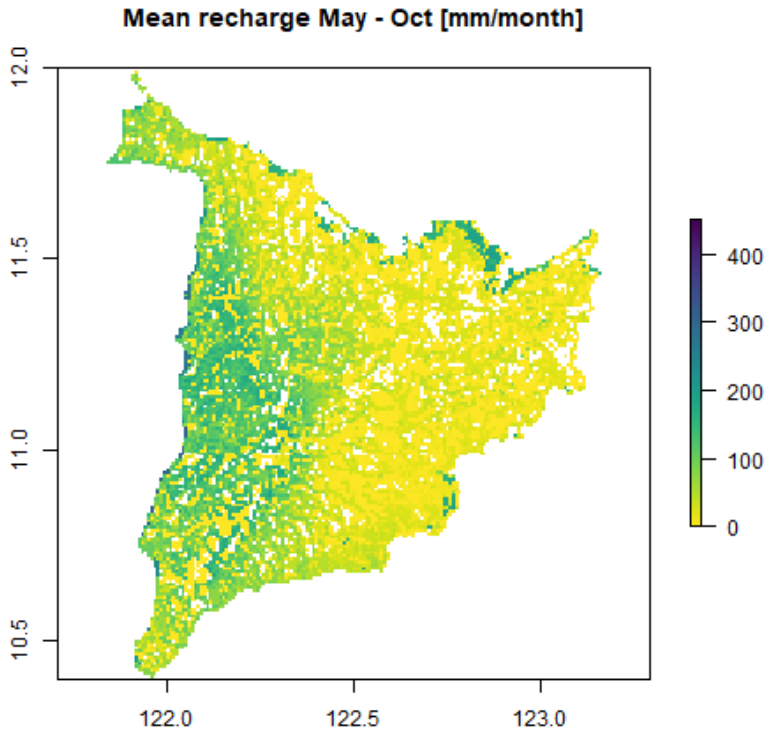

BRITISH GEOLOGICAL SURVEY

Environmental Change, Adaptation & Resilience Programme

OPEN REPORT OR/22/057

Hydrological modelling for Panay and Pampanga, Philippines 1979 - 2089

Johanna M Scheidegger, Christopher R Jackson, Andrew Barkwith, Lei Wang, Maria Aileen Leah G Guzman

Keywords

Philippines; Hydrological modelling; Climate change projections; Luzon; Pampanga; Panay.

Front cover

Simulated mean historical wet-season groundwater recharge for Panay, Philippines

Bibliographical reference

SCHEIDEGGER, J.M., JACKSON, C.R., BARKWITH, A., WANG, L., GUZMAN, M.A.L.G. 2021. Hydrological modelling for Panay and Pampanga, Philippines 1979 - 2089. *British Geological Survey Open Report*, OR/22/057. 71pp.

Keyworth, Nottingham British Geological Survey 2022

BRITISH GEOLOGICAL SURVEY

The full range of our publications is available from BGS shops at Nottingham, Edinburgh, London and Cardiff (Welsh publications only) see contact details below or shop online at www.geologyshop.com

The London Information Office also maintains a reference collection of BGS publications, including maps, for consultation.

We publish an annual catalogue of our maps and other publications; this catalogue is available online or from any of the BGS shops.

The British Geological Survey carries out the geological survey of Great Britain and Northern Ireland (the latter as an agency service for the government of Northern Ireland), and of the surrounding continental shelf, as well as basic research projects. It also undertakes programmes of technical aid in geology in developing countries.

The British Geological Survey is a component body of UK Research and Innovation.

British Geological Survey offices

Nicker Hill, Keyworth,
Nottingham NG12 5GG
Tel 0115 936 3100

BGS Central Enquiries Desk
Tel 0115 936 3143
email enquiries@bgs.ac.uk

BGS Sales
Tel 0115 936 3241
email sales@bgs.ac.uk

The Lyell Centre, Research Avenue South,
Edinburgh EH14 4AP
Tel 0131 667 1000
email scotsales@bgs.ac.uk

Natural History Museum, Cromwell Road,
London SW7 5BD
Tel 020 7589 4090
Tel 020 7942 5344/45
email bgslondon@bgs.ac.uk

Cardiff University, Main Building, Park Place,
Cardiff CF10 3AT
Tel 029 2167 4280

Maclean Building, Crowmarsh Gifford,
Wallingford OX10 8BB
Tel 01491 838800

Geological Survey of Northern Ireland, Department of Enterprise, Trade & Investment, Dundonald House, Upper Newtownards Road, Ballymiscaw, Belfast, BT4 3SB
Tel 01232 666595

www.bgs.ac.uk/gsni/

Natural Environment Research Council, Polaris House, North Star Avenue, Swindon SN2 1EU
Tel 01793 411500 Fax 01793 411501
www.nerc.ac.uk

UK Research and Innovation, Polaris House,
Swindon SN2 1FL
Tel 01793 444000
www.ukri.org

Website www.bgs.ac.uk
Shop online at www.geologyshop.com

Acknowledgements

The project team would like to thank Engr. Susan P. Abaño and her team and the director Dr Sevillo David, Jr, at the National Water Resources Board (NWRB) for providing stream flow and groundwater level data. Also, a significant thanks to the project team and research assistants at Ateneo de Manila University and Department of Science and Technology - Philippine Council for Industry, Energy and Emerging Technology Research and Development (DOST-PCIEERD), for their invaluable help in gathering and formatting data. The project team would also like to thank the Philippine Atmospheric, Geophysical and Astronomical Services Administration (PAGASA) for providing observation data from their network of weather stations.

Contents

FIGURES

TABLES

Summary

This report describes an investigation of the impact of climate change on the hydrological cycle in Panay Island and Pampanga Province, Philippines. We developed an integrated surface water-groundwater model using a version of the widely applied VIC hydrological model that includes a 2D groundwater model: VIC-AMBHAS. The model simulates components of the hydrological cycle, such as soil moisture, evapotranspiration, surface runoff, groundwater recharge, and river baseflow. The model can be used to simulate the hydrological cycle over historical and future time periods. We used data available at a global scale to parameterise the models, which were constructed on a ~1km grid. The meteorological driving data is downscaled to this resolution. Both historical climatology (1979-2018) and future climate projections up to 2089 are used to drive the model to study the impact of climate change on the hydrological cycle.

Over the historical period, Pampanga receives marginally more rainfall (181 mm/month) than Panay (174 mm/month). However, the partitioning of precipitation into the different water fluxes varies for the two regions. In Panay, 72% of the precipitation is partitioned into evapotranspiration whereas in Pampanga this is only 60% of the precipitation. This results in higher surface runoff and groundwater recharge in Pampanga (runoff: 44 mm/month, recharge: 36 mm/month) than Panay (runoff: 33 mm/month, recharge: 18 mm/month). Consequently, on an annual basis, Panay receives half the groundwater recharge compared to Pampanga.

We apply projections of future climate derived from global climate simulations undertaken by the UK Meteorological Office's Hadley Centre – the UKCP18 projections. We also apply two sets of UKCP18 projections that consider different greenhouse gas concentration pathways: RCP2.6 and RCP8.5. In RCP 2.6 carbon dioxide emissions start declining by 2020 and go to zero by 2100. In RCP 8.5 emissions continue to rise throughout the 21st century.

Simulated hydrological changes produced using the RCP2.6 and RCP8.5 projections for the 2050s (Table 1) are relatively similar for each location and indicate the following:

- Panay:
  - Reduction in precipitation of 5%
  - Reduction in groundwater recharge of 11-12%
  - Reduction in surface runoff of 6%
  - Reduction in river baseflow of 12-13%
- Pampanga
  - No change in precipitation
  - Reduction in groundwater recharge of 2-4%
  - No clear change in surface runoff
  - Reduction in river baseflow of 1-3%

2050	Panay		Pampanga	
	RCP 2.6	RCP8.5	RCP 2.6	RCP8.5
Precipitation	-5.1	-5.3	0.0	-0.9
Evapotranspiration	-2.1	-2.4	-0.1	0.0
Groundwater recharge	-11.0	-12.1	-2.0	-3.9
Surface runoff	-5.6	-5.6	1.0	-0.3
River baseflow	-12.2	-13.3	-1.4	-2.9

% change
-30
-20
-10
0
1

Table 1. Simulated hydrological change (%) for the 2050 based on UKCP18 RCP2.6 and RCP8.5 projections. Shading indicates the percentage change relative to historic periods.

Simulated hydrological changes for 2080s (Table 2) are in less agreement between the RCP2.6 and RCP8.5 than the 2050s:

- Panay:
  - Reduction in precipitation of 6-15%
  - Reduction in groundwater recharge 13-29%
  - Reduction in surface runoff 6-17%
  - Reduction in river baseflow 15-33%
- Pampanga
  - Reduction in precipitation of 2-4%
  - Reduction in groundwater recharge 4-12%
  - Reduction in surface runoff 3-4%
  - Reduction in river baseflow 3-9%

	Panay		Pampanga		% change
2080	RCP 2.6	RCP8.5	RCP 2.6	RCP8.5	
Precipitation	-5.6	-14.9	-2.0	-4.3	-30
Evapotranspiration	-2.1	-7.6	0.2	-0.5	-20
Groundwater recharge	-12.7	-29.4	-3.6	-11.5	-10
Surface runoff	-6.1	-16.6	-2.7	-4.1	0
River baseflow	-15.4	-32.6	-2.5	-8.6	1

Table 2. Simulated hydrological change (%) for the 2080 based on UKCP18 RCP2.6 and RCP8.5 projections. Shading indicates the percentage change relative to historic periods.

The model simulations highlight regional differences in the groundwater and surface water availability for Panay and Pampanga for both the historical and future climate periods. Panay receives less groundwater recharge and is projected to be more affected by impacts of climate change than Pampanga. The effects of climate change will result in a larger reduction in precipitation, groundwater, and surface water for periods later in the century.

Whilst the VIC-AMBHAS model has been applied to Pampanga and Panay, an associated modelling framework has been developed which supports the application of the model to other Philippine islands or to the whole of the Philippines. For example, this framework facilitates the processing and downscaling of global climate datasets to create the related input files required by the model. Following on from this project, the British Geological Survey are extending this work by developing a national-scale hydrological model for the whole of the Philippines. This national model will seek to inform the water resource sector and policy makers about regional differences in water availability and predicted response to climate change to help with decision making and policy development.

1 Introduction

Water security is of particular concern for Philippine cities, which have been designated amongst the worst in Asia for urban water security (Asian Development Bank 2016). Changing climate and increasing urban population are putting more stress on water resources. Decreasing rainfall during the dry season and more intense rainfall during the wet season will exacerbate both water availability during periods of drought and the magnitude of flood events during periods of heavy rainfall.

This report investigates the impact of climate change on the hydrology in Panay Island and the Province of Pampanga, Philippines, with a focus on groundwater recharge. We use the VIC hydrological model to investigate the effects of climate change up to 2089 on the magnitude of groundwater recharge.

The report is structured as follows: first parameterisation of the VIC hydrological model is described. Then we compare the modelled river flow to observational data for model calibration. Finally, we present the historical simulations for Panay and Pampanga followed by those considering future climate change.

2 Groundwater recharge modelling for Panay Island and Pampanga Province

2.1 RECHARGE MODEL DESCRIPTION

To simulate groundwater recharge in the Philippines, we use the integrated VIC hydrological model coupled to a lateral groundwater flow model (VIC_AMHAS), as developed by Scheidegger et al. (2021). The VIC hydrological model is a macro-scale hydrological model, applied widely for water and energy balance studies (Hamman et al. 2018). The model describes water and energy transport over a grid cell and calculates evapotranspiration (ET), runoff, infiltration, soil moisture and river baseflow for each cell. When precipitation reaches the land surface, it is partitioned into runoff and infiltration, according to the variable infiltration curve (Wood et al. 1992). It assumes that surface runoff from the upper two soil layers is generated by those areas for which precipitation and the soil moisture exceeds the storage capacity of the soil. The volume of water that flows vertically between the soil layers is calculated using a 1D Richards equation (Gao et al. 2010), assuming free drainage and using the Brooks-Corey relationship for hydraulic conductivity (Gao et al. 2010). In the standard version of VIC (Hamman et al. 2018) river baseflow, which leaves the top of the soil column, is calculated as a function of the relative moisture of the bottom soil layer according to the Arno model formulation (Franchini and Pacciani 1991). To accumulate flows at river gauging stations, routing of runoff and baseflow is performed a-posteriori by post-processing model output (Lohmann et al. 1996).

The lateral groundwater model coupled to VIC is a distributed, one-layer, two-dimensional groundwater model driven by groundwater recharge and groundwater pumping. Groundwater recharge is derived from interaction of the groundwater model with the VIC soil hydrology by allowing bi-directional exchange of water between the aquifer and the soil. This is achieved by calculating a vertical flux, q_v, as a function of soil moisture and water table level following the SIMGM model approach (Niu et al. 2007). This replaces the baseflow formulation of the standard version of VIC. A full description of the lateral groundwater model and coupling to VIC is given by Scheidegger et al. (2021).

2.2 CALCULATION OF GROUNDWATER RECHARGE TO DRIVE MODFLOW GROUNDWATER MODELS

The output from the VIC hydrological model is used to drive groundwater models using MODFLOW. MODFLOW requires recharge for each stress period, which is the flux from the soil to the aquifer but does not include losses from the aquifer to the soil. In VIC-AMBHAS, for each model cell, the vertical flux of water between the soil and the aquifer is either in downward or upward direction. This vertical flux of VIC-AMBHAS differs from the recharge required in MODFLOW. Therefore, we present the following methodology.

When the water table is close to the land surface, q_v is in upward direction. As in reality, model grid cells that are discharging will be recharging as well, we made a work around and adjusted this vertical flux q_v to represent groundwater recharge, q_r. This vertical flux, q_v, between the soil and the aquifer is used as groundwater recharge, q_r, if the flux is downwards, from the soil to the aquifer. If the flux between the soil and the aquifer is upwards, e.g., if the cell is discharging due to high groundwater levels, then we use the VIC variable 'runoff' q_{run} as the groundwater recharge. This is equivalent to:

$$q_r = \begin{cases} q_v, & for\ q_v > 0 \\ P - E - q_v + dS = q_{run}, & for\ q_v < 0 \end{cases}$$

where P is precipitation reaching the soil, E evaporation, q_v upward flow across the bottom boundary of the soil, and dS the change in soil storage. Where the vertical flux between the soil and the aquifer is upwards, all water that reaches the model cell through precipitation that is not evaporated minus the upward flux q_v and considering changes in soil storage is used as recharge into the groundwater model. This is equivalent to the VIC variable 'runoff' q_{run}. At these model cells, where the water table is shallow, the groundwater model will then act as a combined surface and groundwater model.

In this report, we use the term groundwater recharge as the vertical flux q_r from the soil to the aquifer for $q_v > 0$. Groundwater discharge is defined as the vertical flux from the aquifer to the soil ($q_v < 0$).

2.3 VIC MODEL PARAMETERISATION

The VIC model parameterisation is described in detail in the VIC documentation *(University of Washington Computational Hydrology Group 2021)*. The model is parameterised with spatially distributed parameters from a range of sources describing the land surface, including soil properties and vegetation properties. The soil properties such as field capacity, plant available water, wilting point, saturated hydraulic conductivity and residual saturation for the VIC model are taken from a global high-resolution map of soil hydraulic properties (Zhang and Marcel 2018). Quartz fraction and bulk density values are from SoilGrid1km (Hengl et al. 2014). Landcover vegetation parameters are taken from Modis (Friedl and Sulla-Menashe 2015), LAI and albedo from Copernicus (Smets et al. 2019), and vegetation height from LiDAR-derived Global Estimates of Forest Canopy Height (Healey et al. 2015). A full list of parameters, units, dimensions, description and data sources is given in Table 7 and Table 8 (Appendix 1). The model is set up using a grid of 1/120° cells. For Iloilo, this translates to a cell width of between 907.5 and 921.8 m.

The VIC model is driven by meteorological forcing data using a gridded, sub-daily time-series of meteorological variables as input. Average air temperature, total precipitation, atmospheric pressure, incoming shortwave radiation, incoming longwave radiation, vapor pressure and wind speed are required. For the historical simulation (1979 – 2018), we use ERA5 hourly data on single levels from 1979 to present (Hersbach et al. 2018). For the future climate projections (1980 – 2089), we use UKCP Global 60 km simulations of two greenhouse gas concentration pathways: RCP 2.6 and RCP 8.5 (Met Office Hadley Centre 2018).

The meteorological forcing data is at 0.25°, and hence a much coarser resolution than the soil and vegetation parameters. Therefore, the meteorological forcing data were downscaled to match the model grid using the delta method (Moreno and Hasenauer 2016). This approach uses long-term monthly averages of several climate variables at 1/120° developed by WorldClim (Fick and Hijmans 2017) to obtain of 1/120° resolution climate data set.

The groundwater part of the model requires hydraulic conductivity and specific yield, which are obtained from (Gleeson et al. 2014). However, for calibration purposes, hydraulic conductivity and specific yield are multiplied by a factor (described in the next section). The coastlines are set to a hydraulic head of 0 m, representing mean sea level. The groundwater is allowed to discharge at river locations defined by the (National Mapping and Resource Information Authority (NAMRIA) 2015). A full list of parameters used is given in Table 9.

Two models are set up, the first one for the entire island of Panay (Figure 1b), the second one for parts of Luzon (Figure 1c). In Luzon we only considered an area containing the catchment of Pampanga, an area to the east of this to the coast, and a small catchment adjacent to the south-east of the Pampanga catchment. This was because the model is run at a high spatial resolution (~1 km) and requires a large amount of model forcing data.

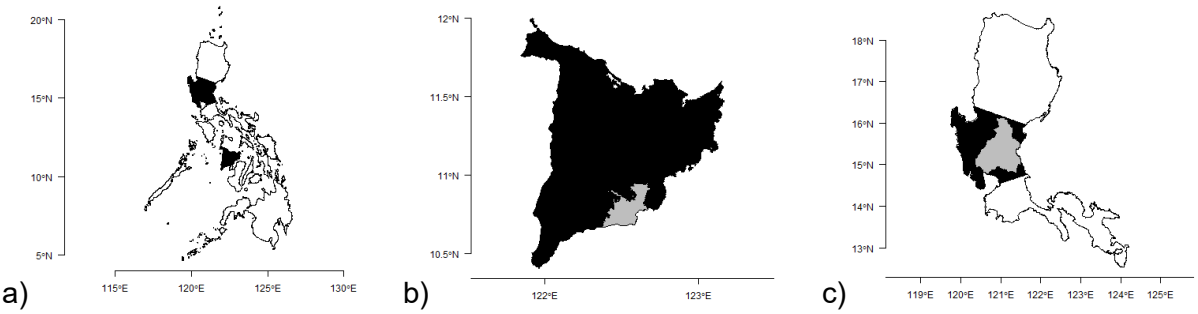

Figure 1. Model domains of a) the Philippines with the two model areas b) Panay with Iloilo and c) Luzon with the Pampanga model domains (Global Administrative Areas 2012).

2.4 VIC MODEL CALIBRATION

The model was manually calibrated against river flow data, altering the following VIC parameters:

- infilt, used to describe the variable infiltration curve;
- the soil thickness;
- saturated hydraulic conductivity, Ksat;
- C_in, defining the river-bed conductance;
- the multiplying factors for specific yield and hydraulic conductivity.

A full description is given in Table 8 for the VIC parameters and Table 9 for the groundwater parameters.
For Panay, we first compared the mean simulated recharge of the Calayan catchment amongst the different model runs. The Calayan catchment also includes the gauging stations Simsiman and Poblacion. For the catchment of Calyan, the simulated mean monthly recharge ranges from 13.6 to 24.4 mm/month, with the median value at 20.7 mm/month. Seven out of the 13 runs have a mean recharge between 20 and 21 mm/month. Amongst the recharge values around the median, we compared the Nash Sutcliffe Efficiency (NSE), the percentage bias, the root mean squared error and absolute error of simulated river flow, and ranked the runs which preformed best for high and low flow conditions. The scores for the selected runs are presented Table 3.

The observed and simulated river flows for Panay are given in Figure 2 and the scores for each station in Table 3. The overall NSE for Calyan, Simsiman and Pampang are around 0.5, and for Lana 0.37, and the simulated river flow represents the dynamics of the observed river flow generally well. The percentage bias for the Calayan Simsiman is below 10% for the wet season and around 20% for the dry season. For the other stations, the overall NSE is lower, and the percentage bias is higher. Some of the peak-flows are not well represented in the model.

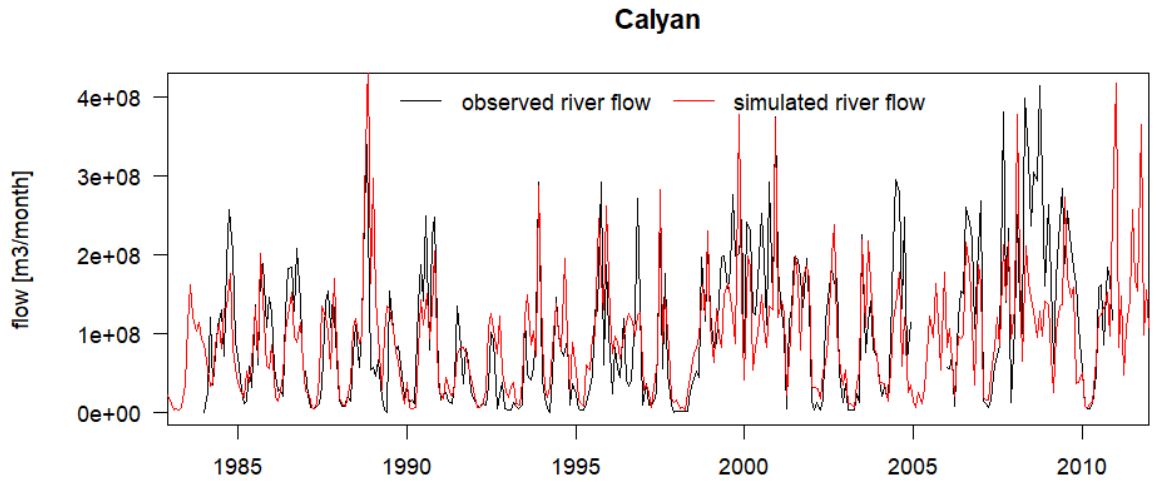

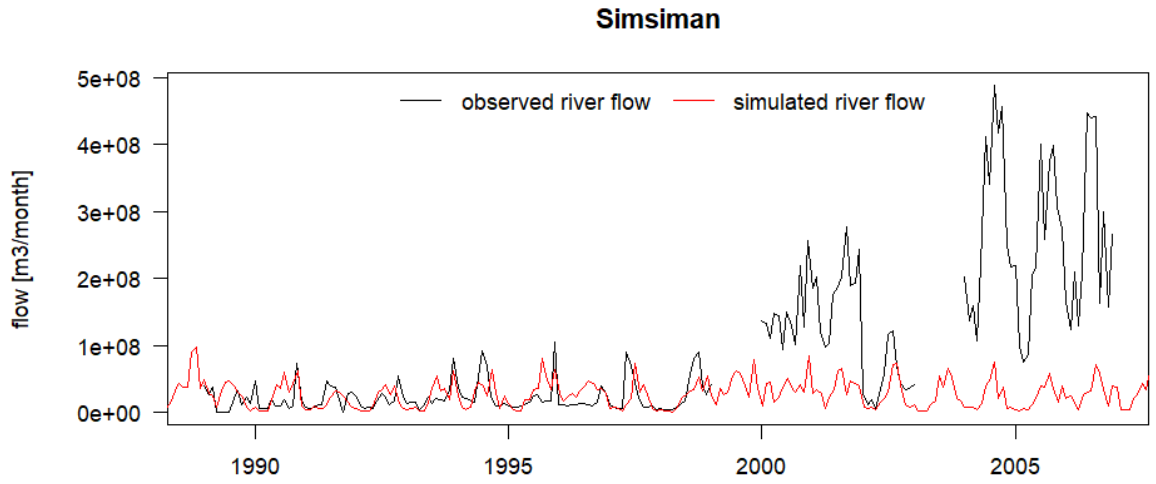

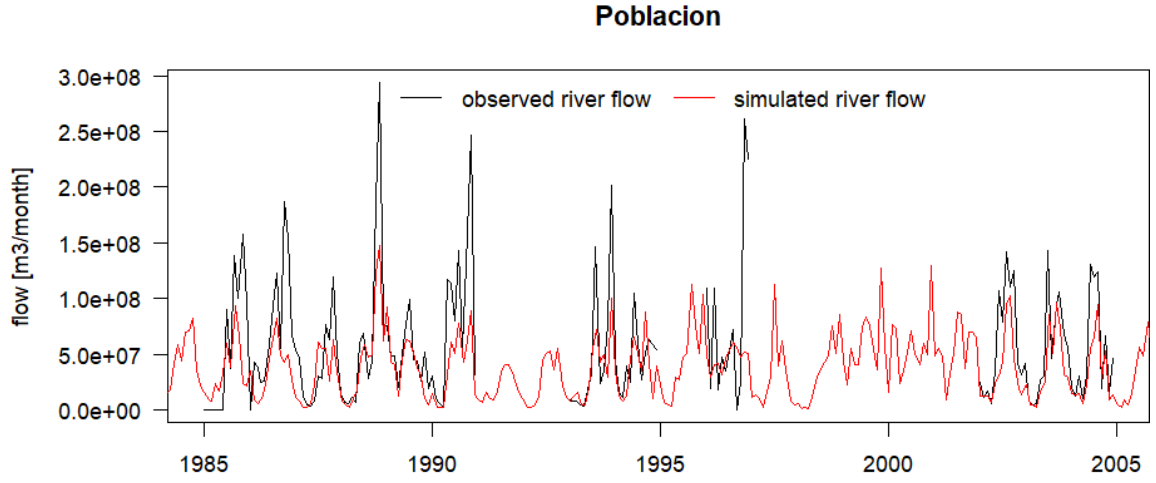

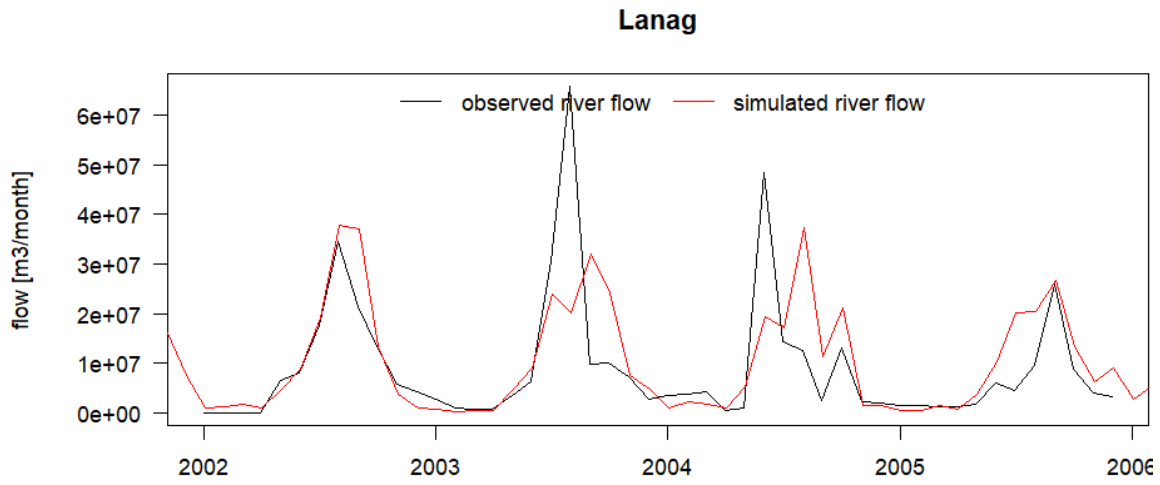
Lanag
observed river flow
simulated river flow
flow [m3/month]
6e+07
5e+07
4e+07
3e+07
2e+07
1e+07
0e+00
2002
2003
2004
2005
2006

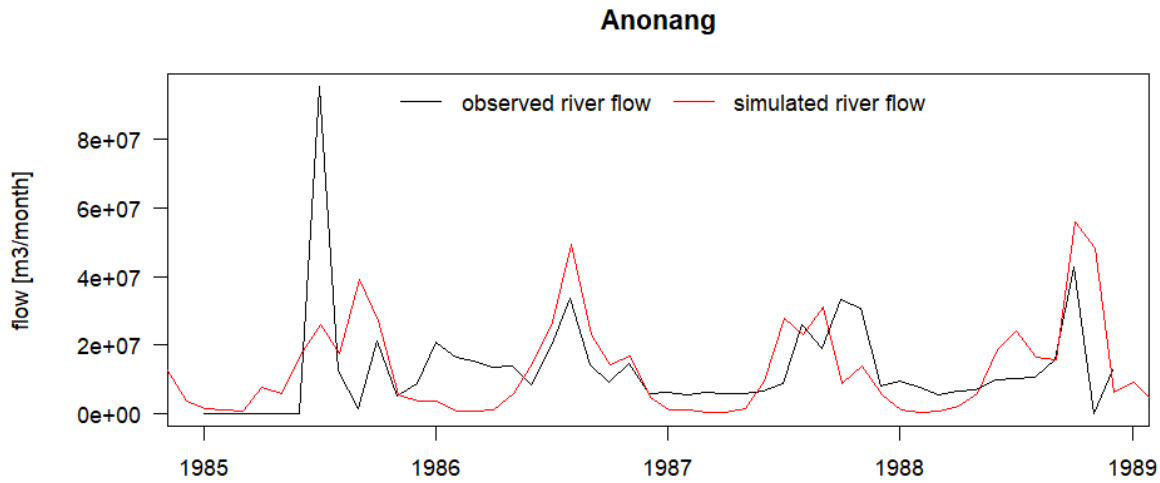
Anonang
observed river flow
simulated river flow
flow [m3/month]
8e+07
6e+07
4e+07
2e+07
0e+00
1985
1986
1987
1988
1989

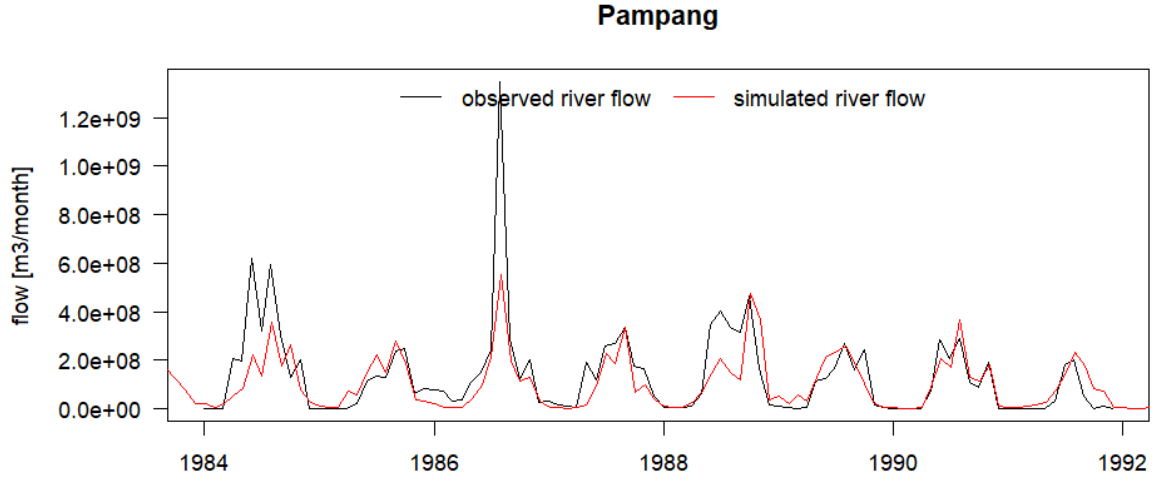
Pampang
observed river flow
simulated river flow
flow [m3/month]
1.2e+09
1.0e+09
8.0e+08
6.0e+08
4.0e+08
2.0e+08
0.0e+00
1984
1986
1988
1990
1992

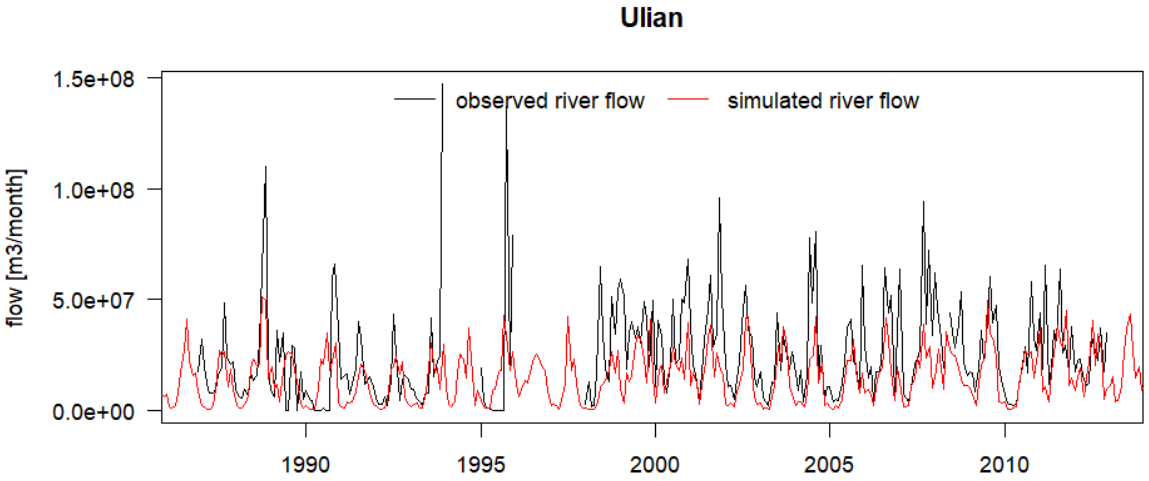

Figure 2. Observed and simulated river flow for the Panay model. Observed flows from (Department of Public Works and Highways 2016).

Measure	Calyan	Poblacion	Simsiman	Anonang	Lanag	Pampang	Ulian
NSE_Dry	0.53	0.50	-0.32	-3.04	-0.59	0.18	-0.05
NSE_Wet	0.24	0.38	-0.31	0.03	0.14	0.32	-0.20
NSE_all	0.49	0.53	-0.26	0.03	0.37	0.51	-0.01
Pbias_Dry	22.60	-18.90	-79.40	-80.90	-25.90	-31.70	-66.50
Pbias_Wet	1.40	-7.30	-70.80	-15.90	-11.40	-29.10	-43.30
Pbias_all	7.90	-10.60	-74.00	-34.60	-13.00	-29.40	-52.10
RMSE_Dry	5.30E+07	2.92E+07	8.83E+07	8.91E+06	1.95E+06	4.96E+07	2.04E+07
RMSE_Wet	7.43E+07	4.59E+07	1.55E+08	1.91E+07	1.40E+07	1.72E+08	2.37E+07
RMSE_all	6.45E+07	3.87E+07	1.26E+08	1.53E+07	1.04E+07	1.31E+08	2.21E+07
AE_Dry	3.42E+07	1.67E+07	5.37E+07	7.71E+06	1.56E+06	2.87E+07	1.31E+07
AE_Wet	5.58E+07	3.18E+07	9.29E+07	9.55E+06	8.29E+06	1.04E+08	1.63E+07
AE_all	4.26E+07	2.94E+07	7.24E+07	1.02E+07	5.96E+06	6.77E+07	1.34E+07

Table 3. Scores for simulated river flows for Iloilo. Each score is taken for the dry season, wet season and for the entire time series. NSE: Nash Sutcliffe Efficiency, Pbias: percentage bias, RMSE: root mean squared error, and AE: absolute error.

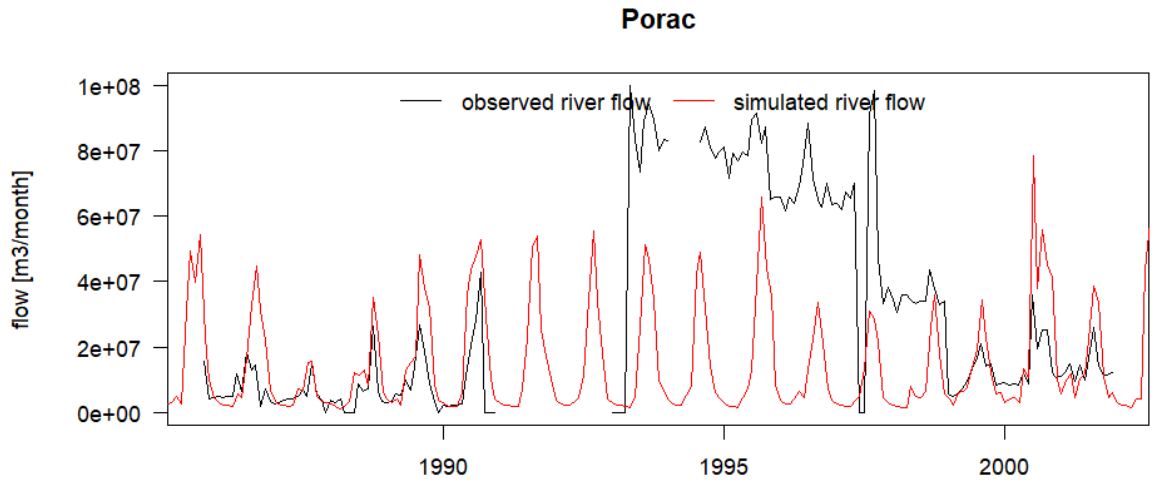
Porac
observed river flow
simulated river flow
flow [m3/month]
1e+08
8e+07
6e+07
4e+07
2e+07
0e+00
1990
1995
2000

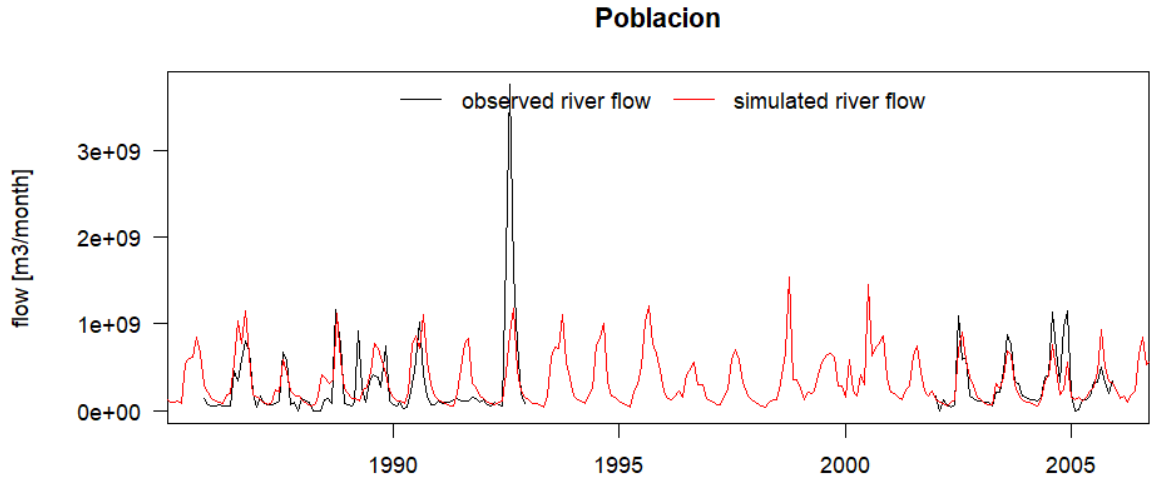
Poblacion
observed river flow
simulated river flow
flow [m3/month]
3e+09
2e+09
1e+09
0e+00
1990
1995
2000
2005

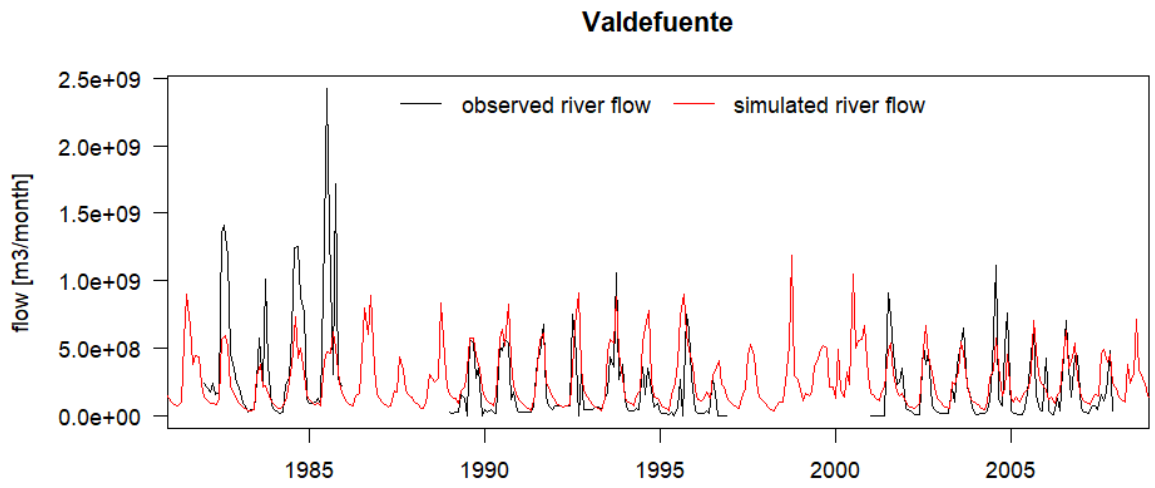
Valdefuente
observed river flow
simulated river flow
flow [m3/month]
2.5e+09
2.0e+09
1.5e+09
1.0e+09
5.0e+08
0.0e+00
1985
1990
1995
2000
2005

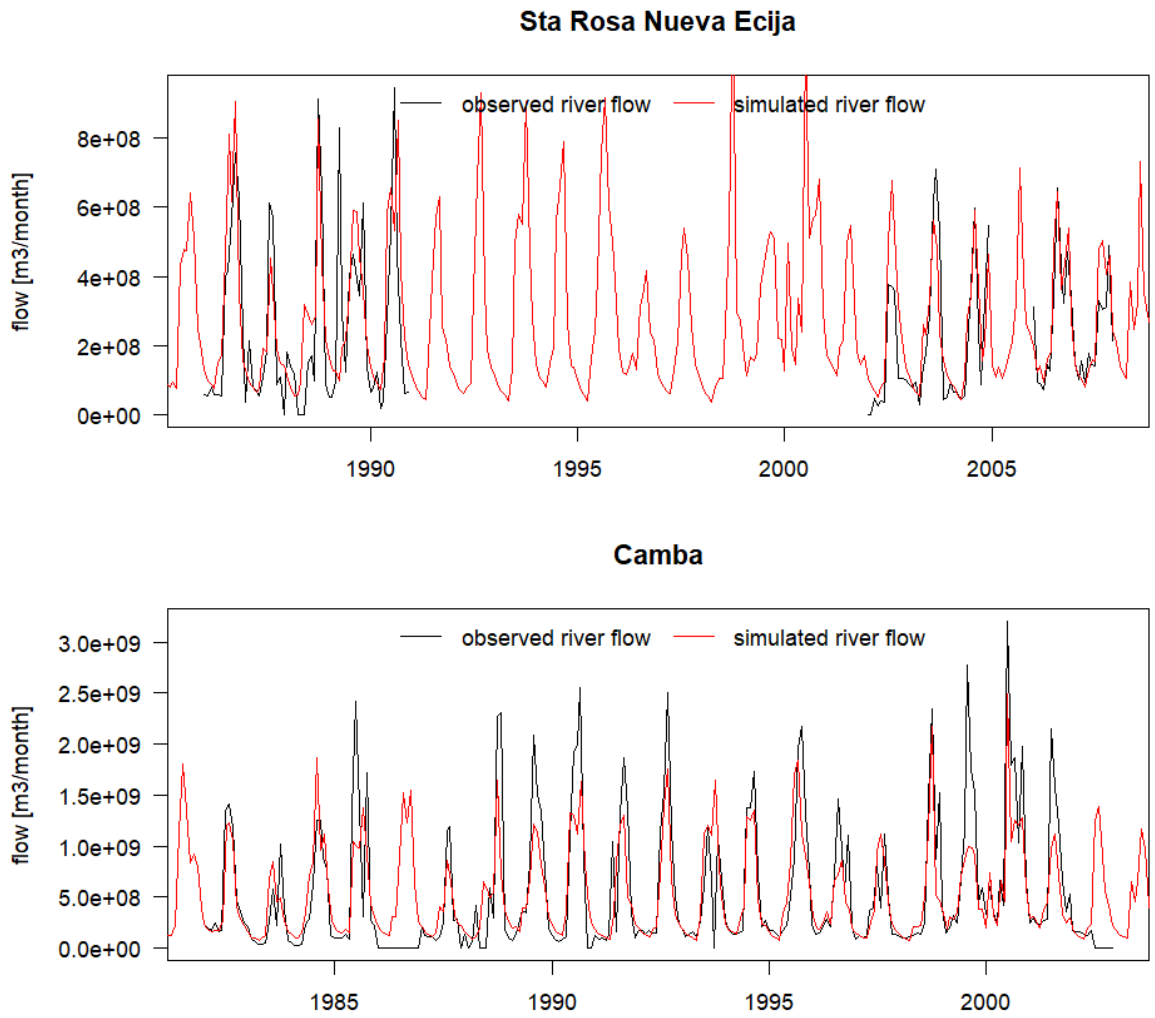

Figure 3. Observed and simulated river flow for the Pampanga model. Observed flows from (Department of Public Works and Highways 2016).

Similarly, for Pampanga the run was selected using the same assessment criteria as the model in Panay. The simulated and observed river flows are given in Figure 3 and the scores are given in Table 4. The selected run performs well at all stations, particularly in Camba, with an overall NSE of 0.69 and around 0.5 for wet and dry seasons only. For Poblacion, the peak flow in 1993 is not represented, and in Porac, the observed flows appear to have increased in the 1990s. This might be related to lahars in the Porac river following the 1991 eruption of Mount Pinatubo. Volcanic deposits lead to a reduction in infiltration and enhanced overland flow. This alteration in watershed hydrology by volcanic deposits in conjunction with heavy rainfall generated the lahars (Major et al. 1996).

Measure	Valdefuente	Sta Rosa Nueva Ecija	Poblacion	Camba
NSE_Dry	0.38	0.23	0.33	0.52
NSE_Wet	0.21	0.41	0.22	0.50
NSE_all	0.43	0.54	0.35	0.69
Pbias_Dry	38.3	3.9	-0.5	6.1
Pbias_Wet	-14	17.7	1.2	-17.5
Pbias_all	-5.8	14.3	0.8	-13.5
RMSE_Dry	8.74E+07	1.17E+08	1.43E+08	1.29E+08
RMSE_Wet	3.67E+08	1.71E+08	4.84E+08	5.01E+08
RMSE_all	2.66E+08	1.48E+08	3.61E+08	3.63E+08
AE_Dry	6.97E+07	6.36E+07	7.36E+07	7.16E+07
AE_Wet	2.28E+08	1.39E+08	2.84E+08	3.65E+08
AE_all	1.49E+08	9.89E+07	1.84E+08	2.18E+08

Table 4. Scores for simulated river flows for Pampanga. Each score is taken for the dry season, wet season and for the entire time series. NSE: Nash Sutcliffe Efficiency, Pbias: percentage bias, RMSE: root mean squared error, and AE: absolute error.

2.5 VIC HISTORICAL SIMULATION

2.5.1 Panay Island

The mean fluxes for the wet (May to October) and dry (November to April) seasons during the historical period in Panay are presented in Figure 4 and the time series of the spatially-averaged fluxes for the Iloilo groundwater model domain in Figure 5. These figures illustrate the spatial and temporal variation in the water fluxes. During the wet season, the rate of groundwater recharge is greater on the east side of the island, where precipitation is higher. Similarly, during the dry season, precipitation is highest in the north of the island, which results in greater rates of recharge there. Where the water table is very shallow (i.e., near the land surface) and within the soil layers, the flux of water between the aquifer and the soil can be from the aquifer to the soil, resulting in a zero recharge and a groundwater discharge, as observed in Figure 4. For an annual cycle, Panay receives 173 mm/month of precipitation. Averaged annually, the precipitation is partitioned to 72% evapotranspiration, 19% runoff, 10% groundwater recharge. The percentage of evapotranspiration from precipitation increases during the dry season to 82% and decreases during the wet season to 69%. Groundwater recharge equates to 9% of the precipitation during the wet season and 13% during the dry season.

Wet season (May – October)

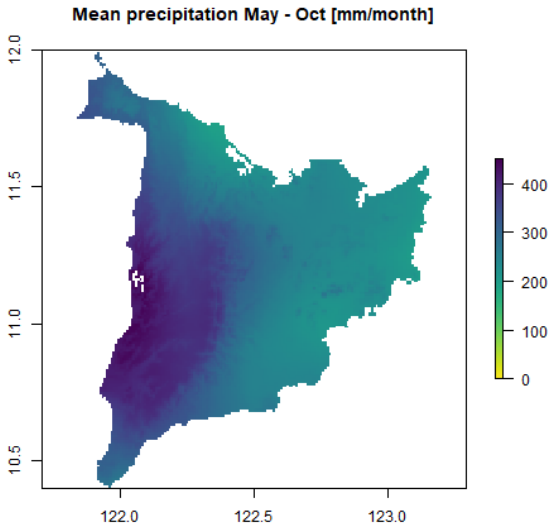

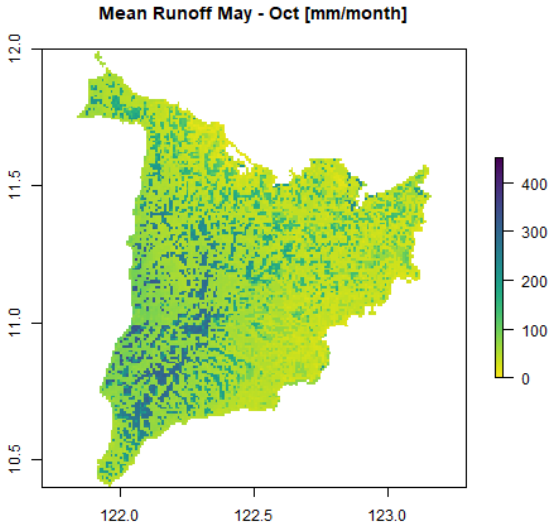

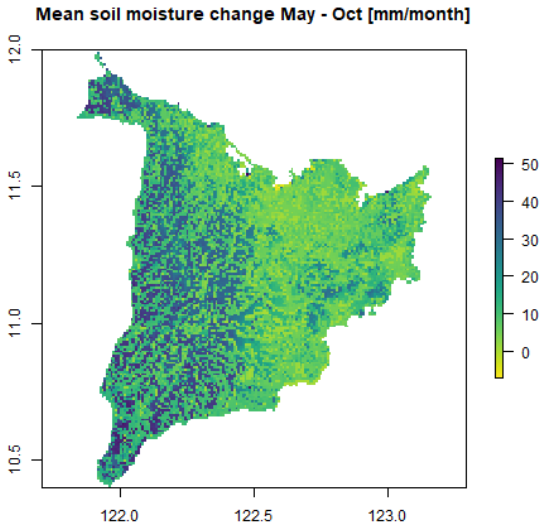

Dry season (November – April)

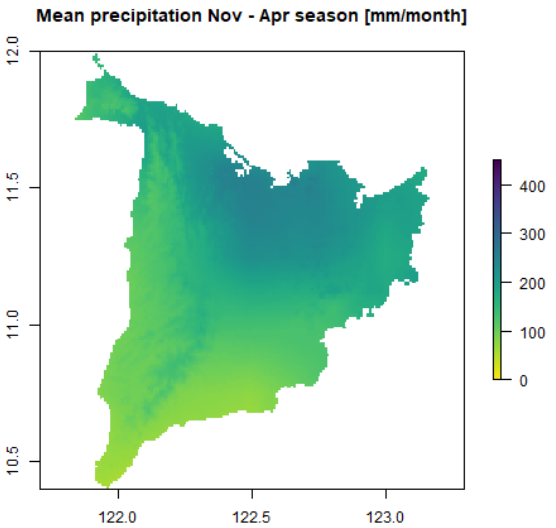

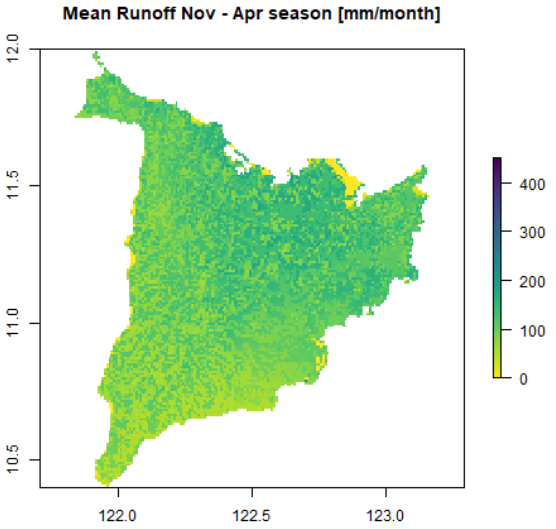

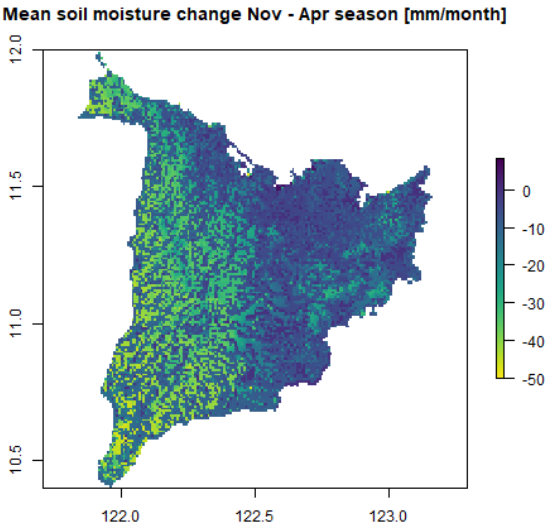

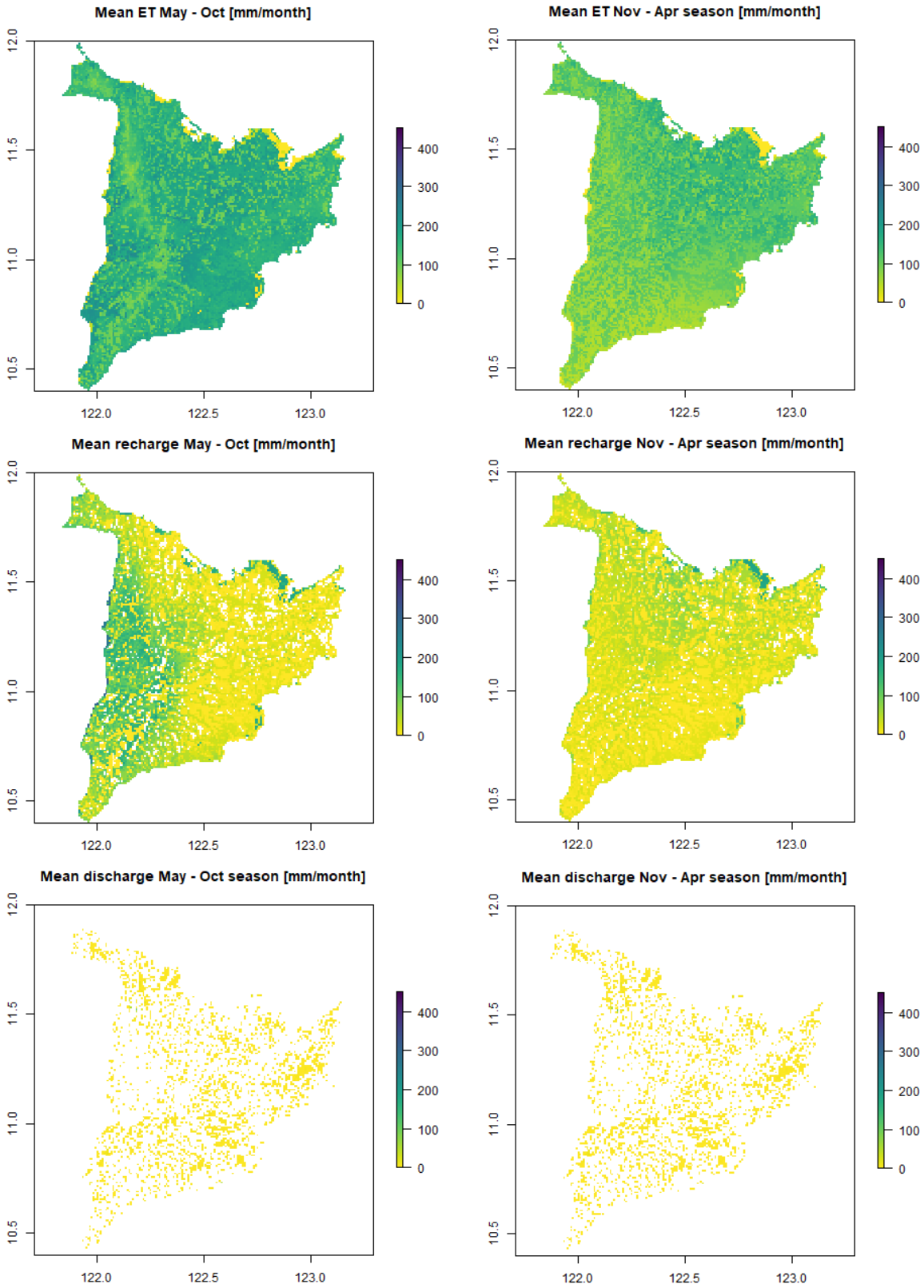

Figure 4. Modelled mean monthly fluxes for Panay 1979 – 2018 for wet (May – October) and dry season (November – April). Precipitation, evapotranspiration (ET), change in soil moisture, groundwater recharge and groundwater discharge.

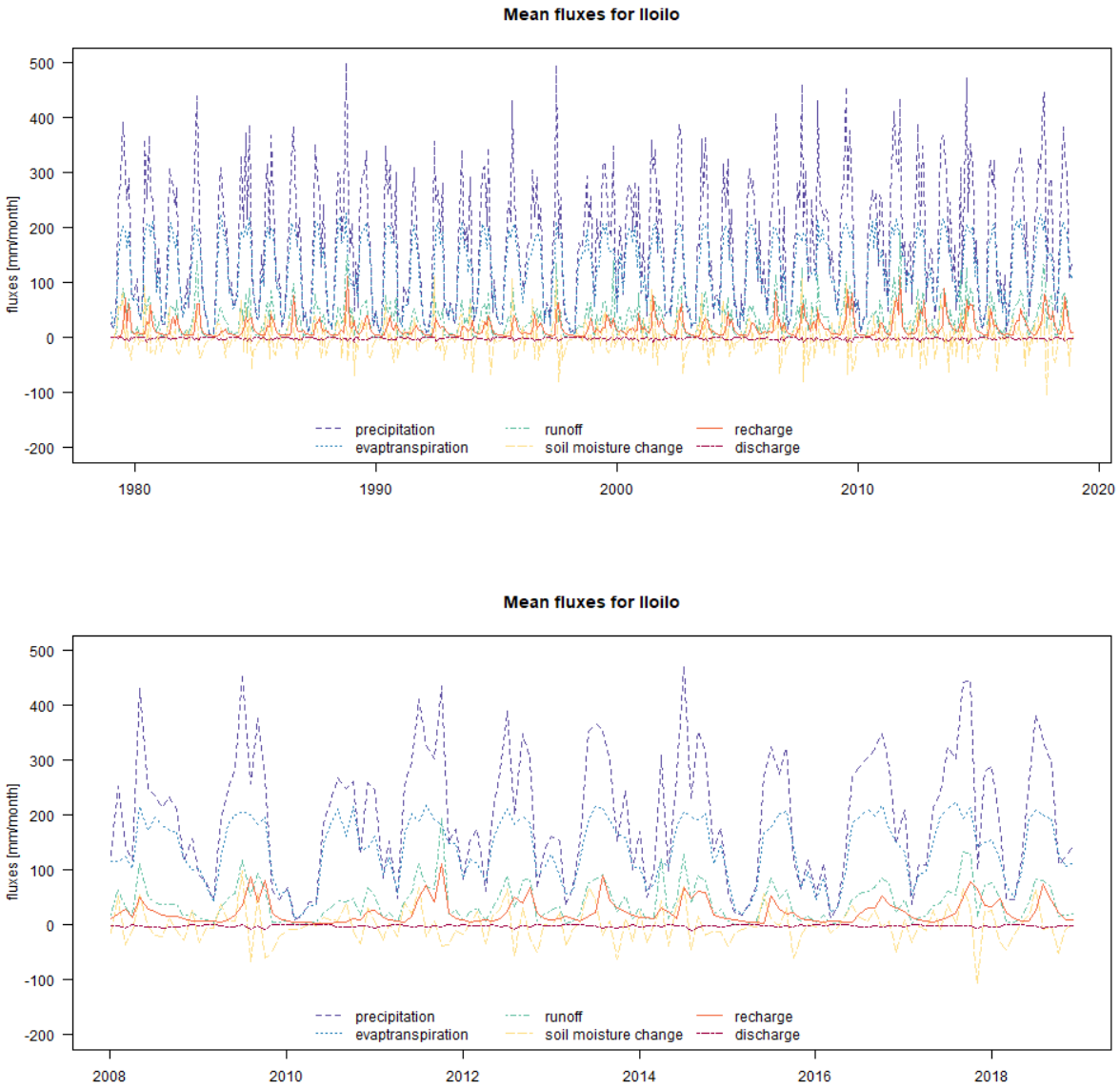

Figure 5. Time-series of modelled mean monthly fluxes for the model domain of Iloilo.

Table 5. Historical fluxes for Panay for annual, wet season and dry season. Absolute values and percentage of rainfall.

	annual		wet season		dry season	
	mm/month	%	mm/month	%	mm/month	%
Precipitation	173.9	100.0	253.9	100.0	93.9	100.0
ET	125.6	72.2	174.3	68.6	76.8	81.8
Runoff	32.9	18.9	49.9	19.7	15.9	17.0
Recharge	17.8	10.2	23.3	9.2	12.3	13.1
Discharge	-1.8	-1.0	-2.5	-1.0	-1.1	-1.2
Soil moisture change	0.3	0.2	9.4	3.7	-8.8	-9.3

2.5.2 Pampanga Province

The mean fluxes for the wet and dry season during the historical period in Pampanga are presented in Figure 6 and the time series of the spatially-averaged fluxes for the Pampanga groundwater model domain given in Figure 7. These figures illustrate the spatial and temporal variation in the water fluxes.

During the wet season, rates of groundwater recharge are greatest on the eastern, southern, and south-western parts of the island, which is due to a combination of precipitation and land cover. Similarly, during the dry season, precipitation is highest in the east of the island, which results in higher recharge there. Where the water table is very shallow and within the soil layers, the flux between the aquifer and the soil can be from the aquifer to the soil, resulting in a zero recharge and a groundwater discharge, as observed in Figure 6.

For an annual cycle, Pampanga receives 181 mm/month of precipitation. The precipitation is partitioned annually to 60% evapotranspiration, 24% runoff, 20% groundwater recharge. The percentage of evapotranspiration from precipitation increases during the dry season to 76% and decreases during the wet season to 56%. Groundwater recharge equates to 18% of precipitation during the wet season and 27% during the dry season (see Table 6).

Wet season (May – October)

Dry season (November – April)

Mean precipitation May - Oct [mm/month]

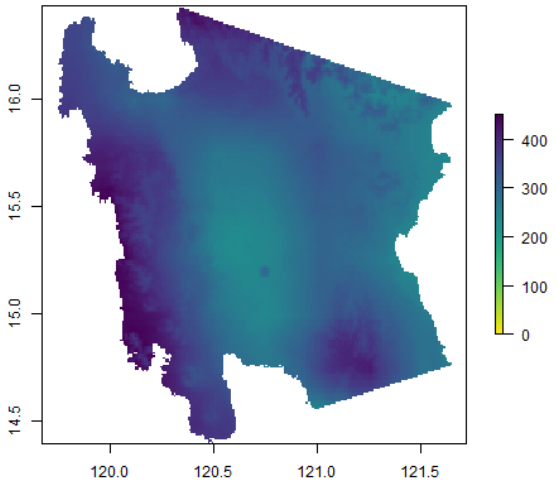

Mean precipitation Nov - Apr season [mm/month]

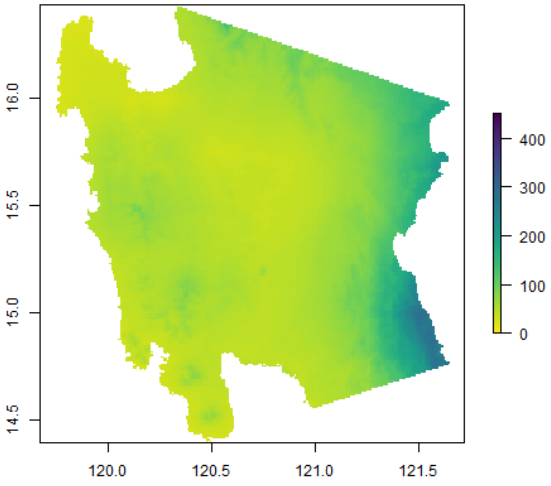

Mean Runoff May - Oct [mm/month]

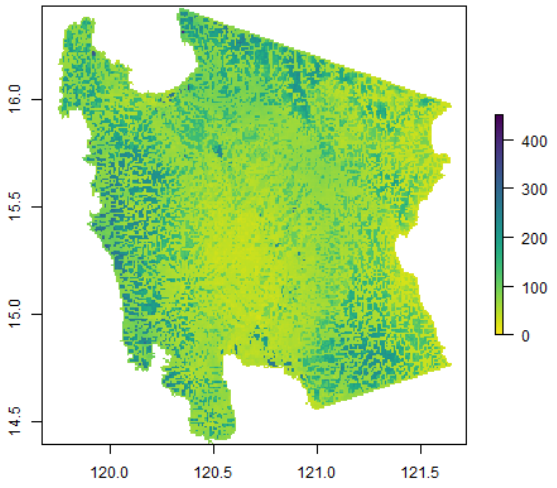

Mean Runoff Nov - Apr season [mm/month]

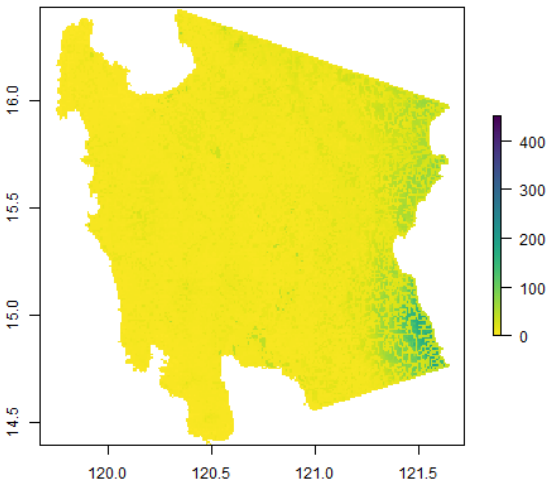

Mean soil moisture change May - Oct [mm/month]

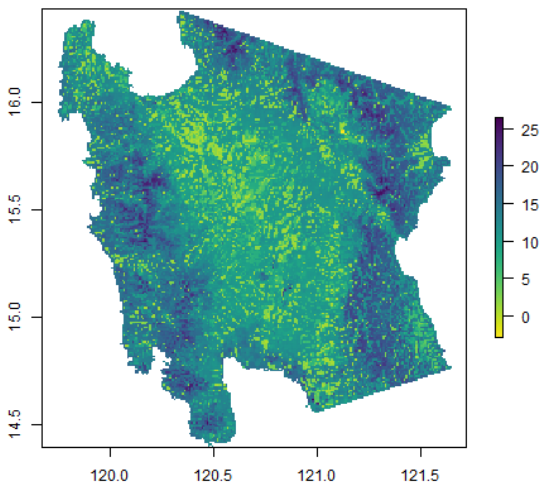

Mean soil moisture change Nov - Apr season [mm/month]

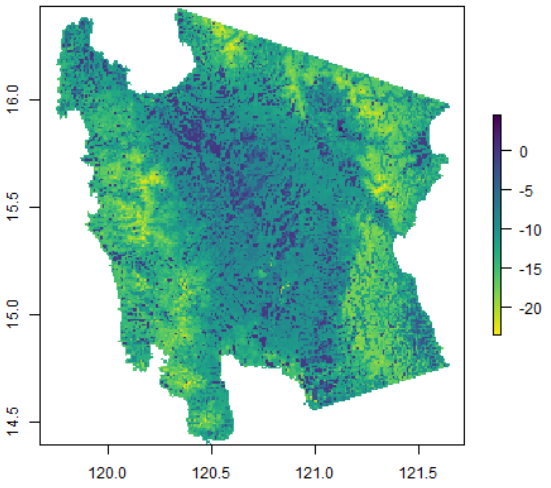

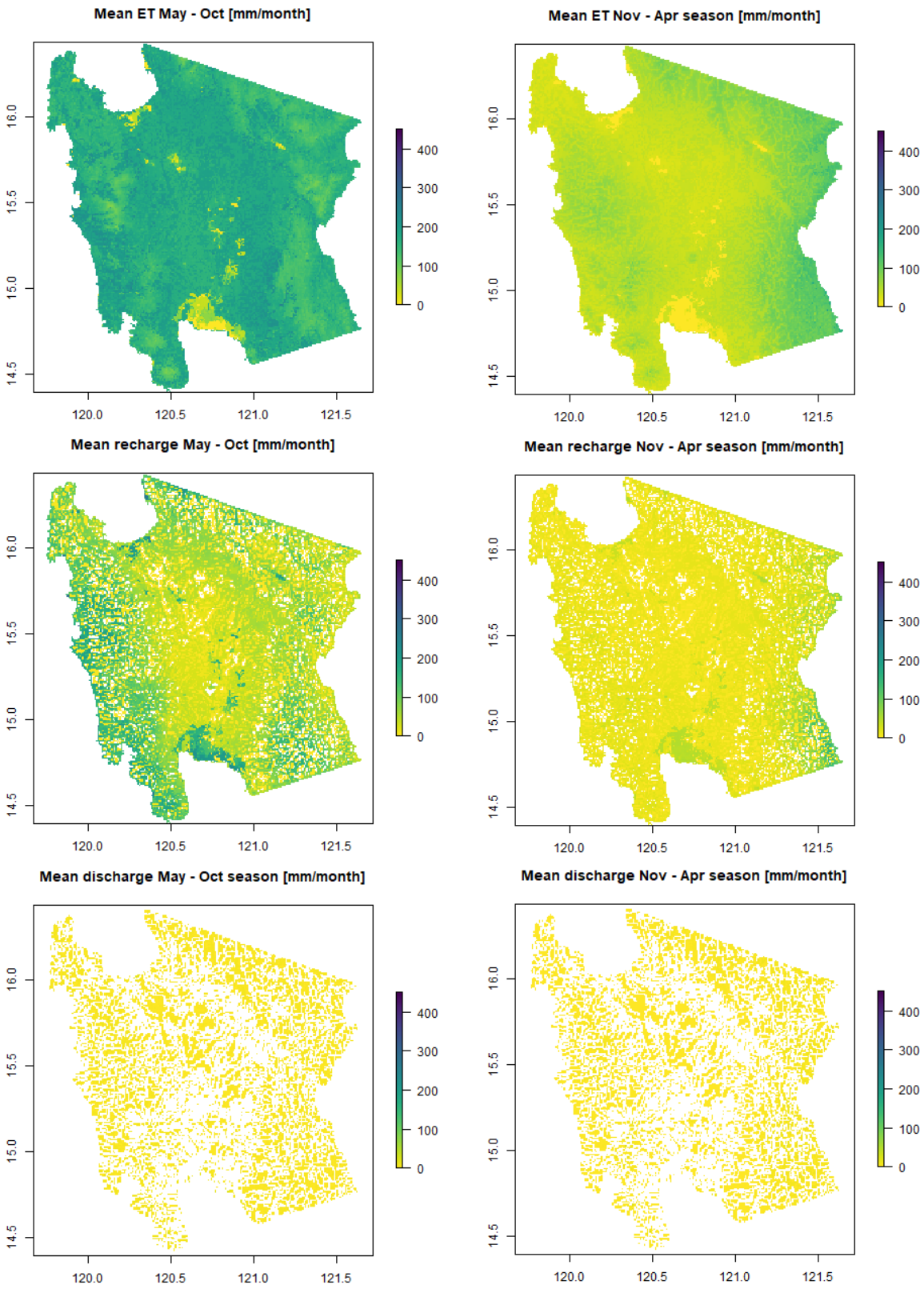

Figure 6. Modelled mean monthly fluxes for Pampanga 1979 – 2018 for wet (Mai – October) and dry season (November – April). Precipitation, evapotranspiration (ET), change in soil moisture, groundwater recharge and groundwater discharge.

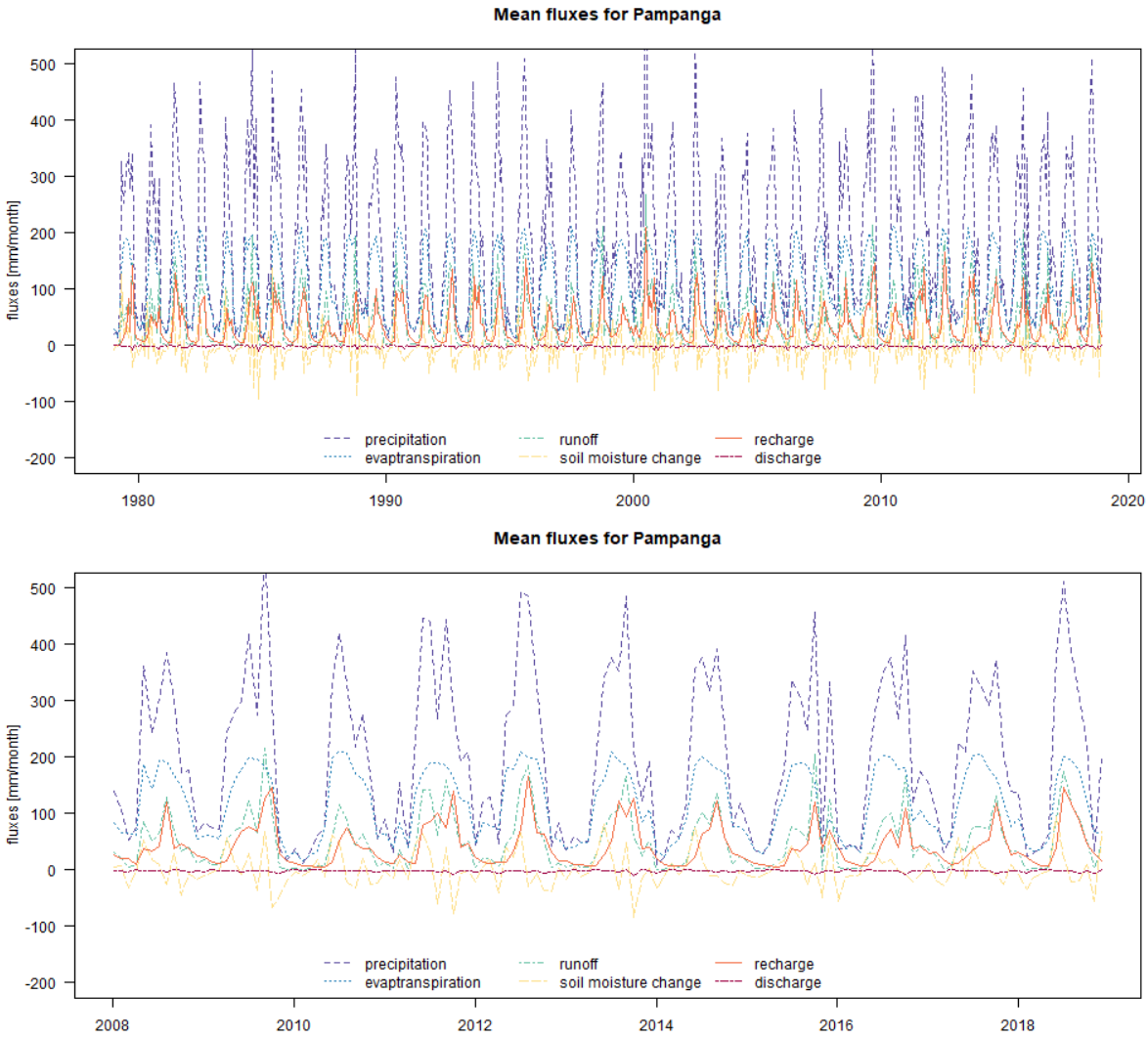

Figure 7. Time-series of modelled mean monthly fluxes for the model domain of Pampanga.

Table 6. Historical fluxes for Pampanga for annual, wet season and dry season. Absolute values and percentage of rainfall.

	Annual		Wet season		Dry season	
	mm/month	%	mm/month	%	mm/month	%
Precipitation	181.7	100.0	291.8	100.0	71.6	100.0
ET	109.6	60.3	164.4	56.3	54.7	76.4
Runoff	44.0	24.2	74.7	25.6	13.2	18.5
Recharge	35.8	19.7	52.5	18.0	19.2	26.8
Discharge	-1.8	-1.0	-1.8	-0.6	-1.7	-2.4
Soil moisture change	0.6	0.3	11.3	3.9	-10.2	-14.2

2.5.3 Summary of historical simulations

Pampanga (181 mm/month) receives more rainfall than Iloilo (174 mm/month) over the historical period. In addition, absolute values in evapotranspiration are lower for Pampanga (110 mm/month) than Iloilo (126 mm/month). This results in higher surface runoff and groundwater recharge in Pampanga (runoff: 44 mm/month, recharge: 36 mm/month) than Iloilo (runoff: 33 mm/month, recharge: 18 mm/month). On an annual basis, Iloilo receives half the groundwater recharge compared to Pampanga (Table 5 and Table 6).

2.6 FUTURE SCENARIOS

Two future scenarios of representative concentration pathways (RCPs) for greenhouse gas emissions are presented: UKCP18 ensemble RCP 2.6 and RCP 8.5. The UKCP18 is a global dataset with 15 ensemble members for each RCP scenario at 60 km spatial resolution. Simulation of climate variables is subject to substantial biases, or errors due to limited spatial resolution, simplified physical representation and incomplete understanding of the system (Copernicus Climate Change Service 2021). Comparing ERA5 and the UKCP18 data sets for the historical periods show a bias of one or both data sets (Figure 8). The bias is larger for Pampanga than for Iloilo. Because of the bias in precipitation for the UKCP18 data set, we present the difference of the future periods to the historical time period, rather than absolute values of the future scenarios. This delta method approach is valid, if we assume that the model bias is constant over time (Beyer et al. 2020). Further work should investigate other methods of bias correction of climate scenarios.

First, we present the mean monthly values for the historical period (1990-2019) and 2050s (2030-2059) and 2080s (2060-2089). Second, we present the mean change in the value for the 2050s and 2080s from the historical values. Third, we present boxplots considering the three time periods and grouping into wet season (May – October), dry season (November – April) and annual periods. Finally, we consider the change in extreme values for the future time periods; for each ensemble member, the percentile range is presented and classified for the distribution of values for each month considering the historical time period. For the future time periods, the historical classification is used and a shift from the normal historical climatology can be observed. The classification considers the following percentiles to align with the PhiGO seasonal groundwater forecasting system (Mackay et al. 2022):

- Exceptionally low < 5%
- Notably low 5 - 12.5 %
- Below normal 12.5 - 27.5%
- Normal 27.5 - 72.5%
- Above normal 72.5 - 87.5%
- Notably high 87.5 - 95%
- Exceptionally high > 95%

Results for Panay are shown in Figure 9 - Figure 13 and for Pampanga in Figure 14 to Figure 18.

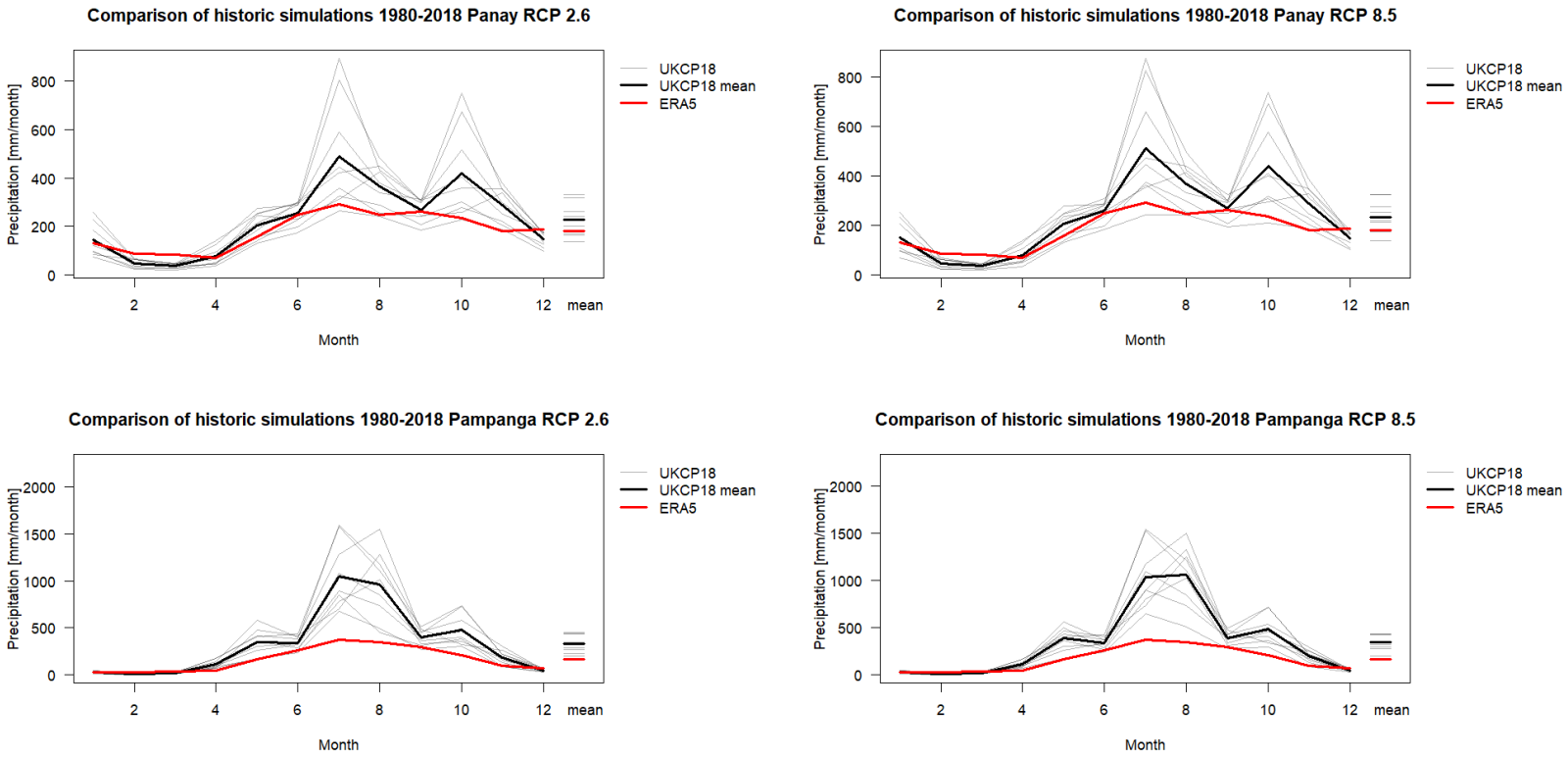

Figure 8. Comparison of ERA5 (historical reanalysis) and UKCP18 (simulated) data sets for the mean climatology 1980-2018 for Iloilo and Panay considering RCP 2.6 and 8.5.

2.6.1 Panay Island

2.6.1.1 Precipitation

For Panay, the mean monthly precipitation follows a bimodal distribution, with peaks in July and October. The mean monthly precipitation for RCP 2.6 and RCP 8.5, the mean monthly change, and the seasonal distributions for the historical (1990-2019), and future time periods of 2050s and 2080s are shown in Figure 9. The ensemble mean precipitation for future scenarios is lower for the 2050s and 2080s time slices (Figure 9 a-b).

For RCP 2.6, both future time slices have very similar mean annual values of 11.5 and 12.5 mm/month below historical values. Seasonally, the wet season (May-October) shows a greater decrease than the dry season (November – April). During the wet season, differences in precipitation are greatest during peak rainfall in July and October (Figure 9 c).

For RCP 8.5, the ensemble mean of annual precipitation for the 2050s decreases by 9.3 mm/month and for 2080s by 29 mm/month, with higher change during the wet season than the dry season (Figure 9 d). Similar to RCP 2.6, the differences in precipitation are greatest during peak rainfall in July and October.

For RCP 8.5 the decrease in precipitation is higher compared to RCP 2.6 for the 2080s and lower for the 2050s considering mean annual, wet and dry season monthly means.

For both RCPs, the simulated spread of the mean monthly precipitation amongst the different ensemble members is large. For example, the mean monthly precipitation of the historical period for RCP 2.6 ranges from 235.5 to 893.9 mm/month amongst the different ensemble members (Figure 9 e-f).

The percentile range of months with ‘normal’ precipitation decreases for RCP 2.6 from 45% to 37% and for RCP 8.5 from 45% to 29%. This is balanced by an increase in the months below normal precipitation, which is especially pronounced for RCP 8.5. For RCP 8.5, months with exceptionally low precipitation increase from 3% to 11% in the 2050s and 21% in 2080s (Figure 9 g-h).

2.6.1.2 Evapotranspiration

The simulated evapotranspiration increases during the wet season and decreases with the onset of the dry season.

The ensemble mean evapotranspiration for future scenarios is lower than that of the historical time slices, with 2.5 and 2.6 mm/month for RCP 2.5 and 2.4 and 8.1 mm/month below historic values for RCP 8.5 for the 2050s and 2080s respectively (Figure 10 c-d). The differences are greater during the dry season than in the wet season, implying that the change in evapotranspiration is driven by increasing temperatures (Figure 10 c-d).

There is a decrease in months with a normal range in evapotranspiration for the 2050s and 2080s, with an increase in months with exceptionally low evapotranspiration, and a slight increase in months with an exceptionally high evapotranspiration during the wet season for RCP 8.5. There is only little change for RCP 2.6 (Figure 10 g-h)

2.6.1.3 Groundwater recharge

The large spread in precipitation amongst different ensemble members is reflected in a large spread in mean monthly groundwater recharge. The seasonality of groundwater recharge lags the seasonality of precipitation by a month, and peaks in August and November.

The ensemble mean for the future scenarios shows an annual decrease in groundwater recharge of 4.5 and 5.2 mm/month and 4.1 and 10.6 mm/month for RCP 2.6 and RCP 8.5 for the 2050s and 2080s respectively (Figure 11 c-d). The largest decrease in groundwater

recharge is simulated during the wet season, specifically for August and November (Figure 10 c-d).

There is a slight increase in months with notably low or exceptionally low recharge for RCP 2.6, due to a decrease in months with a normal or higher than normal distribution of recharge. For RCP 8.5 the decrease in months with a normal range of recharge is from 45% in the historical period to 28% for the 2080s, accompanied with an increase in notably low and exceptionally low months (Figure 10 g-h).

2.6.1.4 Runoff

The large spread in precipitation is also reflected in the spread of mean monthly runoff. The seasonality of runoff reflects the seasonality of precipitation, with the highest values during the wet season. There is a bi-modal distribution of runoff, with peaks in July and October.

The ensemble means of runoff for the mean annual future scenarios decreases by 5.3 and 57 mm/month for RCP 2.6 and 3.9 and 13.3 mm/month for RCP 8.5 (Figure 12 c-d). The highest decrease in runoff occurs during the wet season, in July and October (Figure 12 c-d).

The number of months with a notably low or exceptionally low runoff are increases for RCP 8.5, from 10% during historical periods to 20% for the 2050s and 36% for the 2080s. For RCP 2.6, this decrease is to 19% for both 2050s and 2080s (Figure 12 g-h).

2.6.1.5 Baseflow

The large spread in precipitation is again reflected in the spread in mean monthly baseflow values. As with recharge, the seasonality of baseflow lags the seasonality of precipitation by a month, and peaks in August and November.

The annual ensemble means of baseflow for the future scenarios decrease by 9.7 and 12.2 mm/month for RCP 2.6 and 8.4 and 22.9 mm/month for RCP 8.5 (Figure 13 c-d). The decrease is greatest during the wet season for both the time periods. The baseflow contribution is lower for the 2080s period than the 2050s (Figure 13 c-d).

Under RCP 2.6 there is a decrease in months with a normal or higher than normal baseflow (75% to 61% for both 2050s and 2080s), and an increase in months with below normal or lower baseflow (25% to 39% for both 2050s and 2080s). For RCP 8.5 this pattern is more extreme, with a further reduction in months with normal or higher than normal baseflow especially for periods more distant in the future (75% to 61% in 2050s and 43% in 2080s) and an increase in months with below normal or lower baseflow (25 to 40% in 2050s and 57% in 2080s) (Figure 13 g-h).

2.6.2 Pampanga Province

2.6.2.1 Precipitation

The monthly mean precipitation for Pampanga reflects a less distinct bimodal distribution than Panay. The highest values occur in July with a secondary peak in October. The spread in precipitation across different ensemble members is large, with the greatest divergence in July and August. For example, the simulated mean monthly precipitation for July for RCP 2.6 ranges from 653.1 mm/month to 2249 mm/month.

The annual ensemble mean for the 2050s has little change from the historical period (+ 0.1 to -2.8 mm/month), whereas for the 2080s, the mean annual precipitation decreases by 6.7 and 14.0 mm/month for RCP 2.6 and 8.5 (Figure 14 c-d). For both scenarios, there is little change during the dry season, whereas for the wet season, the mean monthly precipitation decreases under RCP 8.5. For both RCPs, there is a decrease in precipitation during July and October and a slight increase in August and September (Figure 14 c-d).

In Panay, there is a consistent decrease in mean annual precipitation in the future, whereas for Pampanga the mean annual decrease in precipitation can only be seen for the 2080s.

There is a decrease in months with a normal amount of precipitation, with values below normal or lower as well as values above normal or higher increasing. Especially for RCP 8.5, there is an increase in months with exceptionally high rainfall (Figure 14 g-h).

2.6.2.2 Evapotranspiration

There is no annual change in evapotranspiration considering the ensemble means for the 2050s and 2080s compared to the historical simulation. For both RCPs there is a slight increase in evapotranspiration during the wet season and a decrease during the dry season (Figure 15 a - d).

Following the precipitation, the number of months with a normal amount of evapotranspiration decreases and months with above normal or below normal evapotranspiration increases. For RCP 8.5, exceptionally high evapotranspiration is most pronounced during the wet season, with 27% in the 2050s or 34% in the 2080s classified as months with exceptionally high evapotranspiration (Figure 15 g-h).

2.6.2.3 Groundwater recharge

The large spread in precipitation across ensemble members is reflected in a large spread in mean monthly groundwater recharge. The seasonality of groundwater recharge lags the seasonality of precipitation by a month, and peaks in August. There is a clear unimodal distribution of recharge, with the secondary peak of precipitation being lost in the groundwater recharge signal (Figure 16 a-b).

There is a decrease in mean annual groundwater recharge for both RCPs and time periods. For RCP 2.6 the mean annual decrease in recharge is 1.4 and 2.6 mm/month and for RCP 8.5 2.8 and 8.2 mm/month for the 2050s and 2080s retrospectively. The decrease is most pronounced during the wet season (Figure 16 c-d).

For RCP 2.6, there is a slight increase in the number of months with below normal or lower groundwater recharge, increasing from 25% to 31% and 32% for the 2050s and 2080s. This is more pronounced for RCP 8.5, increasing from 25% to 35% and 46% for the 2050s and 2080s. Therefore, there will be more months with less than normal groundwater recharge (Figure 16 g-h).

2.6.2.4 Runoff

The large spread in precipitation across ensemble members is reflected in the spread of mean monthly runoff values. The seasonality of runoff reflects the seasonality of precipitation, with the highest values during the wet season. Peak runoff is in July (Figure 17 a-b). The change of mean runoff is not clear for the 2050s, as RCP 2.6 shows an increase in 1.6 mm/month and RCP 8.5 a decrease in 0.4 mm/month. In contrast, for 2080s, runoff is expected to decrease by 4.5 and 5.9 mm/month RCP 2.6 and 8.2. The decrease in runoff occurs during the wet season, reflecting a decrease in precipitation (Figure 17 c-d).

The number of months with exceptionally high and low runoff are expected to increase, resulting in more extreme high and low river flow events (Figure 17 g-h).

2.6.2.5 Baseflow

The peak in baseflow lags the peak in precipitation by 2 months. For RCP 2.6 there is a decrease in mean annual baseflow of 1.1 and 2.1 mm/month for 2050s and 2080s, and for RCP 8.5, the decrease is 2.4 and 6.9 mm/month (Figure 18 a-d).

The number of months with a normal baseflow values decreases under both RCPs, resulting in an increased number of months with below normal flow and fewer months above normal

flow. For RCP 2.6, the months with exceptionally low baseflow are increase from 2% to 7% and 12% for the 2050s and 2080s, whereas for RCP 8.5, to 10% and 18% for the 2050s and 2080s (Figure 18 g-h).

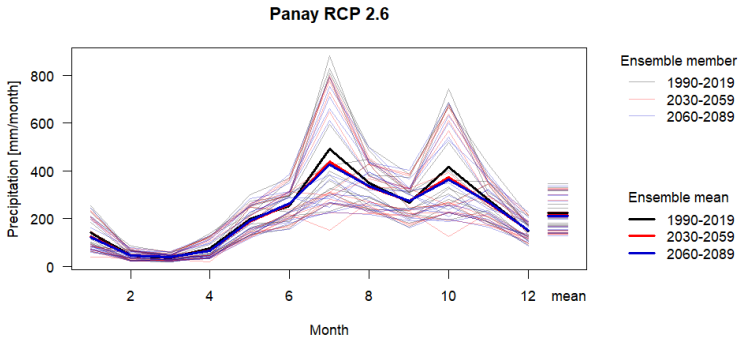
Panay RCP 2.6
Precipitation [mm/month]
0
200
400
600
800
2
4
6
8
10
12
mean
Month
Ensemble member
1990-2019
2030-2059
2060-2089
Ensemble mean
1990-2019
2030-2059
2060-2089

a)

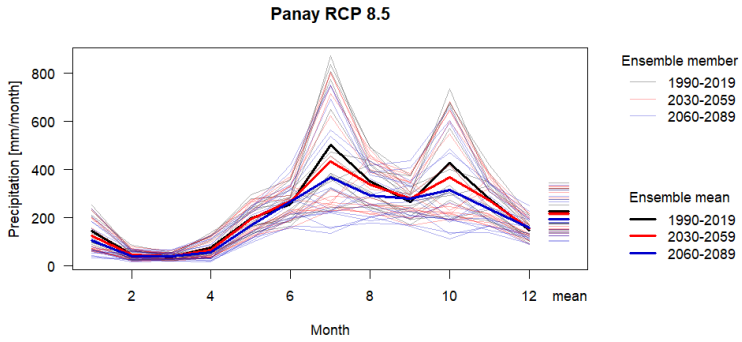
Panay RCP 8.5
Precipitation [mm/month]
0
200
400
600
800
2
4
6
8
10
12
mean
Month
Ensemble member
1990-2019
2030-2059
2060-2089
Ensemble mean
1990-2019
2030-2059
2060-2089

b)

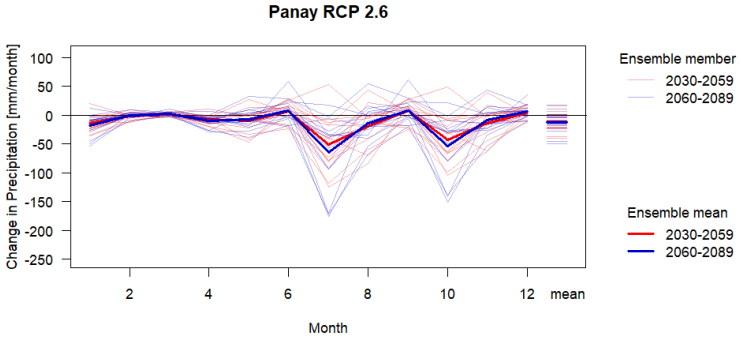
Panay RCP 2.6
Change in Precipitation [mm/month]
-250
-200
-150
-100
-50
0
50
100
2
4
6
8
10
12
mean
Month
Ensemble member
2030-2059
2060-2089
Ensemble mean
2030-2059
2060-2089

c)

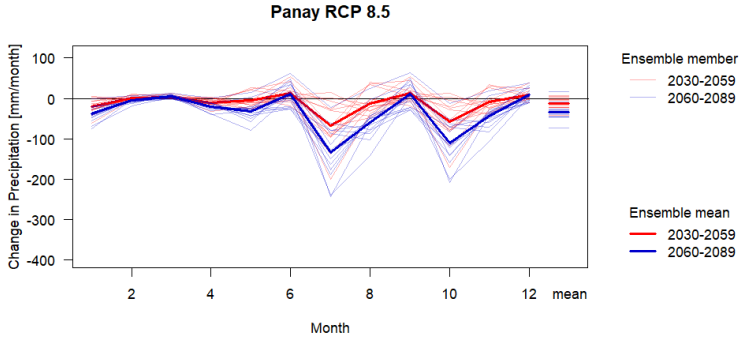
Panay RCP 8.5
Change in Precipitation [mm/month]
-400
-300
-200
-100
0
100
2
4
6
8
10
12
mean
Month
Ensemble member
2030-2059
2060-2089
Ensemble mean
2030-2059
2060-2089

d)

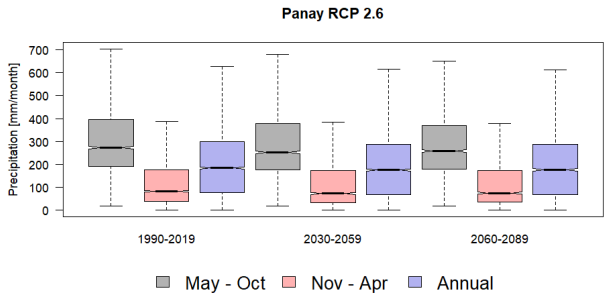
Panay RCP 2.6
Precipitation [mm/month]
0
100
200
300
400
500
600
700
1990-2019
2030-2059
2060-2089
May - Oct
Nov - Apr
Annual

e)

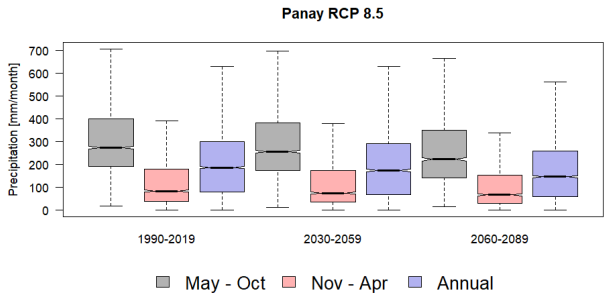
Panay RCP 8.5
Precipitation [mm/month]
0
100
200
300
400
500
600
700
1990-2019
2030-2059
2060-2089
May - Oct
Nov - Apr
Annual

f)

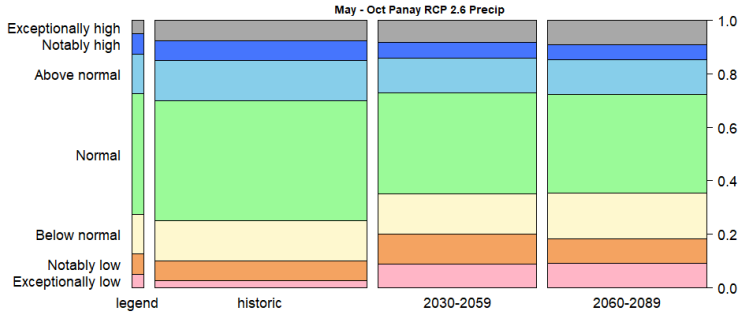

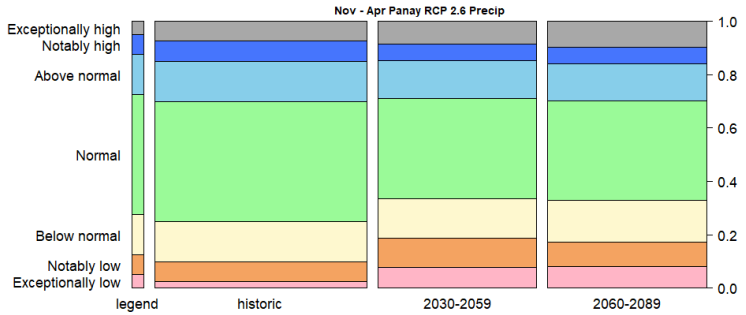

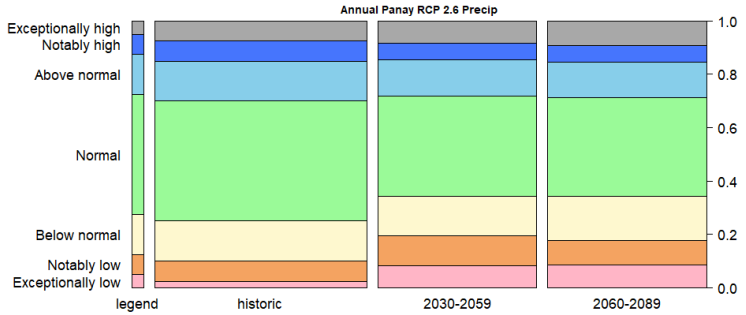

g)

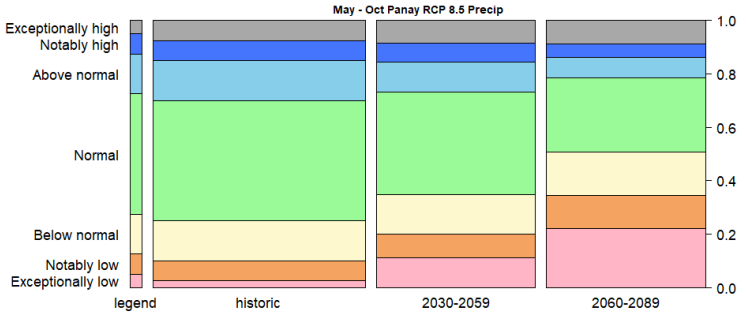

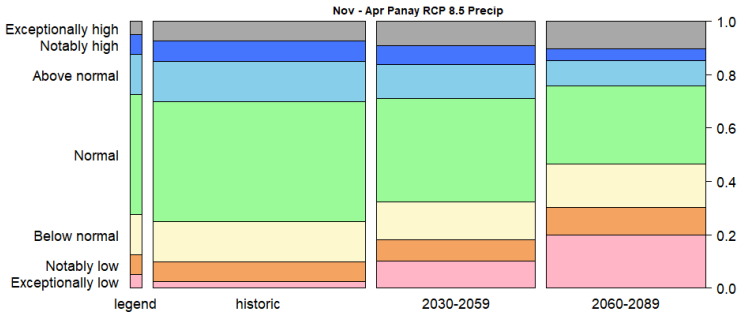

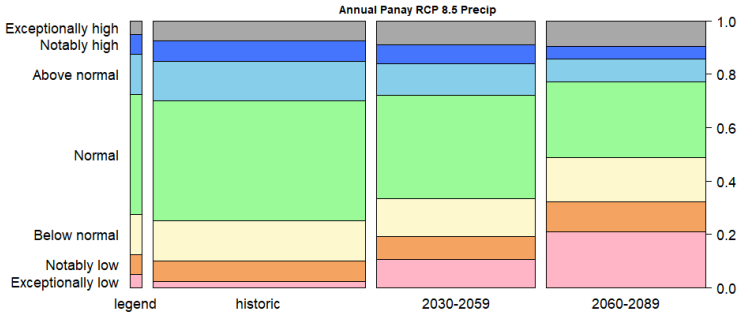

h)

Figure 9. Mean monthly precipitation (a-b), change in mean monthly precipitation (c-d), box plot (e-f) of mean seasonal values, and percentile range compared to historical monthly values for wet season (May – Oct), dry season (Nov-Apr) and annual values considering the historical (1990-2019), 2030-2059 and 2060-2089 time slices for Panay using RCP 2.6 and 8.5.

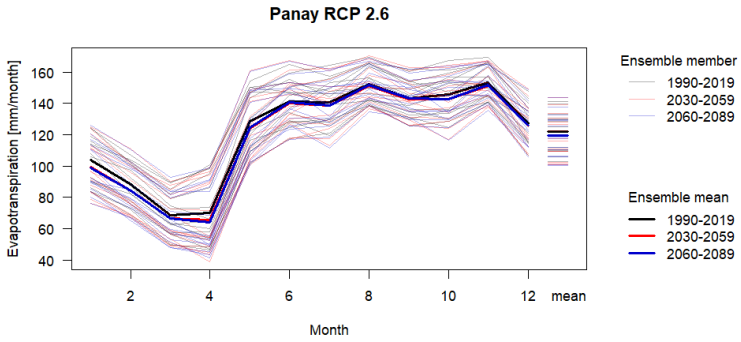
Panay RCP 2.6
Evapotranspiration [mm/month]
160
140
120
100
80
60
40
2
4
6
8
10
12
mean
Month
Ensemble member
1990-2019
2030-2059
2060-2089
Ensemble mean
1990-2019
2030-2059
2060-2089

a)

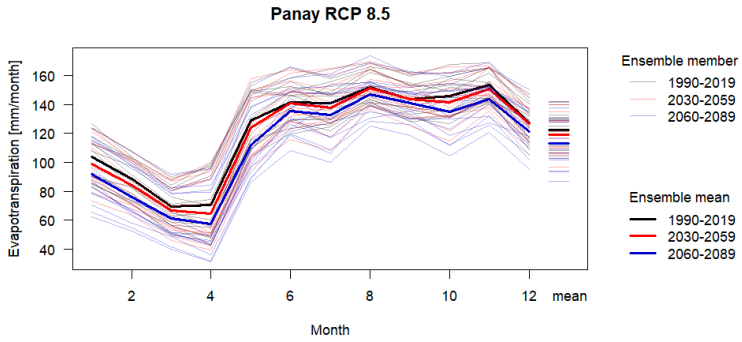
Panay RCP 8.5
Evapotranspiration [mm/month]
160
140
120
100
80
60
40
2
4
6
8
10
12
mean
Month
Ensemble member
1990-2019
2030-2059
2060-2089
Ensemble mean
1990-2019
2030-2059
2060-2089

b)

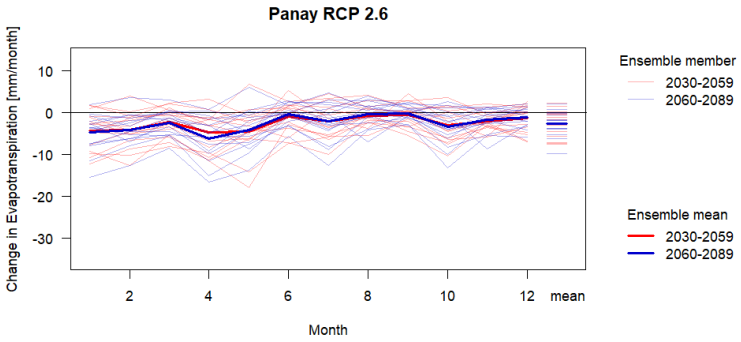
Panay RCP 2.6
Change in Evapotranspiration [mm/month]
10
0
-10
-20
-30
2
4
6
8
10
12
mean
Month
Ensemble member
2030-2059
2060-2089
Ensemble mean
2030-2059
2060-2089

c)

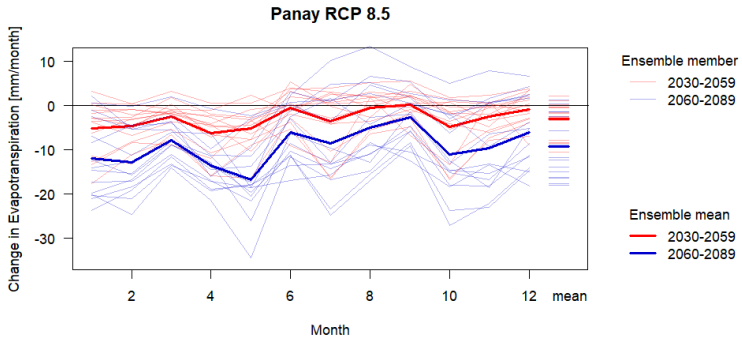
Panay RCP 8.5
Change in Evapotranspiration [mm/month]
10
0
-10
-20
-30
2
4
6
8
10
12
mean
Month
Ensemble member
2030-2059
2060-2089
Ensemble mean
2030-2059
2060-2089

d)

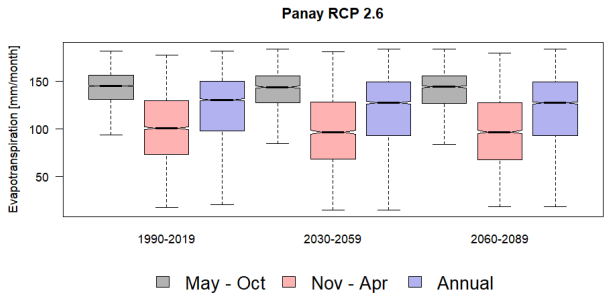
Panay RCP 2.6
Evapotranspiration [mm/month]
150
100
50
1990-2019
2030-2059
2060-2089
May - Oct
Nov - Apr
Annual

e)

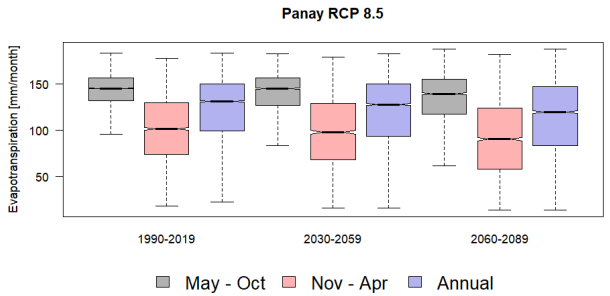
Panay RCP 8.5
Evapotranspiration [mm/month]
150
100
50
1990-2019
2030-2059
2060-2089
May - Oct
Nov - Apr
Annual

f)

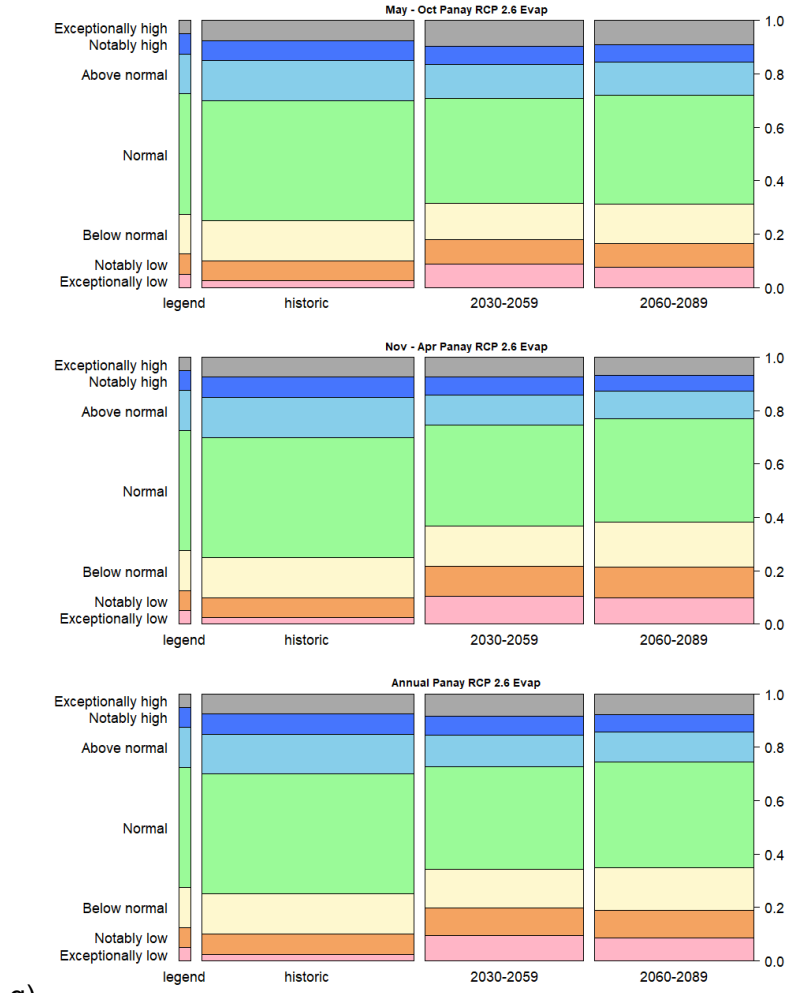

g)

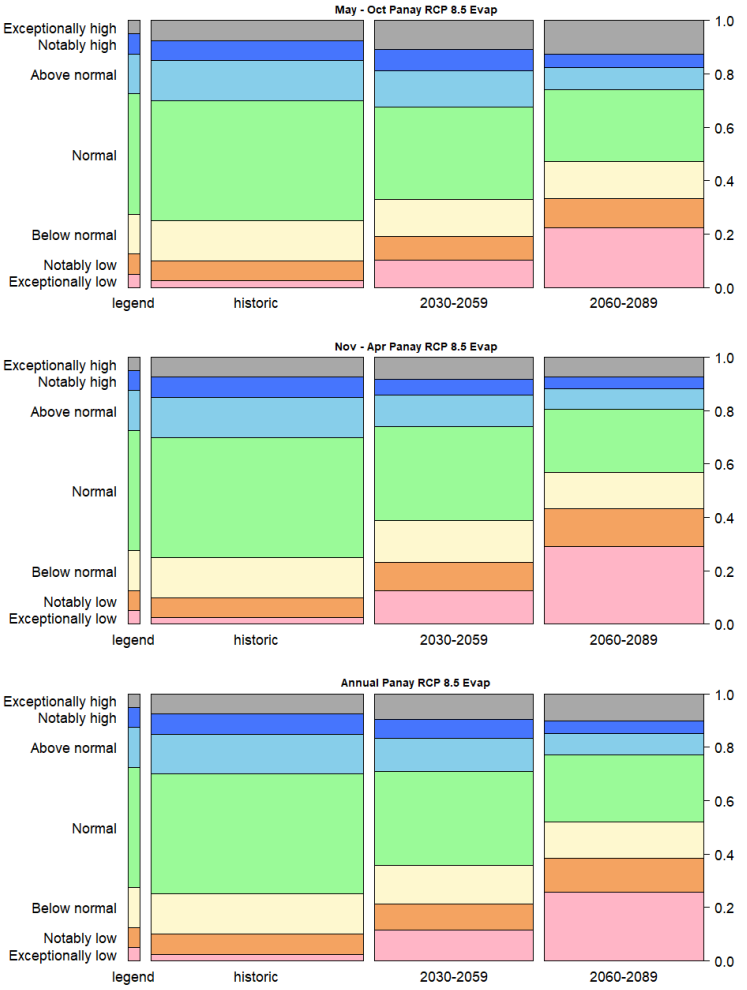

h)

Figure 10. Mean monthly evapotranspiration (a-b), change in mean monthly precipitation (c-d), box plot (e-f) of mean seasonal values, and percentile range compared to historical monthly values for wet season (May – Oct), dry season (Nov-Apr) and annual values considering the historical (1990-2019), 2030-2059 and 2060-2089 time slices for Panay using RCP 2.6 and 8.5.

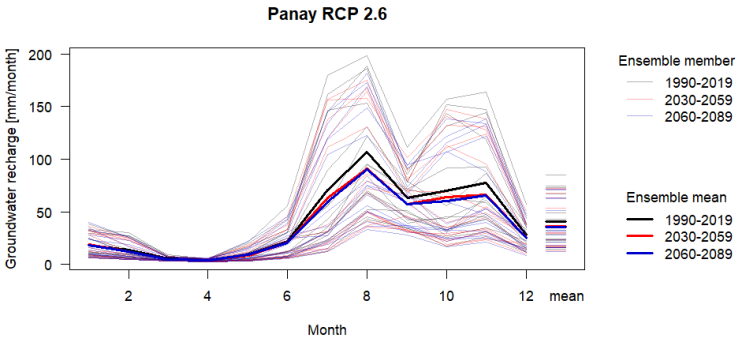
Panay RCP 2.6
Groundwater recharge [mm/month]
Month
Ensemble member
1990-2019
2030-2059
2060-2089
Ensemble mean
1990-2019
2030-2059
2060-2089

a)

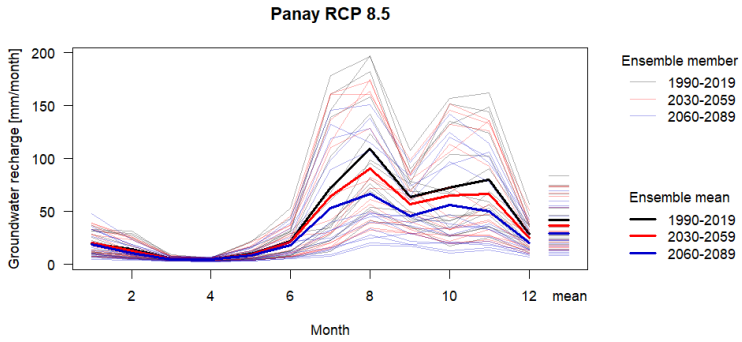
Panay RCP 8.5
Groundwater recharge [mm/month]
Month
Ensemble member
1990-2019
2030-2059
2060-2089
Ensemble mean
1990-2019
2030-2059
2060-2089

b)

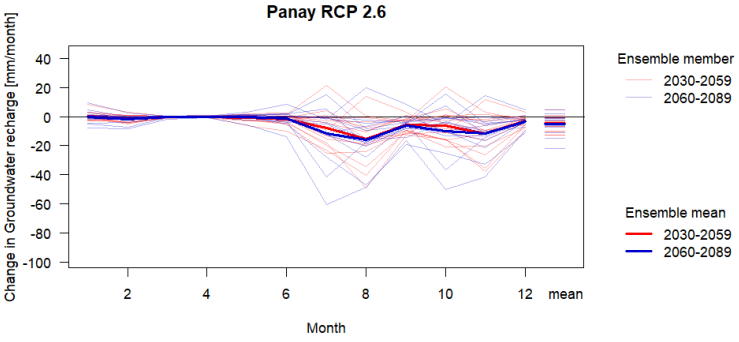
Panay RCP 2.6
Change in Groundwater recharge [mm/month]
Month
Ensemble member
2030-2059
2060-2089
Ensemble mean
2030-2059
2060-2089

c)

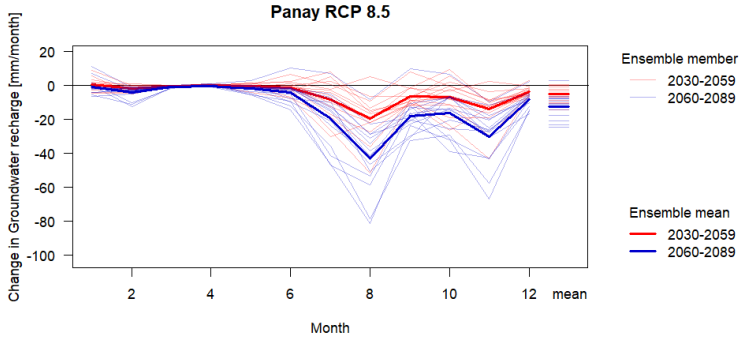
Panay RCP 8.5
Change in Groundwater recharge [mm/month]
Month
Ensemble member
2030-2059
2060-2089
Ensemble mean
2030-2059
2060-2089

d)

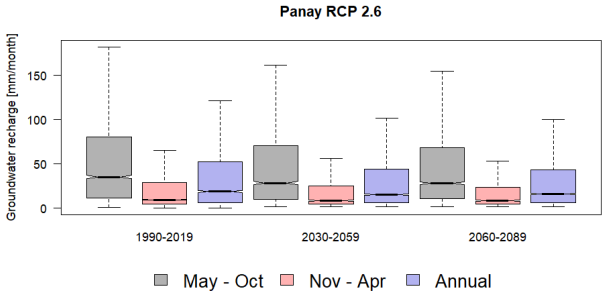
Panay RCP 2.6
Groundwater recharge [mm/month]
1990-2019
2030-2059
2060-2089
May - Oct
Nov - Apr
Annual

e)

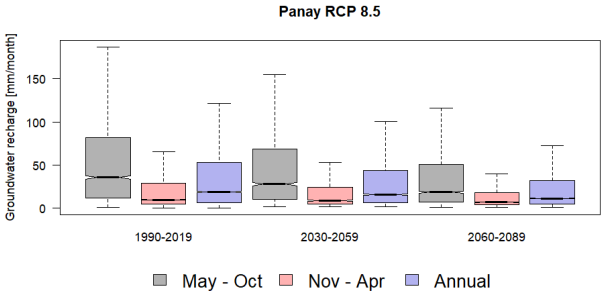
Panay RCP 8.5
Groundwater recharge [mm/month]
1990-2019
2030-2059
2060-2089
May - Oct
Nov - Apr
Annual

f)

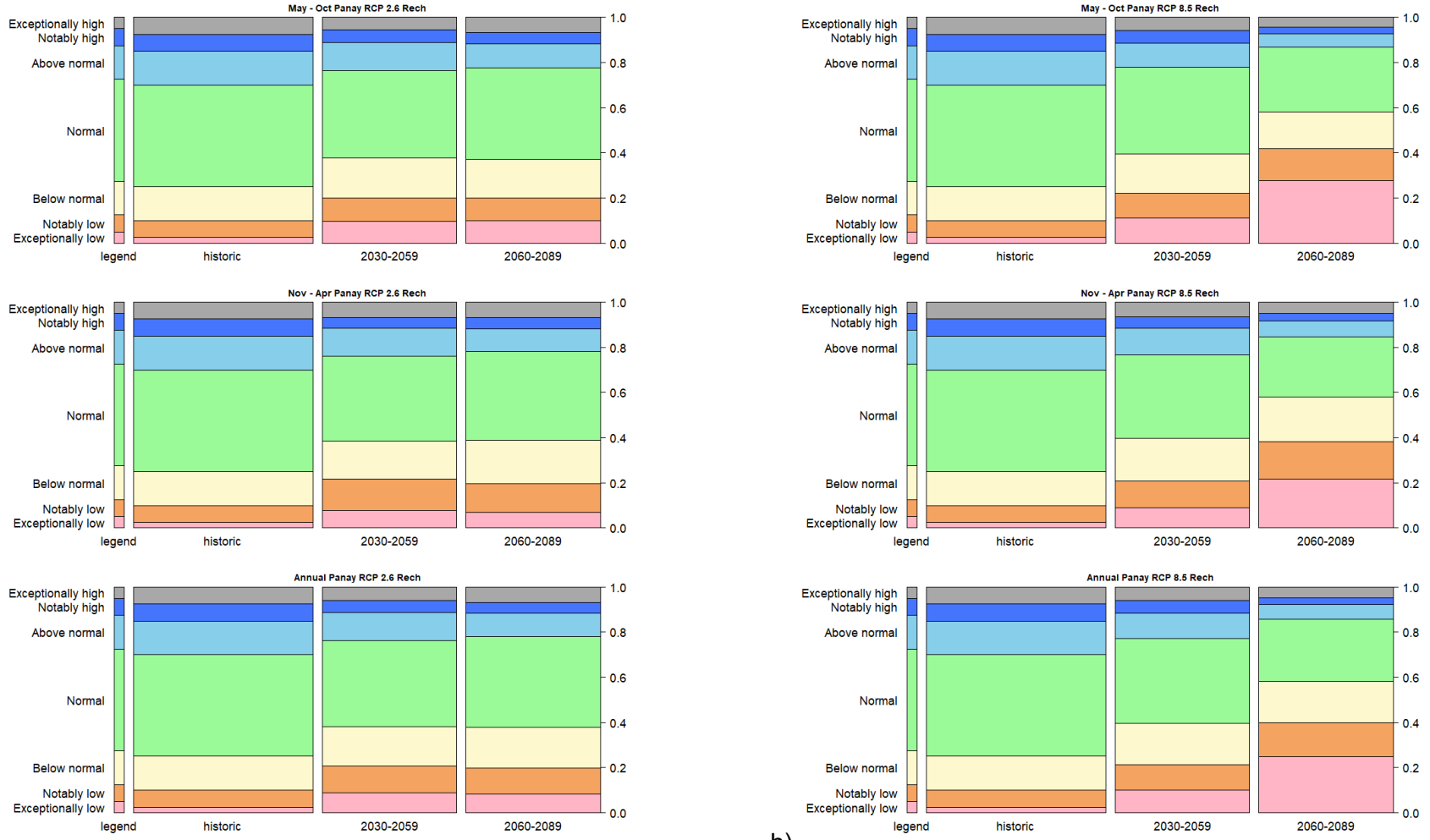

g) h)

Figure 11. Mean monthly groundwater recharge (a-b), change in mean monthly precipitation (c-d), box plot (e-f) of mean seasonal values, and percentile range compared to historical monthly values for wet season (May – Oct), dry season (Nov-Apr) and annual values considering the historical (1990-2019), 2030-2059 and 2060-2089 time slices for Panay using RCP 2.6 and 8.5.

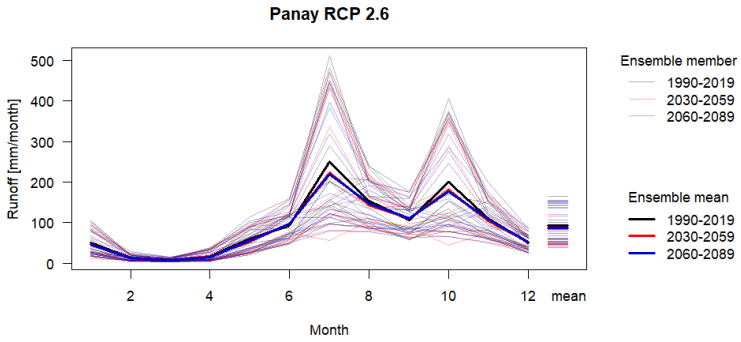
Panay RCP 2.6
Runoff [mm/month]
Month
mean
Ensemble member
1990-2019
2030-2059
2060-2089
Ensemble mean
1990-2019
2030-2059
2060-2089

a)

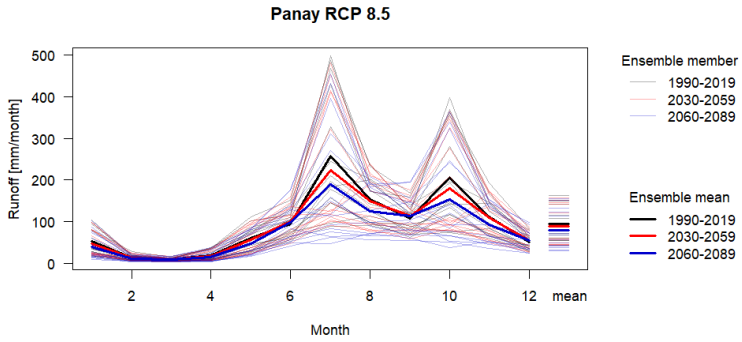
Panay RCP 8.5
Runoff [mm/month]
Month
mean
Ensemble member
1990-2019
2030-2059
2060-2089
Ensemble mean
1990-2019
2030-2059
2060-2089

b)

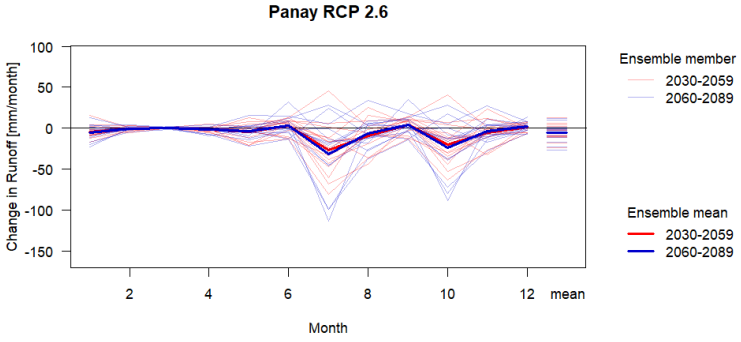
Panay RCP 2.6
Change in Runoff [mm/month]
Month
mean
Ensemble member
2030-2059
2060-2089
Ensemble mean
2030-2059
2060-2089

c)

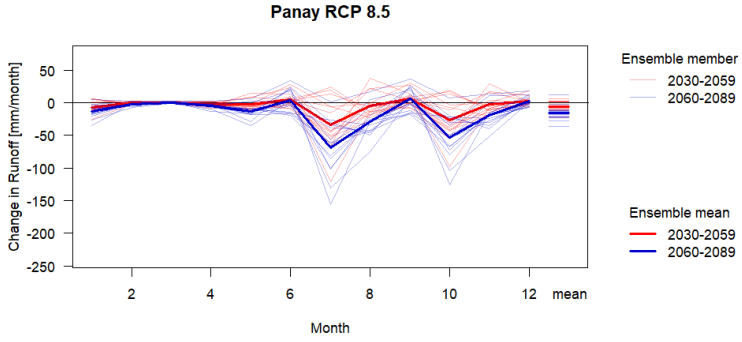
Panay RCP 8.5
Change in Runoff [mm/month]
Month
mean
Ensemble member
2030-2059
2060-2089
Ensemble mean
2030-2059
2060-2089

d)

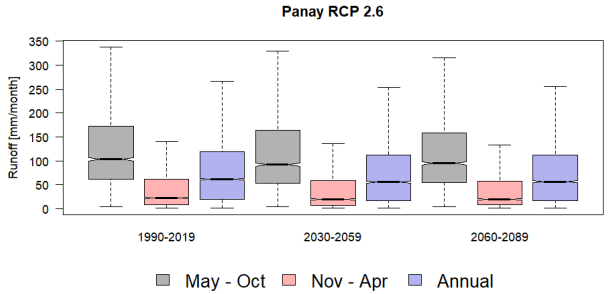
Panay RCP 2.6
Runoff [mm/month]
1990-2019
2030-2059
2060-2089
May - Oct
Nov - Apr
Annual

e)

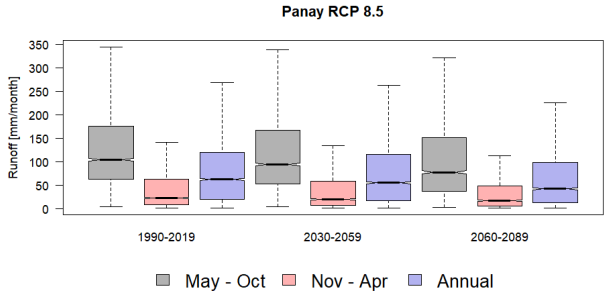
Panay RCP 8.5
Runoff [mm/month]
1990-2019
2030-2059
2060-2089
May - Oct
Nov - Apr
Annual

f)

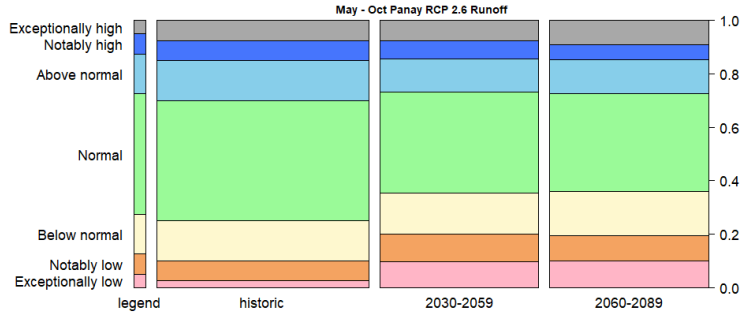

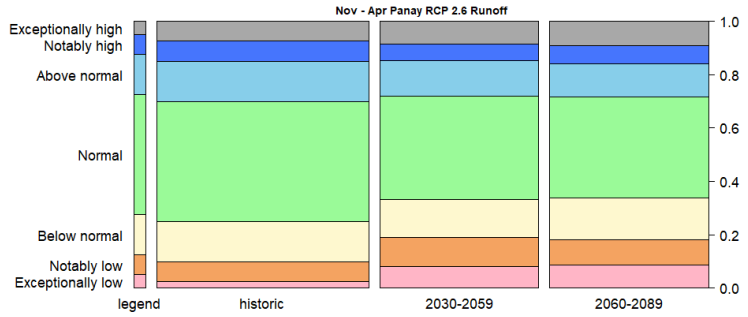

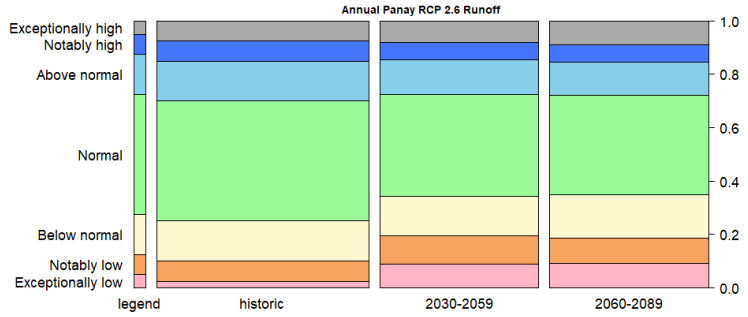

g)

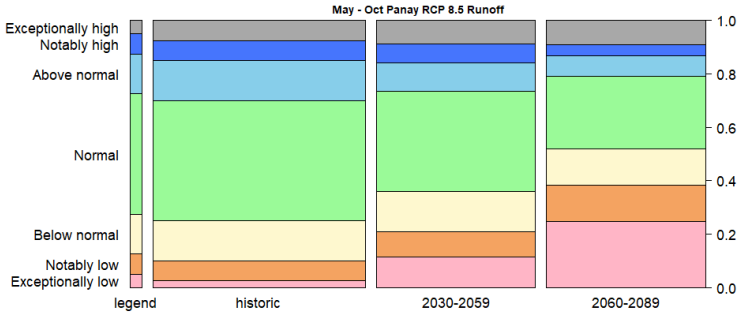

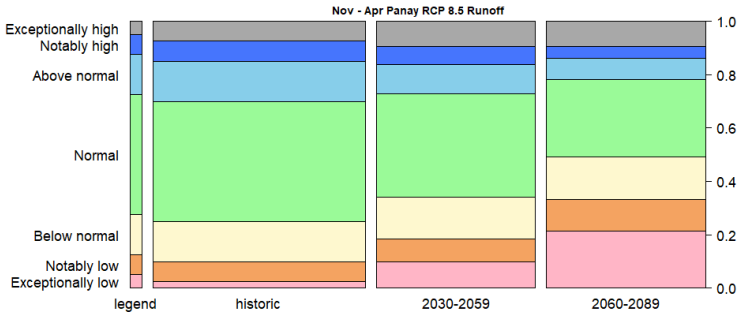

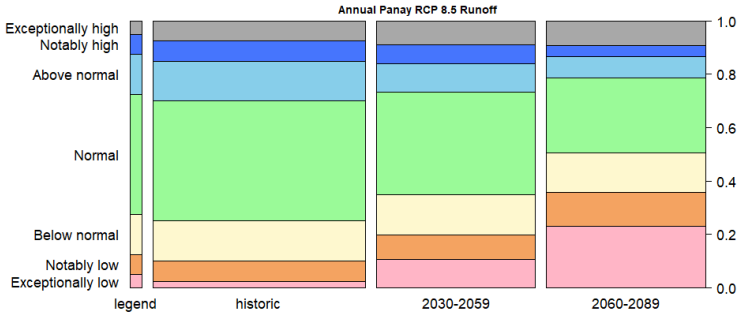

h)

Figure 12. Mean monthly runoff (a-b), change in mean monthly precipitation (c-d), box plot (e-f) of mean seasonal values, and percentile range compared to historical monthly values for wet season (May – Oct), dry season (Nov-Apr) and annual values considering the historical (1990-2019), 2030-2059 and 2060-2089 time slices for Panay using RCP 2.6 and 8.5.

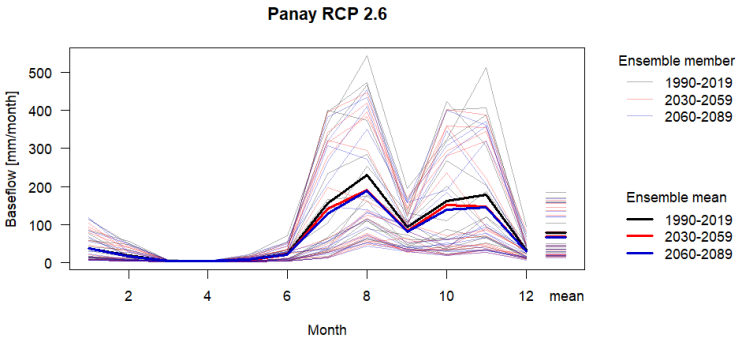
Panay RCP 2.6
Baseflow [mm/month]
0
100
200
300
400
500
2
4
6
8
10
12
mean
Month
Ensemble member
1990-2019
2030-2059
2060-2089
Ensemble mean
1990-2019
2030-2059
2060-2089

a)

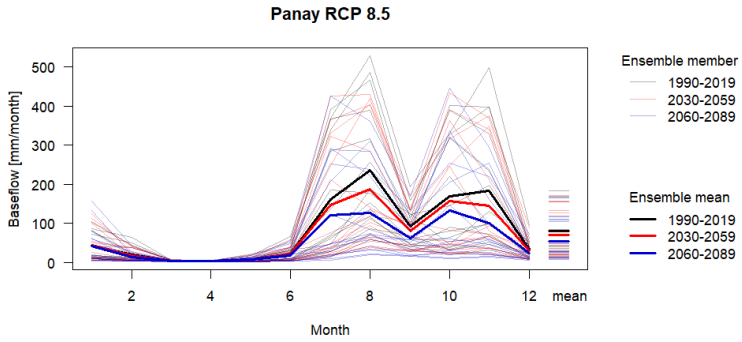
Panay RCP 8.5
Baseflow [mm/month]
0
100
200
300
400
500
2
4
6
8
10
12
mean
Month
Ensemble member
1990-2019
2030-2059
2060-2089
Ensemble mean
1990-2019
2030-2059
2060-2089

b)

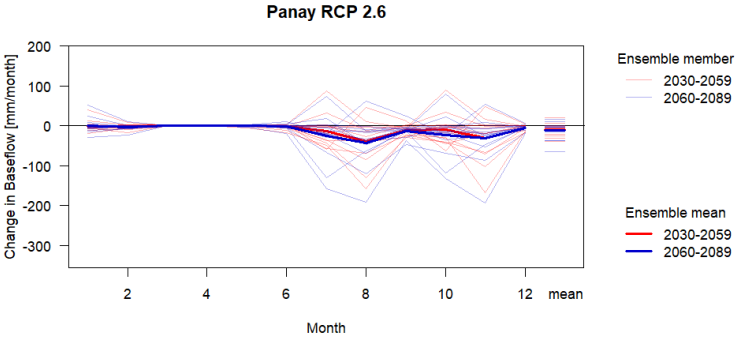
Panay RCP 2.6
Change in Baseflow [mm/month]
-300
-200
-100
0
100
200
2
4
6
8
10
12
mean
Month
Ensemble member
2030-2059
2060-2089
Ensemble mean
2030-2059
2060-2089

c)

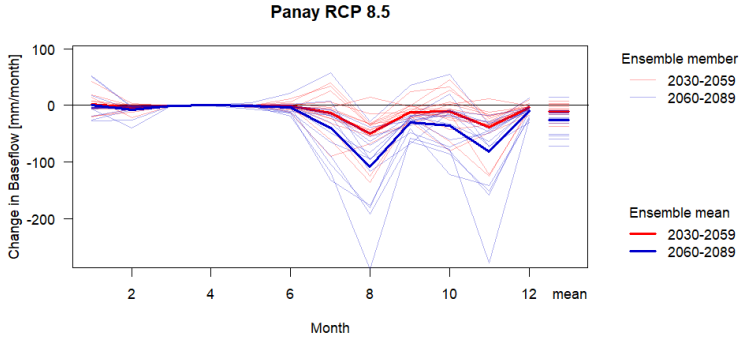
Panay RCP 8.5
Change in Baseflow [mm/month]
-200
-100
0
100
2
4
6
8
10
12
mean
Month
Ensemble member
2030-2059
2060-2089
Ensemble mean
2030-2059
2060-2089

d)

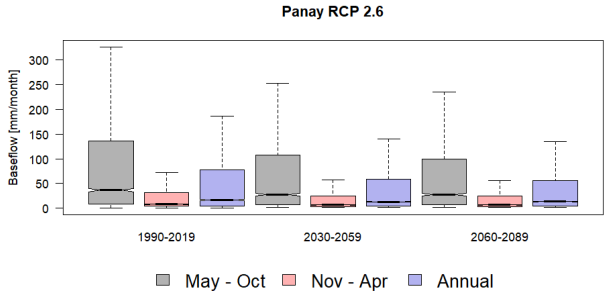
Panay RCP 2.6
Baseflow [mm/month]
0
50
100
150
200
250
300
1990-2019
2030-2059
2060-2089
May - Oct
Nov - Apr
Annual

e)

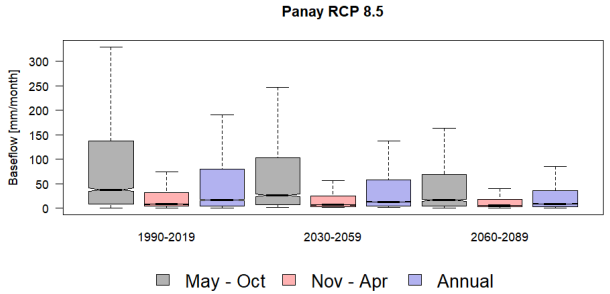
Panay RCP 8.5
Baseflow [mm/month]
0
50
100
150
200
250
300
1990-2019
2030-2059
2060-2089
May - Oct
Nov - Apr
Annual

f)

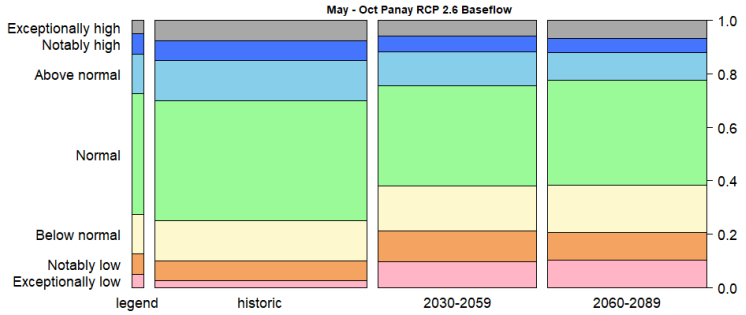

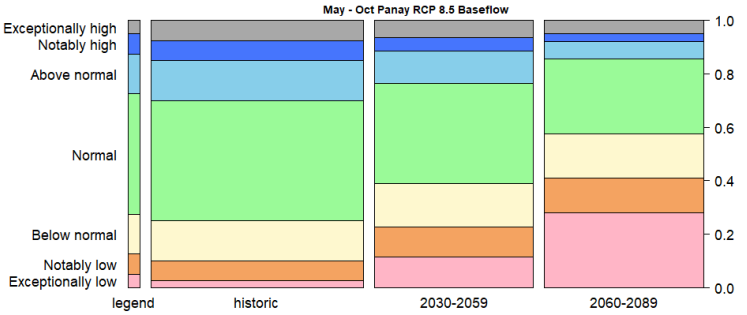

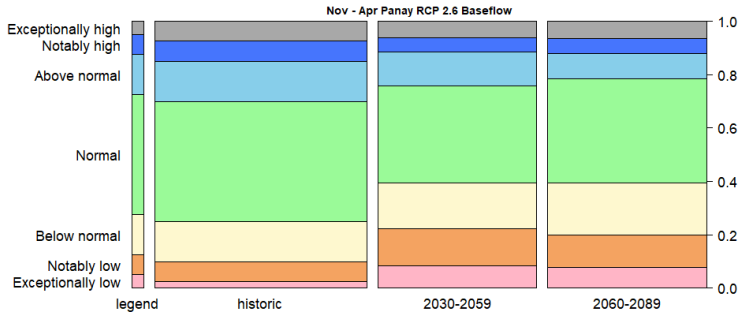

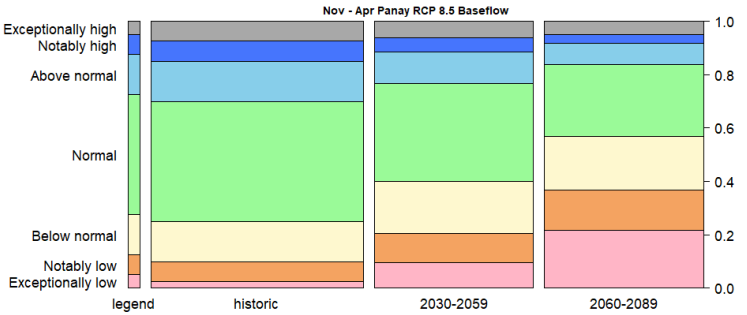

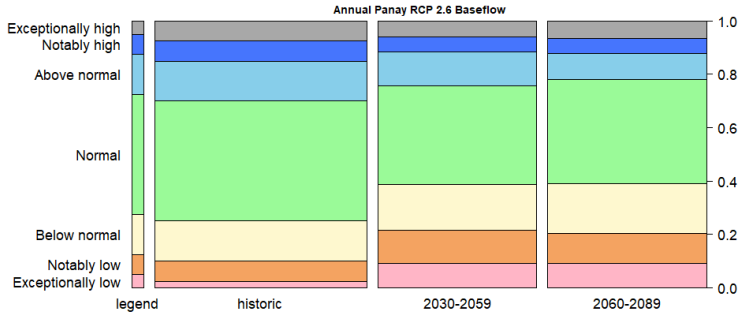

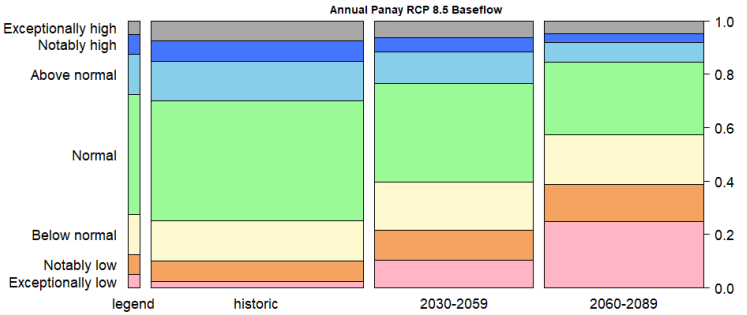

g) h)

Figure 13. Mean monthly baseflow (a-b), change in mean monthly precipitation (c-d), box plot (e-f) of mean seasonal values, and percentile range compared to historical monthly values for wet season (May – Oct), dry season (Nov-Apr) and annual values considering the historical (1990-2019), 2030-2059 and 2060-2089 time slices for Panay using RCP 2.6 and 8.5.

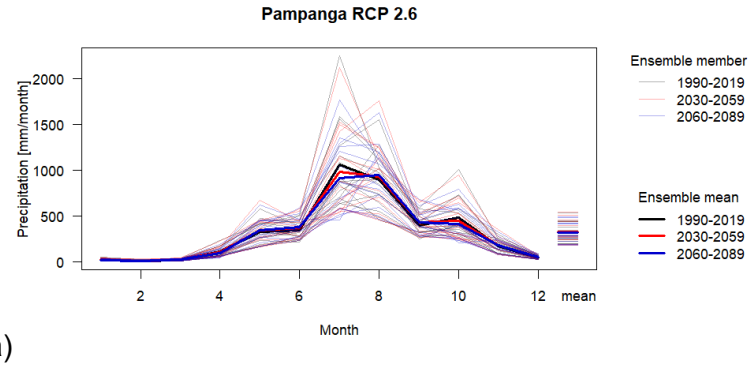
Pampanga RCP 2.6
Precipitation [mm/month]
0
500
1000
1500
2000
2
4
6
8
10
12
mean
Month
Ensemble member
1990-2019
2030-2059
2060-2089
Ensemble mean
1990-2019
2030-2059
2060-2089

a)

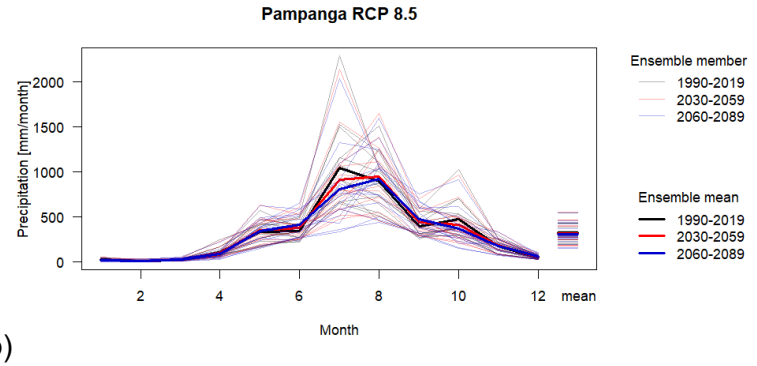
Pampanga RCP 8.5
Precipitation [mm/month]
0
500
1000
1500
2000
2
4
6
8
10
12
mean
Month
Ensemble member
1990-2019
2030-2059
2060-2089
Ensemble mean
1990-2019
2030-2059
2060-2089

b)

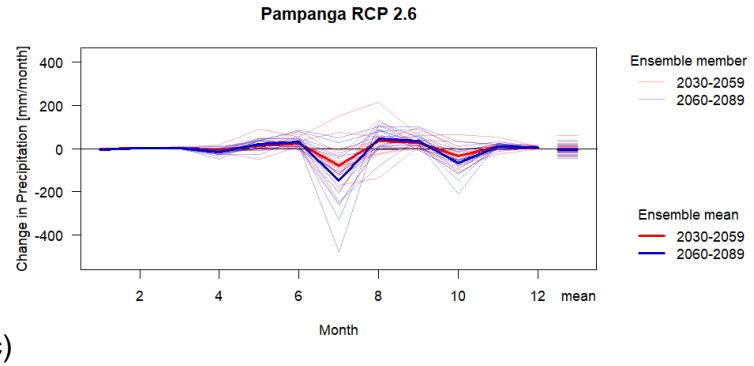
Pampanga RCP 2.6
Change in Precipitation [mm/month]
-400
-200
0
200
400
2
4
6
8
10
12
mean
Month
Ensemble member
2030-2059
2060-2089
Ensemble mean
2030-2059
2060-2089

c)

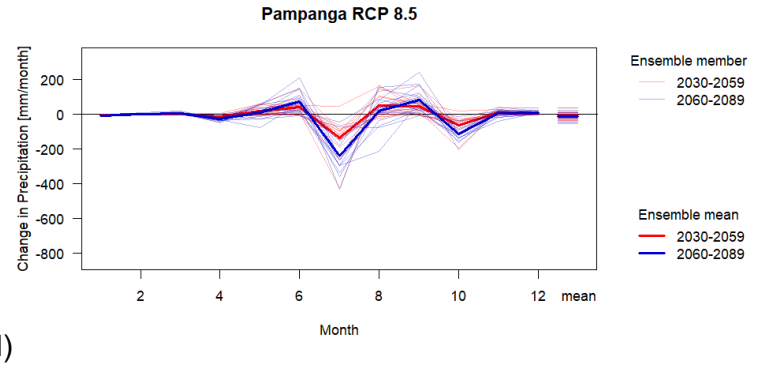
Pampanga RCP 8.5
Change in Precipitation [mm/month]
-800
-600
-400
-200
0
200
2
4
6
8
10
12
mean
Month
Ensemble member
2030-2059
2060-2089
Ensemble mean
2030-2059
2060-2089

d)

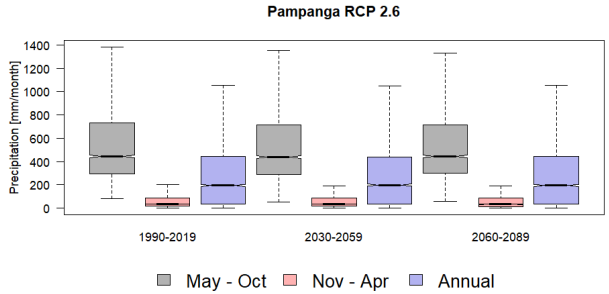
Pampanga RCP 2.6
Precipitation [mm/month]
0
200
400
600
800
1000
1200
1400
1990-2019
2030-2059
2060-2089
May - Oct
Nov - Apr
Annual

e)

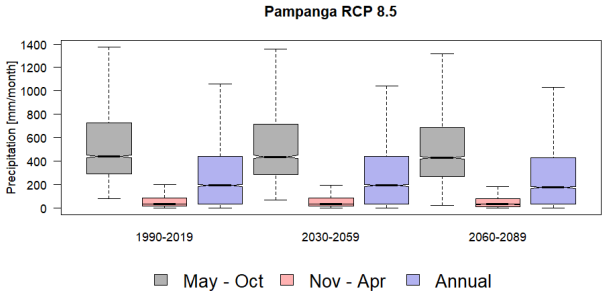
Pampanga RCP 8.5
Precipitation [mm/month]
0
200
400
600
800
1000
1200
1400
1990-2019
2030-2059
2060-2089
May - Oct
Nov - Apr
Annual

f)

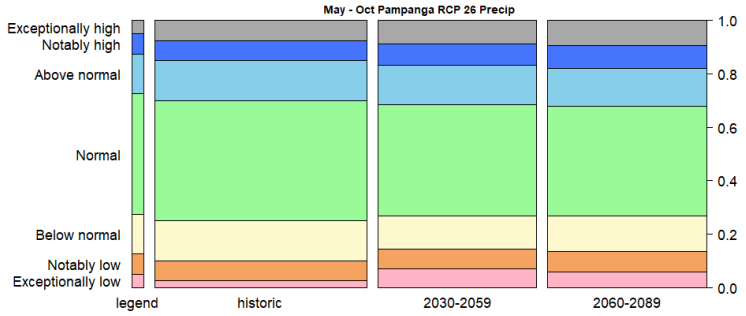

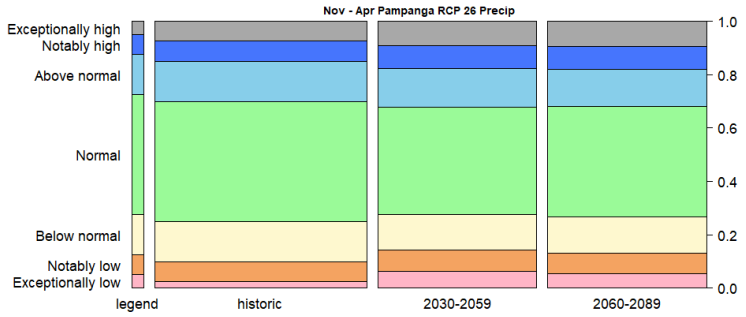

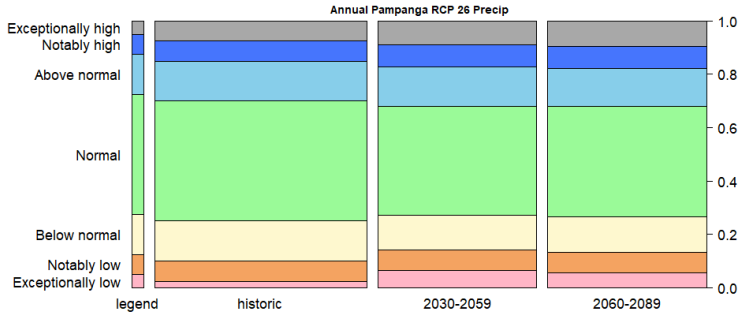

g)

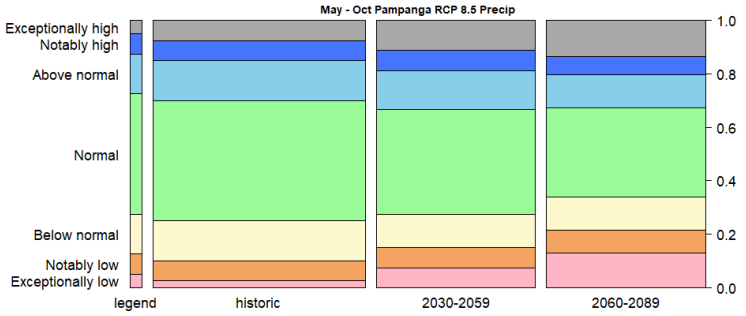

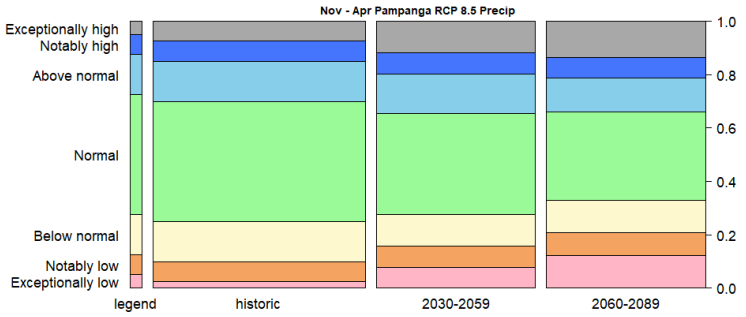

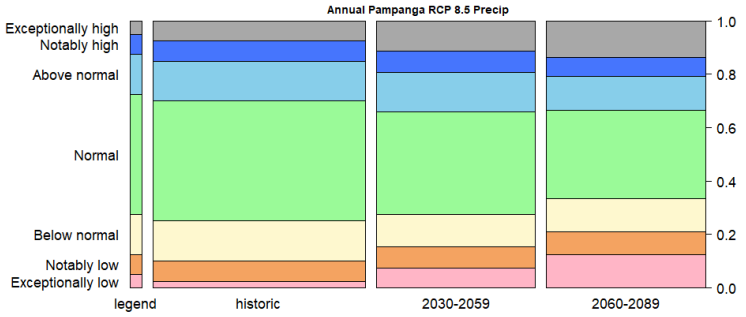

h)

Figure 14. Mean monthly precipitation (a-b), change in mean monthly precipitation (c-d), box plot (e-f) of mean seasonal values, and percentile range compared to historical monthly values for wet season (May – Oct), dry season (Nov-Apr) and annual values considering the historical (1990-2019), 2030-2059 and 2060-2089 time slices for Pampanga using RCP 2.6 and 8.5.

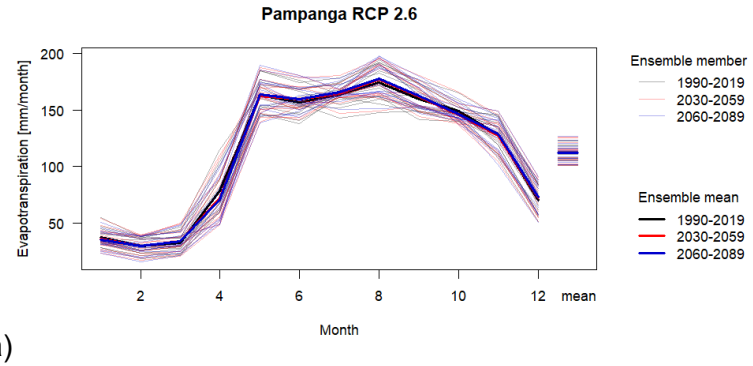
Pampanga RCP 2.6
Evapotranspiration [mm/month]
200
150
100
50
2
4
6
8
10
12
mean
Month
Ensemble member
1990-2019
2030-2059
2060-2089
Ensemble mean
1990-2019
2030-2059
2060-2089

a)

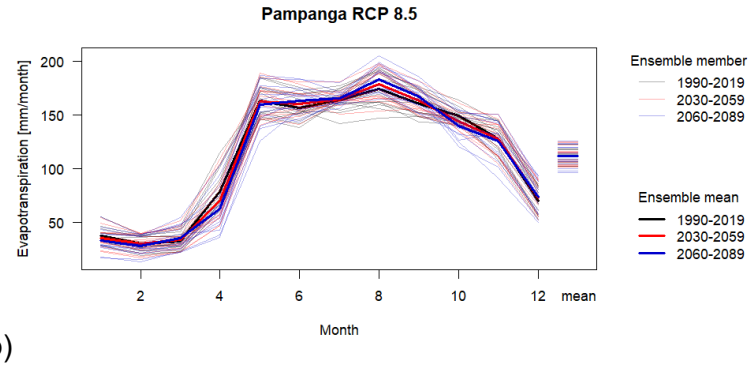
Pampanga RCP 8.5
Evapotranspiration [mm/month]
200
150
100
50
2
4
6
8
10
12
mean
Month
Ensemble member
1990-2019
2030-2059
2060-2089
Ensemble mean
1990-2019
2030-2059
2060-2089

b)

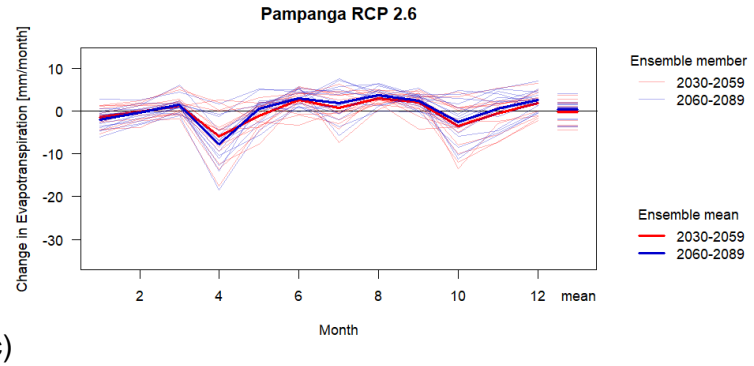
Pampanga RCP 2.6
Change in Evapotranspiration [mm/month]
10
0
-10
-20
-30
2
4
6
8
10
12
mean
Month
Ensemble member
2030-2059
2060-2089
Ensemble mean
2030-2059
2060-2089

c)

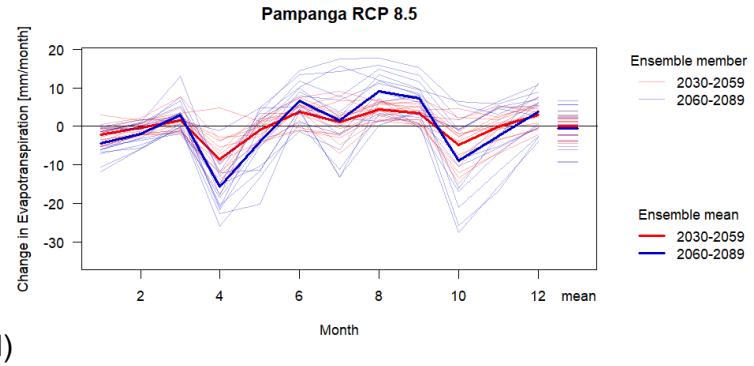
Pampanga RCP 8.5
Change in Evapotranspiration [mm/month]
20
10
0
-10
-20
-30
2
4
6
8
10
12
mean
Month
Ensemble member
2030-2059
2060-2089
Ensemble mean
2030-2059
2060-2089

d)

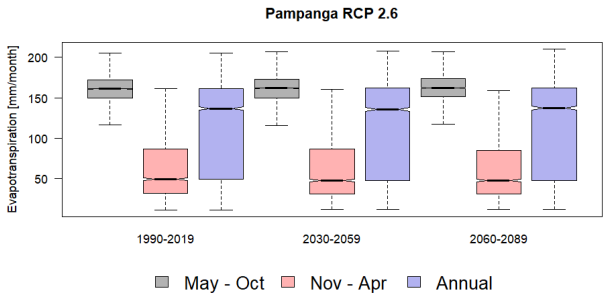
Pampanga RCP 2.6
Evapotranspiration [mm/month]
200
150
100
50
1990-2019
2030-2059
2060-2089
May - Oct
Nov - Apr
Annual

e)

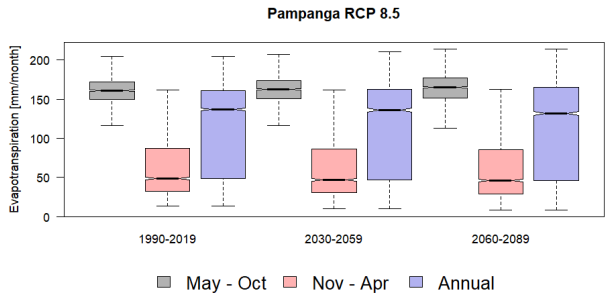
Pampanga RCP 8.5
Evapotranspiration [mm/month]
200
150
100
50
0
1990-2019
2030-2059
2060-2089
May - Oct
Nov - Apr
Annual

f)

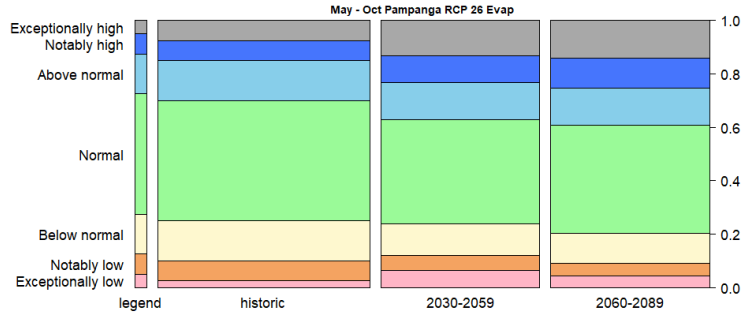

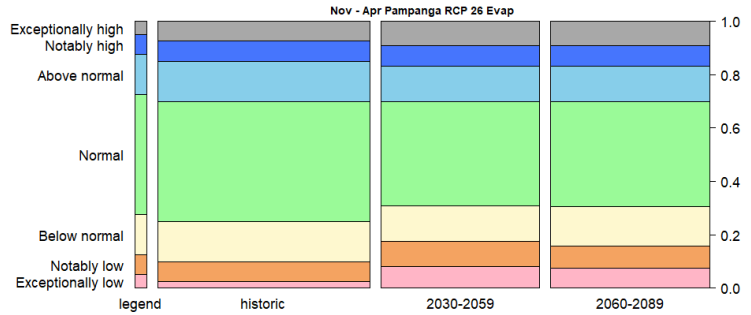

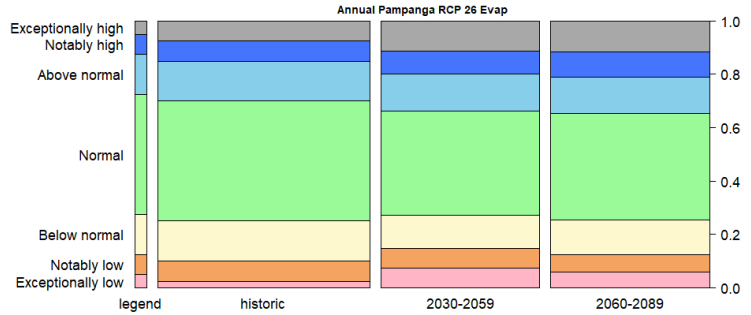

g)

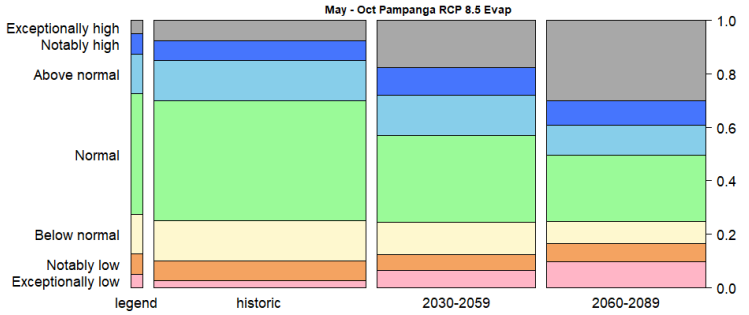

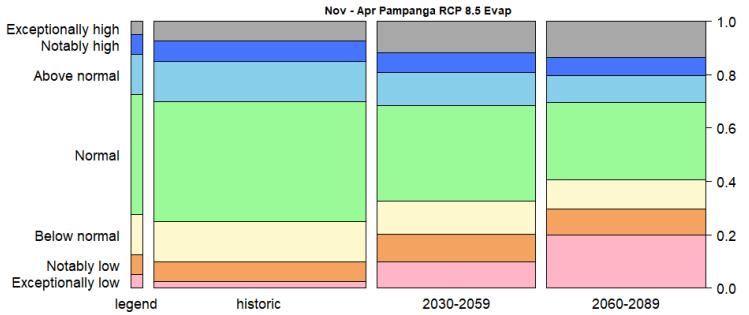

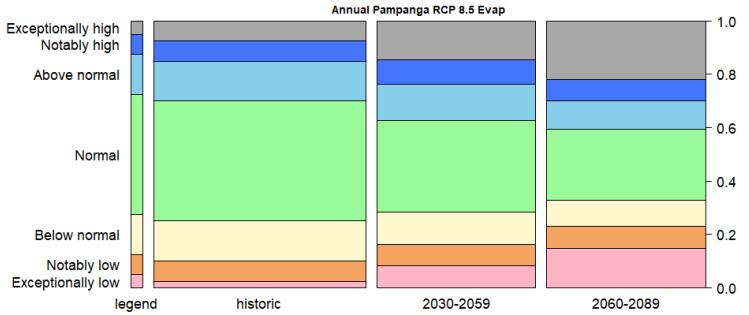

h)

Figure 15. Mean monthly evapotranspiration (a-b), change in mean monthly precipitation (c-d), box plot (e-f) of mean seasonal values, and percentile range compared to historical monthly values for wet season (May – Oct), dry season (Nov-Apr) and annual values considering the historical (1990-2019), 2030-2059 and 2060-2089 time slices for Pampanga using RCP 2.6 and 8.5.

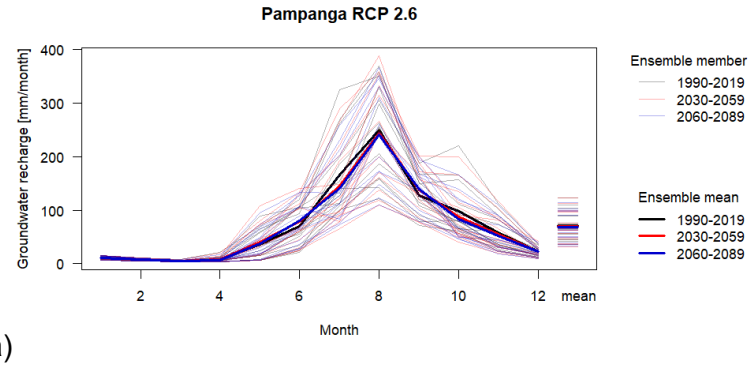
Pampanga RCP 2.6
Groundwater recharge [mm/month]
Month
Ensemble member
1990-2019
2030-2059
2060-2089
Ensemble mean
1990-2019
2030-2059
2060-2089

a)

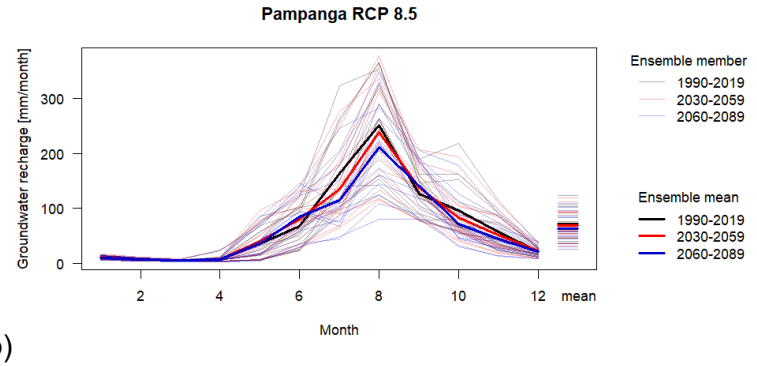
Pampanga RCP 8.5
Groundwater recharge [mm/month]
Month
Ensemble member
1990-2019
2030-2059
2060-2089
Ensemble mean
1990-2019
2030-2059
2060-2089

b)

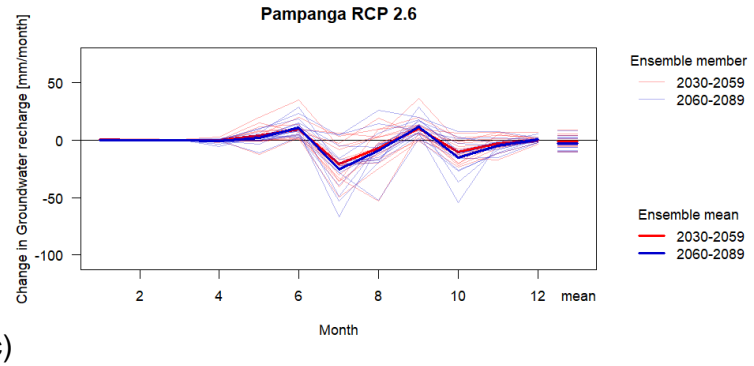
Pampanga RCP 2.6
Change in Groundwater recharge [mm/month]
Month
Ensemble member
2030-2059
2060-2089
Ensemble mean
2030-2059
2060-2089

c)

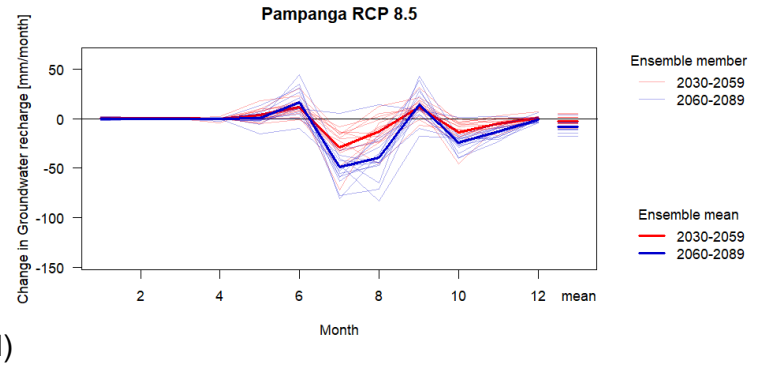
Pampanga RCP 8.5
Change in Groundwater recharge [mm/month]
Month
Ensemble member
2030-2059
2060-2089
Ensemble mean
2030-2059
2060-2089

d)

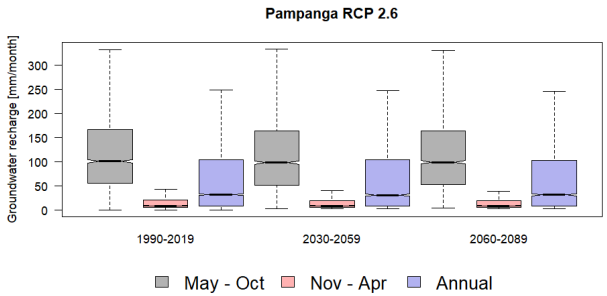
Pampanga RCP 2.6
Groundwater recharge [mm/month]
1990-2019
2030-2059
2060-2089
May - Oct
Nov - Apr
Annual

e)

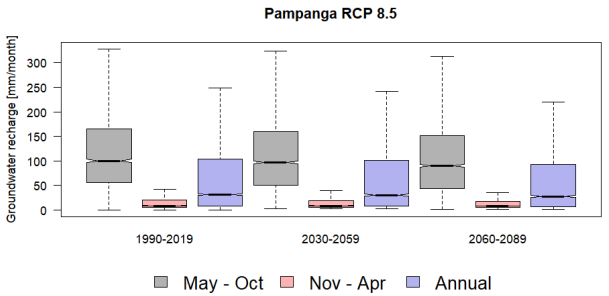
Pampanga RCP 8.5
Groundwater recharge [mm/month]
1990-2019
2030-2059
2060-2089
May - Oct
Nov - Apr
Annual

f)

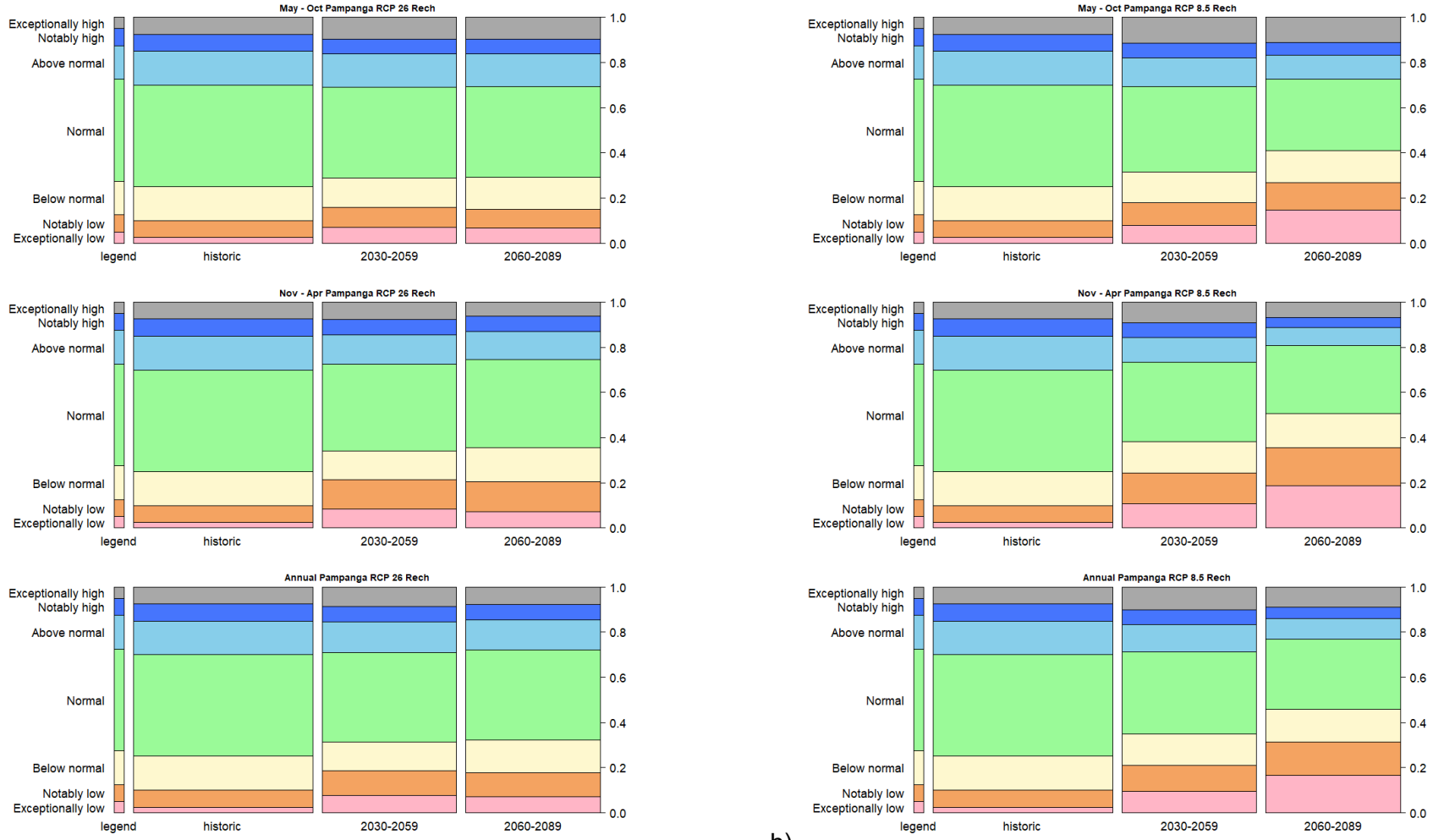

g) h)

Figure 16. Mean monthly groundwater recharge (a-b), change in mean monthly precipitation (c-d), box plot (e-f) of mean seasonal values, and percentile range compared to historical monthly values for wet season (May – Oct), dry season (Nov-Apr) and annual values considering the historical (1990-2019), 2030-2059 and 2060-2089 time slices for Pampanga using RCP 2.6 and 8.5.

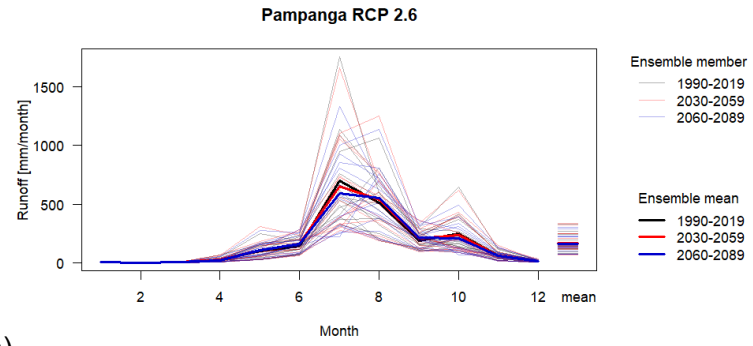
Pampanga RCP 2.6
Runoff [mm/month]
1500
1000
500
0
2
4
6
8
10
12
mean
Month
Ensemble member
1990-2019
2030-2059
2060-2089
Ensemble mean
1990-2019
2030-2059
2060-2089

a)

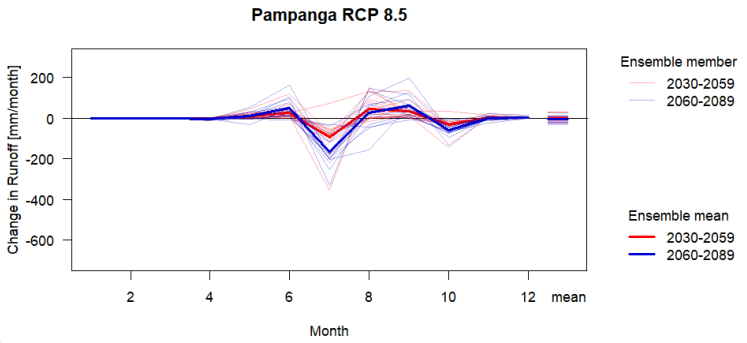
Pampanga RCP 8.5
Change in Runoff [mm/month]
200
0
-200
-400
-600
2
4
6
8
10
12
mean
Month
Ensemble member
2030-2059
2060-2089
Ensemble mean
2030-2059
2060-2089

b)

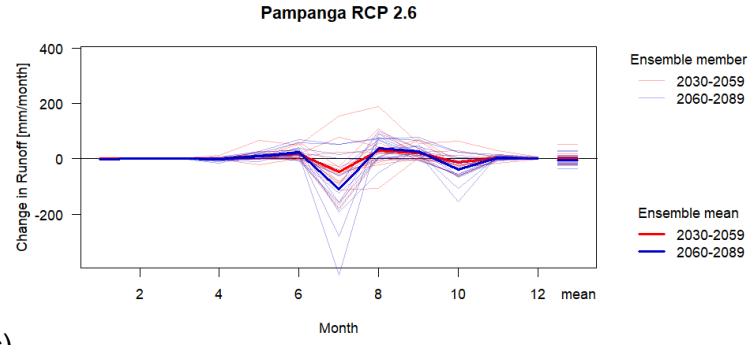
Pampanga RCP 2.6
Change in Runoff [mm/month]
400
200
0
-200
2
4
6
8
10
12
mean
Month
Ensemble member
2030-2059
2060-2089
Ensemble mean
2030-2059
2060-2089

c)

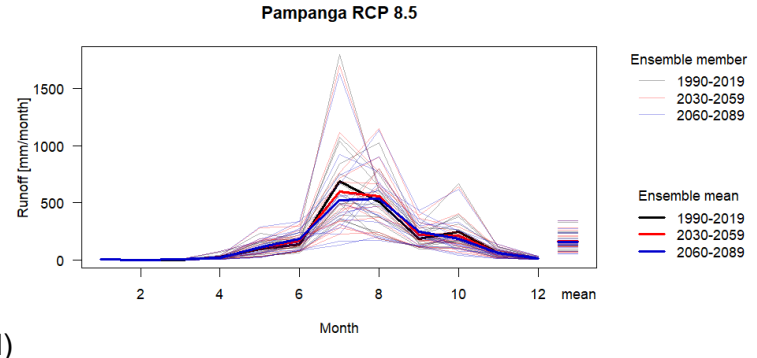
Pampanga RCP 8.5
Runoff [mm/month]
1500
1000
500
0
2
4
6
8
10
12
mean
Month
Ensemble member
1990-2019
2030-2059
2060-2089
Ensemble mean
1990-2019
2030-2059
2060-2089

d)

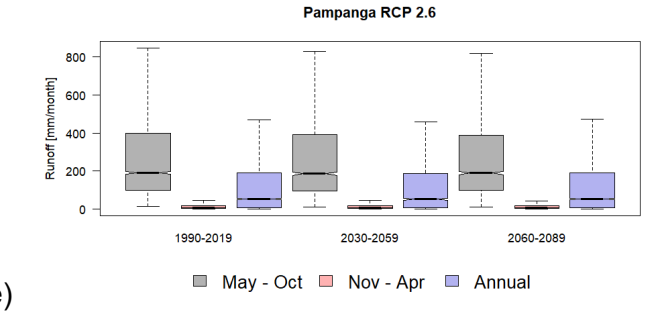
Pampanga RCP 2.6
Runoff [mm/month]
800
600
400
200
0
1990-2019
2030-2059
2060-2089
May - Oct
Nov - Apr
Annual

e)

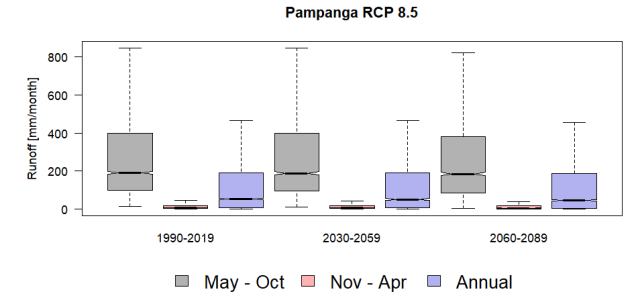
Pampanga RCP 8.5
Runoff [mm/month]
800
600
400
200
0
1990-2019
2030-2059
2060-2089
May - Oct
Nov - Apr
Annual

f)

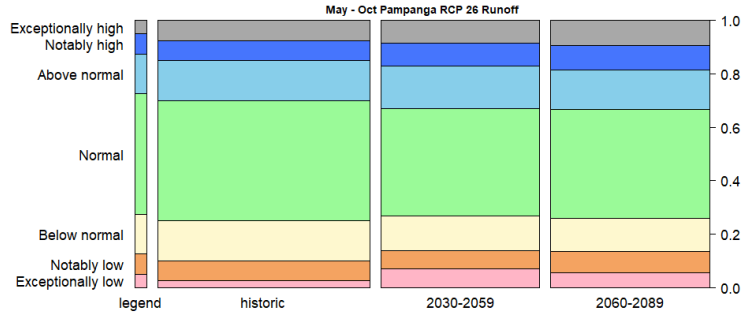

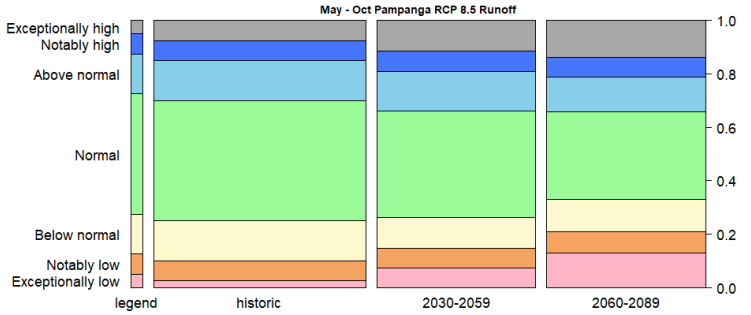

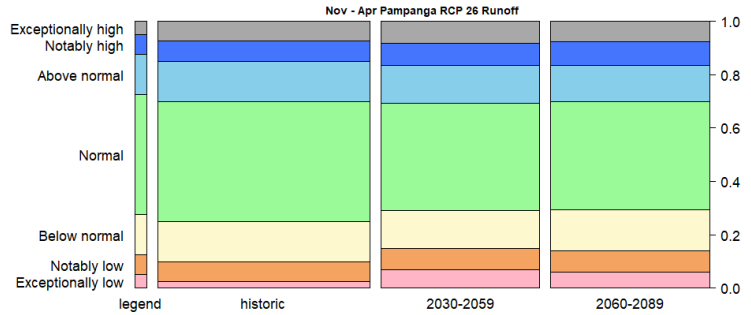

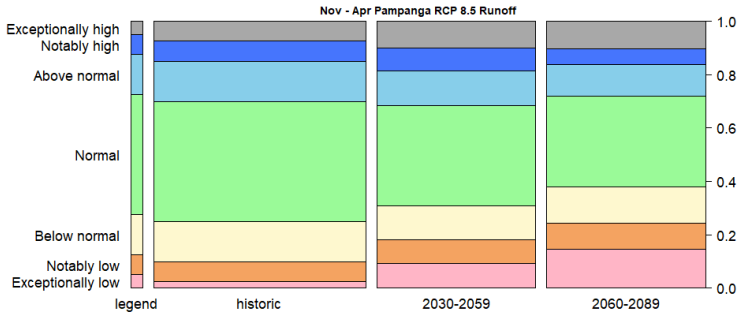

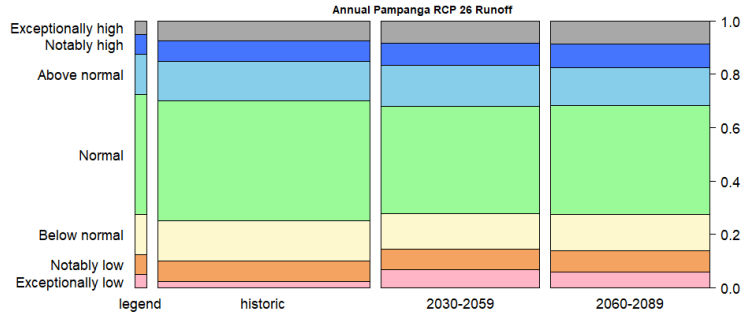

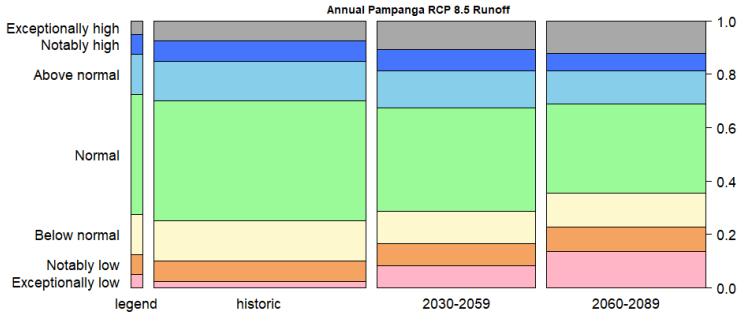

g)

h)

Figure 17. Mean monthly runoff (a-b), change in mean monthly precipitation (c-d), box plot (e-f) of mean seasonal values, and percentile range compared to historical monthly values for wet season (May – Oct), dry season (Nov-Apr) and annual values considering the historical (1990-2019), 2030-2059 and 2060-2089 time slices for Pampanga using RCP 2.6 and 8.5.

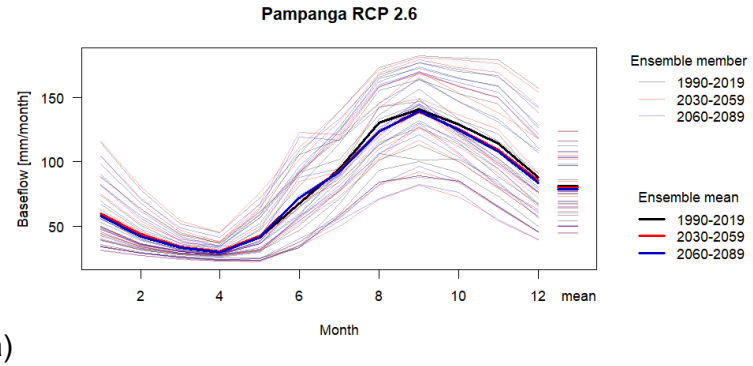
Pampanga RCP 2.6
Baseflow [mm/month]
150
100
50
2
4
6
8
10
12
mean
Month
Ensemble member
1990-2019
2030-2059
2060-2089
Ensemble mean
1990-2019
2030-2059
2060-2089

a)

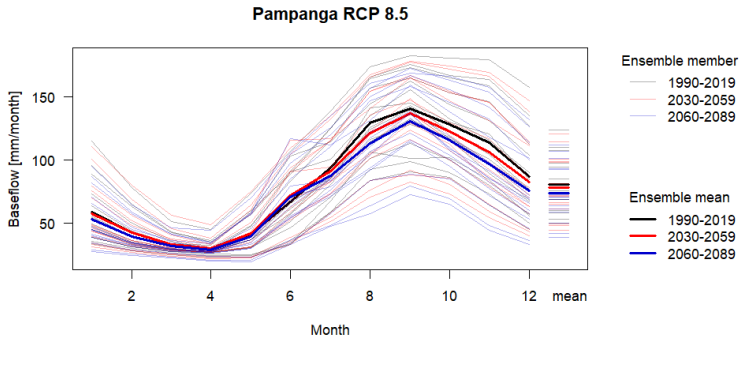
Pampanga RCP 8.5
Baseflow [mm/month]
150
100
50
2
4
6
8
10
12
mean
Month
Ensemble member
1990-2019
2030-2059
2060-2089
Ensemble mean
1990-2019
2030-2059
2060-2089

b)

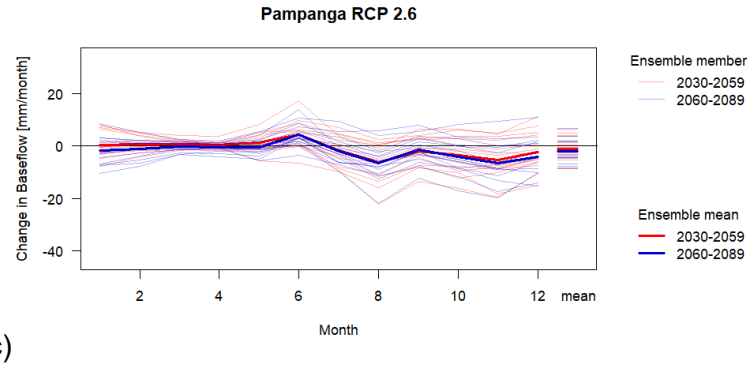
Pampanga RCP 2.6
Change in Baseflow [mm/month]
20
0
-20
-40
2
4
6
8
10
12
mean
Month
Ensemble member
2030-2059
2060-2089
Ensemble mean
2030-2059
2060-2089

c)

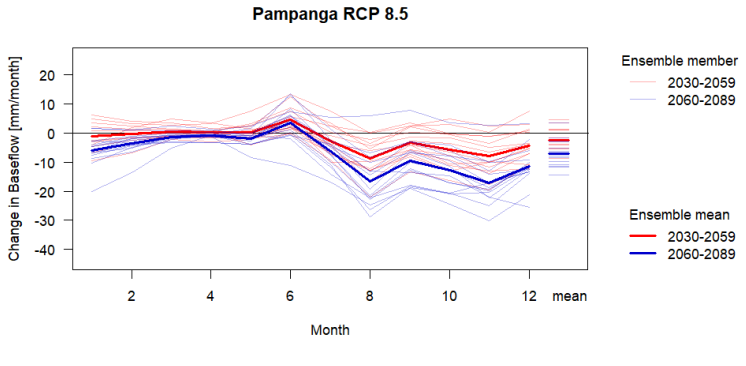
Pampanga RCP 8.5
Change in Baseflow [mm/month]
20
10
0
-10
-20
-30
-40
2
4
6
8
10
12
mean
Month
Ensemble member
2030-2059
2060-2089
Ensemble mean
2030-2059
2060-2089

d)

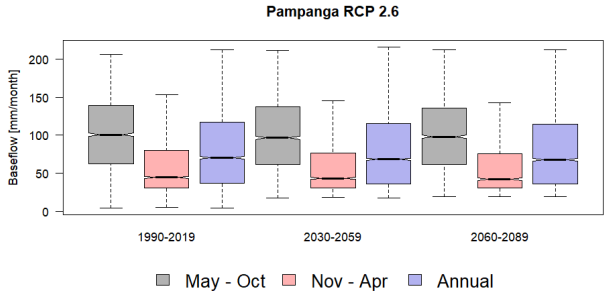
Pampanga RCP 2.6
Baseflow [mm/month]
200
150
100
50
0
1990-2019
2030-2059
2060-2089
May - Oct
Nov - Apr
Annual

e)

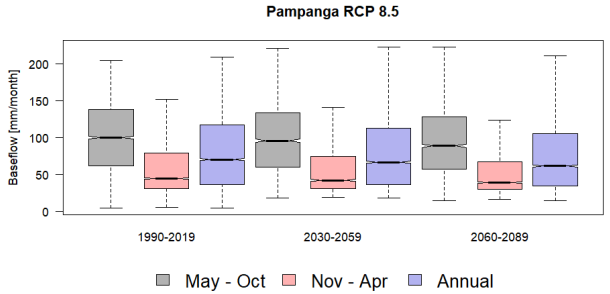
Pampanga RCP 8.5
Baseflow [mm/month]
200
150
100
50
0
1990-2019
2030-2059
2060-2089
May - Oct
Nov - Apr
Annual

f)

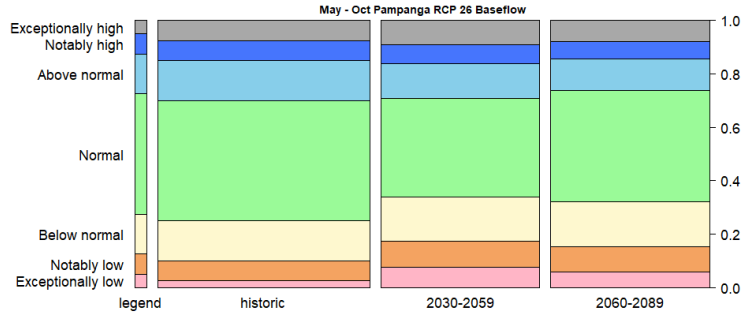

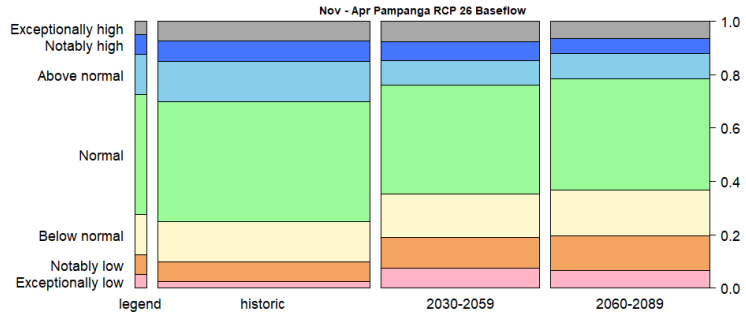

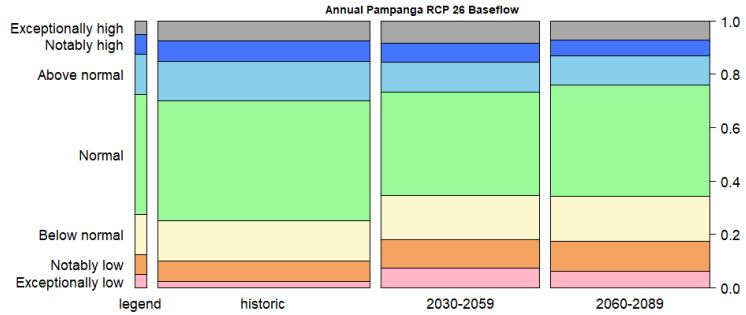

g)

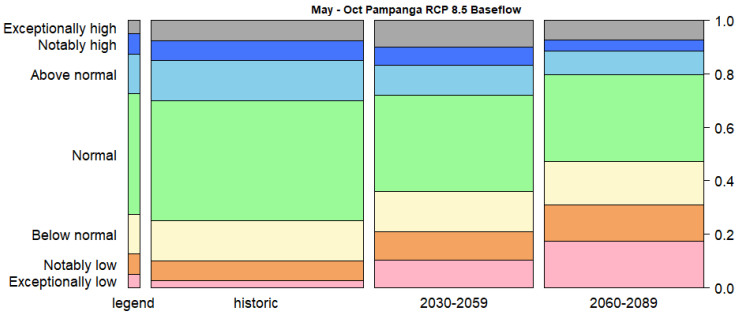

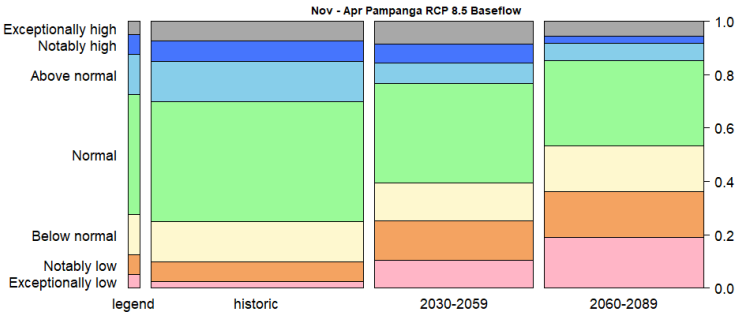

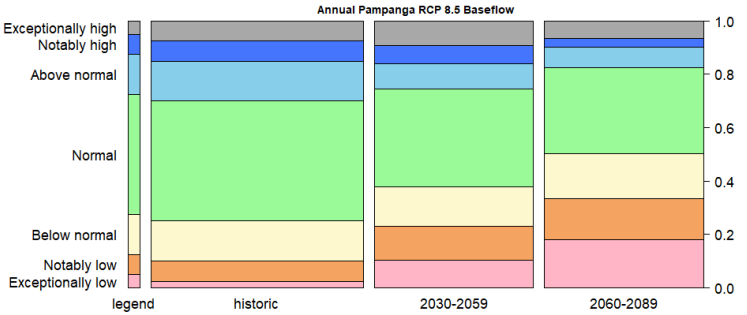

h)

Figure 18. Mean monthly baseflow (a-b), change in mean monthly precipitation (c-d), box plot (e-f) of mean seasonal values, and percentile range compared to historical monthly values for wet season (May – Oct), dry season (Nov-Apr) and annual values considering the historical (1990-2019), 2030-2059 and 2060-2089 time slices for Pampanga using RCP 2.6 and 8.5.

3 Summary of future hydrological change

Hydrological modelling of Panay Island and Pampanga Province for future scenarios considering RCP 2.6 and RCP 8.5 UKCP18 climate ensemble for the 2050s (2030-2059) and 2080s (2060-2089) suggest the following changes to the hydrological system are to be expected (Figure 19 and Figure 20):

- Mean precipitation decreases in Panay between 11.5 – 12 mm/month for the 2050s and 12 – 33.8 mm/month for the 2080s. This is a decrease of 5% in the 2050s and up to 15% in the 2080s. This is accompanied by an increase in in the number of months with exceptionally low precipitation to 21% for the 2080s considering RCP 8.5.
- Mean precipitation decreases in Pampanga for the 2050s by 0-3 mm/month and decreases by 7-14 mm/month for the 2080s, which is a decrease of 2-4.3%. Whereas the mean precipitation changes little for the two future time periods, there is an increase in the number of months with above normal or higher and below normal or lower precipitation.
- Mean evapotranspiration decreases in Panay between 2.5 – 3 mm/month for the 2050s and 2.5 and 9.3 mm/month for the 2080s. There are a greater number of months with below normal or lower evapotranspiration from 25 % to 34-36% for the 2050s and 35-52% for the 2080s. There is a slight decrease in the frequency of months with above normal or higher evapotranspiration for both time periods.
- Mean evapotranspiration does not change in Pampanga, however, there is an increase in the frequency of months with above normal or higher evapotranspiration from 30% to 34-77% in the 2050s and 34-40% in the 2080s. The evapotranspiration increases in the wet season and decreases in the dry season.
- Mean groundwater recharge decreases in Panay in the 2050s between 4.5 – 5 mm/month and 5.2 – 12.2 mm/month in the 2080s. This is a decrease by ~12% for the 2050s and 12-29% for the 2080s. The frequency of months with a groundwater recharge below normal or lower is increasing from 25% to 34-36% for the 2050s and 35-52% in the 2080s.
- Mean groundwater recharge decreases by 1.4 - 2.8 mm/month for the 2050s and 2.6-8.2 mm/month for the 2080s for Pampanga, which is a decrease by 4 - 12% for the 2080s. The frequency of months with groundwater recharge below normal or lower increases and decreases for months with above normal or higher groundwater recharge.
- Mean runoff in Panay decreases by around 5 mm/month for the 2050s and 6-16 mm/months for the 2080s. The frequency of months with above normal runoff or higher decrease, and the frequency of months with below normal or lower runoff increase.
- Mean runoff in Pampanga has no clear signal in the 2050s and decreases by 4.5 – 6.7 mm/month in the 2080s. The frequency of months with above normal runoff or higher and below normal or lower runoff increase for both time periods. This means that both high runoff events and low runoff events are more likely to occur.
- Mean baseflow in Panay is decreasing by 9.7 - 10.8 mm/month by 2050s and by 12.2 - 26.5 mm/month by 2080s. For 2050s this is a reduction in baseflow by 12.2 – 13.3% and for 2080s by 15.4 – 32.6 %. The frequency of months with baseflow above normal or higher is decreasing and below normal or lower are increasing.
- Mean baseflow in Pampanga is expected to decrease by 1.1 – 2.4 mm/month in the 2050s and 2.1 - 6.9 mm/month in the 2080s. This is a decrease in baseflow to up to 2.5% by 2050s and 8.6% by 2080s. The frequency of months with baseflow above normal or higher is decreasing and below normal or lower are increasing.
- Panay shows a decrease in precipitation, whereas Pampanga has little annual change in the 2050s and a decrease in the 2080s comparable to 2050s in Iloilo. Nevertheless, both Panay and Pampanga show a decrease in groundwater recharge and baseflow contribution to rivers for the 2050s and 2080s. For Panay, Runoff and evapotranspiration also decrease, whereas for Pampanga, evapotranspiration remains unchanged and runoff increases in the 2050s and decreases in the 2080s.

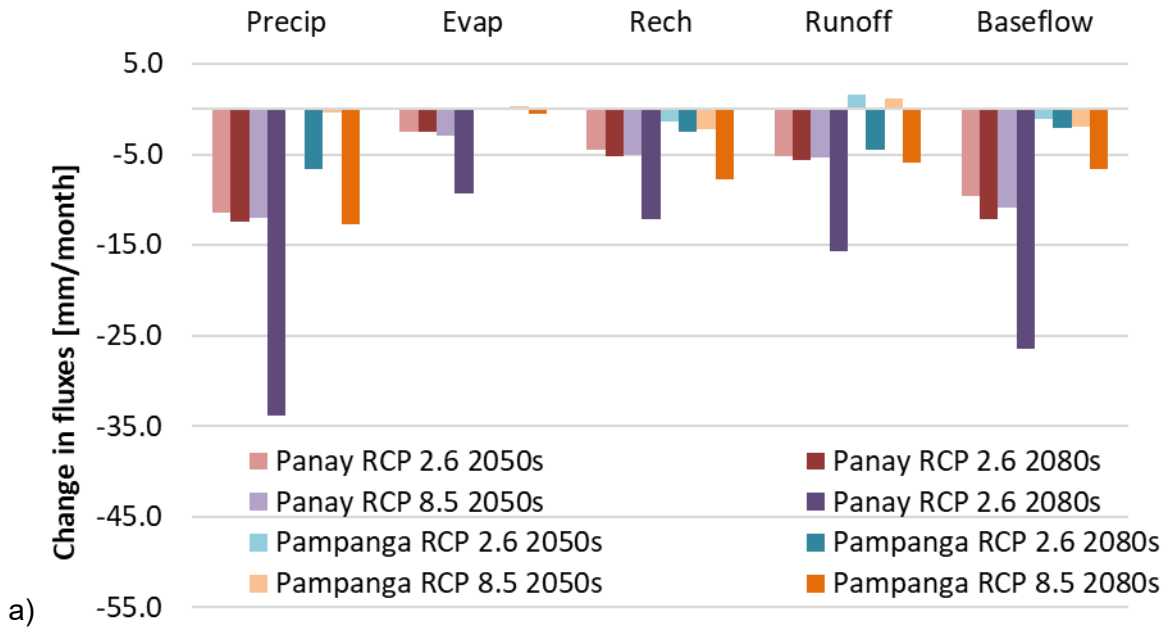

a)

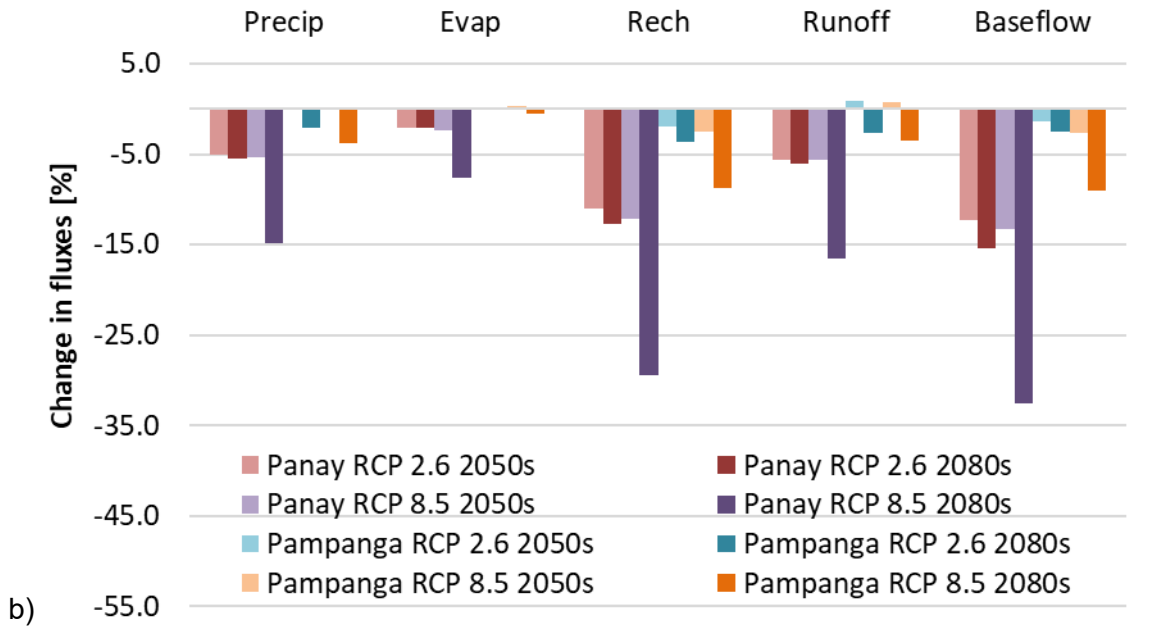

b)

Figure 19. a) absolute and b) relative change in fluxes for Panay and Pampanga regarding RCP 2.6 and 8.5 for the 2050s and 2080s.

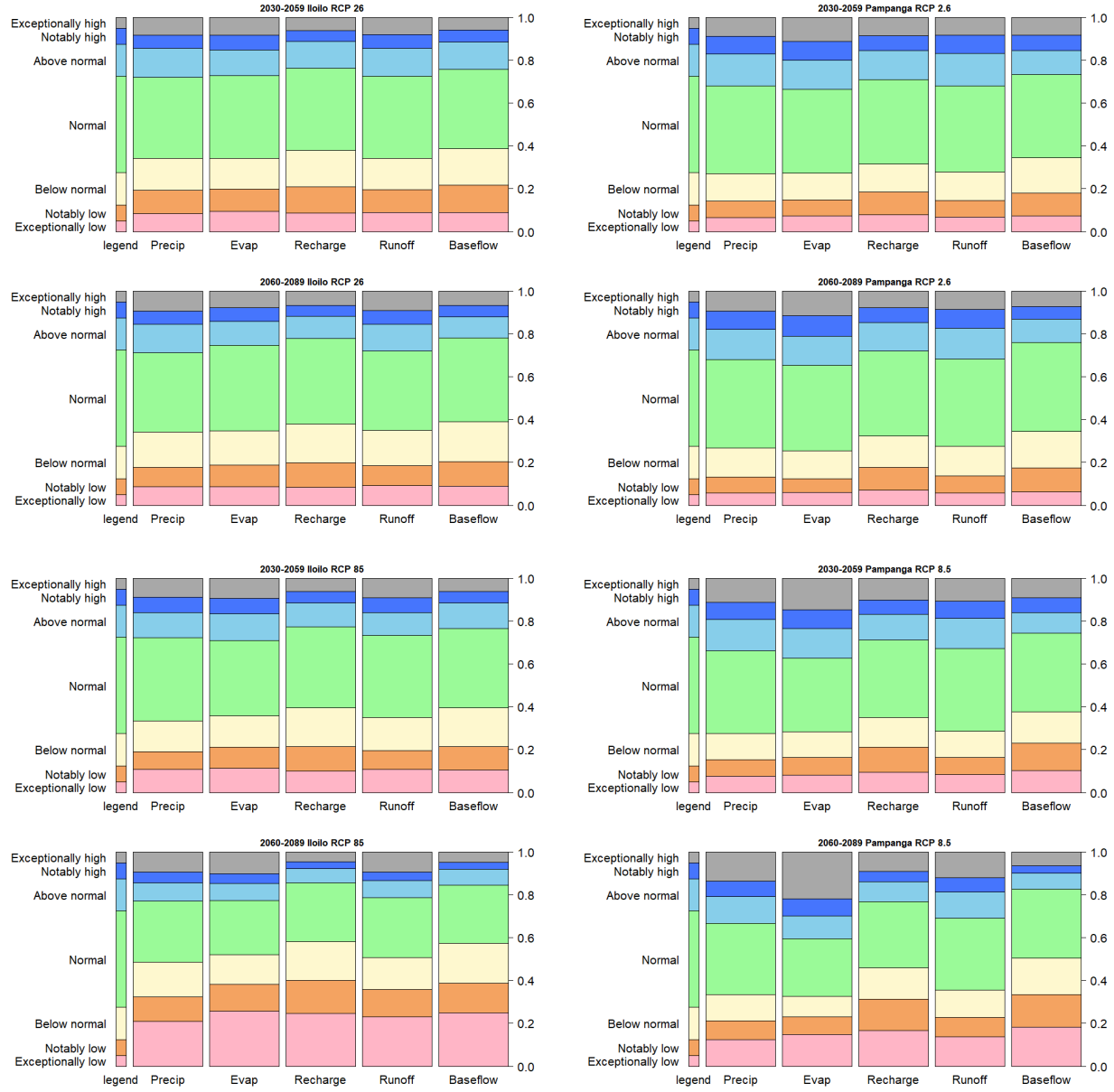

Figure 20. Percentile range compared to historical fluxes for the 2050s and 2080s for Panay and Pampanga considering RCP 2.6 and 8.5.

4 Future work

- As demonstrated in this report, the modelling framework is set up to perform hydrological modelling of the entire Philippines. Therefore, if desired, it could be expanded to cover the remaining islands. This work will form part of the BGS IGRD project ‘National scale hydrological models’.
- The driving data for the future scenarios from UKCP18 show a bias during the historical periods compared to the ERA5 data. To overcome this bias, we presented only the change for the future periods compared to the historical periods for each climate scenario. To get more confidence in the absolute values of the predictions, for future work the UKCP18 data could either be bias corrected by comparing the historical periods with ERA5 climatology, or we could use higher resolution regional climate models, such as CORDEX.

Appendix 1 VIC model parameters

Parameters and sources for the VIC parameters are listed in the tables below:

Table 7. Description of variable name, units and dimensions for the VIC global parameter file.

Variable number	Variable name	Units	Precision	Number of dimensions	Dimensions
1	mask	m2	int	2	lon, lat
2	layer	-	int	1	nlayer
3	run_cell	N/A	int	2	lon, lat
4	gridcell	N/A	int	2	lon, lat
5	lats	degrees	double	2	lon, lat
6	lons	degrees	double	2	lon, lat
7	infilt	mm/day	double	2	lon, lat
8	Ds	fraction	double	2	lon, lat
9	Dsmax	mm/day	double	2	lon, lat
10	Ws	fraction	double	2	lon, lat
11	c	N/A	double	2	lon, lat
12	expt	N/A	double	3	lon, lat, nlayer
13	Ksat	mm/day	double	3	lon, lat, nlayer
14	phi_s	mm/mm	double	3	lon, lat, nlayer
15	init_moist	mm	double	3	lon, lat, nlayer
16	elev	m	double	2	lon, lat
17	depth	m	double	3	lon, lat, nlayer
18	avg_T	C	double	2	lon, lat
19	dp	m	double	2	lon, lat
20	bubble	cm	double	3	lon, lat, nlayer
21	quartz	fraction	double	3	lon, lat, nlayer
22	bulk_density	kg/m3	double	3	lon, lat, nlayer
23	soil_density	kg/m3	double	3	lon, lat, nlayer
24	off_gmt	hours	double	2	lon, lat
25	Wcr_FRACT	fraction	double	3	lon, lat, nlayer
26	Wpwp_FRACT	fraction	double	3	lon, lat, nlayer
27	rough	m	double	2	lon, lat
28	snow_rough	m	double	2	lon, lat
29	annual_prec	mm	double	2	lon, lat

30	resid_moist	fraction	double		3	lon, lat, nlayer
31	fs_active	binary	int		2	lon, lat
32	cellnum	N/A	double		2	lon, lat
33	AreaFract	fraction	double		3	lon, lat, snow_band
34	elevation	m	double		3	lon, lat, snow_band
35	Pfactor	fraction	double		3	lon, lat, snow_band
36	veg_descr	string		1	1	veg_class
37	Nveg	N/A	int		2	lon, lat
38	Cv	fraction	double		3	lon, lat, veg_class
39	root_depth	m	double		4	lon, lat, root_zone, veg_class
40	root_fract	fraction	double		4	lon, lat, root_zone, veg_class
41	LAI	m2/m2	double		4	lon, lat, month, veg_class
42	overstory	N/A	int		3	lon, lat, veg_class
43	rarc	s/m	double		3	lon, lat, veg_class
44	rmin	s/m	double		3	lon, lat, veg_class
45	wind_h	m	double		3	lon, lat, veg_class
46	RGL	W/m^2.	double		3	lon, lat, veg_class
47	rad_atten	fraction	double		3	lon, lat, veg_class
48	wind_atten	fraction	double		3	lon, lat, veg_class
49	trunk_ratio	fraction	double		3	lon, lat, veg_class
50	albedo	fraction	double		4	lon, lat, month, veg_class
51	veg_rough	m	double		4	lon, lat, month, veg_class
52	displacement	m	double		4	lon, lat, month, veg_class

Table 8. Description and data source of variables for the VIC global parameter file.

Variable number	Variable name	Source	Description
1	mask	(Global Administrative Areas 2012)	Country and Island outline
2	layer	-	-
3	run_cell	-	1 = Run Grid cell, 0 = Do not Run
4	gridcell	-	Grid cell number
5	lats	-	Latitude
6	lons	-	Longitude
7	infilt	callibration parameter	Variable Infiltration parameter (binfilt). The binfilt parameter is the parameter used to describe the Variable Infiltration Curve. This is typically a value that is adjusted during the calibration of the VIC model. Parameter values range from 10-5 to 0.4. Higher values The b_infilt parameter is the parameter used to describe the Variable Infiltration Curve. This is typically a value that is adjusted during the calibration of the VIC model. Parameter values range from 10-5 to 0.4. Higher values will produce more runoff. 0.2 is often used as a starting value.
8	Ds	Dummy, not used	The soil parameter Ds represents the fraction of the Dsmax parameter at which non-linear base-flow occurs. This is typically a parameter that is adjusted during the calibration of the VIC model. An initial value of 0.001 may be used. Typically this value is small (less than 1). For the coupled VIC-AMBHAS model, this parameter is not used in the simulation, but needs to be given in the input files.
9	Dsmax	Dummy, not used	The parameter Dsmax is the maximum velocity of baseflow for each grid cell. This can be estimated using

			the saturated hydraulic conductivity, Ksat, for each grid cell multiplied by the slope of the grid cell. The values for Ksat can be averaged for the layers for which baseflow will be included. When working in decimal degrees, the elevation data for the basin should be projected to an equal area map projection, in order to have horizontal dimensions in the same units as the vertical dimensions so that the slopes computed in Arc/Info are meaningful lues. For the coupled VIC-AMBHAS model, this parameter is not used in the simulation, but needs to be given in the input files.
10	Ws	Dummy, not used	The parameter Ws is the fraction of maximum soil moisture where non-linear baseflow occurs. As with the Ds parameter, this is generally adjusted during the calibration phase of applying the VIC model. Values for Ws are typically greater than 0.5. An initial value of 0.9 can be used. For the coupled VIC-AMBHAS model, this parameter is not used in the simulation, but needs to be given in the input files.
11	c	Dummy, not used	c Exponent used in baseflow curve, normally set to 2. For the coupled VIC-AMBHAS model, this parameter is not used in the simulation, but needs to be given in the input files.
12	expt	Calculated from wilting point and field capacity by Zhang and Marcel (2018). https://dataverse.harvard.edu/dataset.xhtml?persistentId=doi:10.7910/DVN/UI5LCE The wilting point is given at h = 15000 cm, and the field capacity at h = 330 cm. b = slope of the retention curve in log – log space expt = 3 + 2*b	Exponent n (=3+2/lambda) in Campbells eqn for hydraulic conductivity, HBH 5.6 (where lambda = soil pore size distribution parameter). Values should be > 3.0

13	Ksat	Zhang and Marcel (2018) https://dataverse.harvard.edu/dataset.xhtml?persistentId=doi:10.7910/DVN/UI5LCE	Saturated hydraulic conductivity mm/d
14	phi_s	Zhang and Marcel (2018) https://dataverse.harvard.edu/dataset.xhtml?persistentId=doi:10.7910/DVN/UI5LCE	Soil moisture diffusion parameter
15	init_moist	Initial soil moisture is set to porosity * layer depth	init_moist in mm Initial moisture content of each layer can be set at any reasonable value. One approach is to use fractional soil moisture content (expressed as a fraction of the maximum soil moisture; max. soil moisture = porosity * layer depth) at the critical point, Wcr, which can be computed for each layer as a depth in i meters by multiplying Wcr by the thickness of the layer in meters, and then multiplying by 1000
16	elev	SRTM dtm 90 m (Jarvis et al. 2008)	Average elevation of grid cell
17	depth		Thickness of each soil moisture layer. This is set to 0.1, 0.5, 2m below ground
18	avg_T	Fick and Hijmans (2017). https://www.worldclim.org/data/worldclim21.html	Average soil temperature. This parameter is the temperature of the soil at the damping depth. This temperature is often assumed to be the same as the average annual air temperature. This temperature is used as the bottom boundary of all thermal flux calculations made for the soil column.
19	dp	4m	This is the soil thermal damping depth. It is defined as the depth in the soil column at which the soil temperature remains nearly constant annually. This is the depth to which soil thermal flux calculations will be made, and is often set to 4m. The constant temperature at this boundary is defined with the parameter avg_T.
20	bubble	bubble =0.32*expt + 4.3	The bubble parameter is the bubbling pressure, h, for the soil texture type (see, e.g., Table 5.3.2 in Rawls, et al (Handbook of Hydrology)). This parameter is necessary for running the VIC model with FULL_ENERGY==TRUE

			or FROZEN_SOIL==TRUE. Values must be > 0.0. If you have a VIC soil parameter file created for water-balance mode runs, in which bubbling pressure has been set to a "nodata" value such as -99, you will not be able to use this soil parameter file for FULL_ENERGY==TRUE or FROZEN_SOIL==TRUE. However, a quick way to estimate bubbling pressure from the existing soil parameters (namely the expt parameter) is: bubble = 0.32*expt + 4.3 This is illustrated in figure 1, generated by taking the data from table 5.3.2 in Rawls, et al (Handbook of Hydrology), computing expt from lambda, and performing a linear regression.
21	quartz	SoilGrid1km variable SNDPPT(Hengl et al. 2014)	Quartz content of soil. Here the sand fraction is used.
22	bulk_density	SoilGrids1km BLDFIE (Hengl et al. 2014)	Bulk density of organic portion of soil.
23	soil_density	Soil particle density, normally 2685 kg/m3	Soil particle density of organic portion of soil.
24	off_gmt	-	Time zone offset from GMT.
25	Wcr_FRACT	Calculated from Zhang using phi_s and the field capacity as follows: phi=phi_s*(0.7*FieldCapacity/psi_s)^(-1/b) Wcr_FRACT=phi/phi_s https://dataverse.harvard.edu/dataset.xhtml?persistentId=doi:10.7910/DVN/UI5LCE	The parameter Wcr_FRACT (Wcr) is the fractional soil moisture (expressed as a fraction of the maximum soil moisture; max. soil moisture = porosity * layer depth) at the critical point, which is the water content below which hydraulic conductivity begins to fall below saturated values, as does transpiration. This is set at 70% of the field capacity, in accordance with the different soil textures. Field Capacity is defined as the water content at a tension of -33kPa.
26	Wpwp_FRACT	Wilting point from Zhang and Marcel (2018) divided by phi_s from Zhang and Marcel (2018) https://dataverse.harvard.edu/dataset.xhtml?persistentId=doi:10.7910/DVN/UI5LCE	The parameter Wpwp_FRACT (wp) is the fractional soil moisture (expressed as a fraction of the maximum soil moisture; max. soil moisture = porosity * layer depth) at the wilting point. Wilting Point is set at the water content at

			a tension of 1500 kPa, and is approximated for the different soil textures.
27	rough	0.001	Surface roughness of bare soil, expressed in meters, can be set to a value 0.001, and adjusted according to local data.
28	snow_rough	0	The surface roughness of the snowpack, expressed in meters, can be set to an initial value of 0.0005, and can then be adjusted according to local data.
29	annual_prec	Fick and Hijmans (2017) https://www.worldclim.org/data/worldclim21.html	Average annual precipitation
30	resid_moist	Zhang and Marcel (2018). https://dataverse.harvard.edu/dataset.xhtml?persistentId=doi:10.7910/DVN/UI5LCE	Soil moisture layer residual moisture content in units of residual moisture content / total layer volume [mm/mm].
31	fs_active	0	If set to 1, then frozen soil algorithm is activated for the grid cell. A 0 indicates that frozen soils are not computed even if soil temperatures fall below 0C
32	cellnum	same as gridcell	Grid cell number
33	AreaFract	1	Fraction of grid cell covered by each elevation band. Sum of the fractions must equal 1.
34	elevation	SRTM dtm (Jarvis et al. 2008)	Mean (or median) elevation of elevation band. This is used to compute the change in air temperature from the grid cell mean elevation
35	Pfactor	1	Fraction of cell precipitation that falls on each elevation band. Total must equal 1. To ignore effects of elevation on precipitation, set these fractions equal to the area fractions
36	veg_descr	MODIS landcover at 0.05 °(Friedl and Sulla-Menashe 2015). https://lpdaac.usgs.gov/products/mcd12c1v006/	Land cover classification
37	Nveg	1	Number of vegetation tiles in the grid cell

38	Cv	1	Fraction of grid cell covered by vegetation tile
39	root_depth	Fan et al. (2017a) and dataset Fan et al. (2017b) https://wci.earth2observe.eu/thredds/catalog/usc/root-depth/catalog.html	Root zone thickness (sum of depths is total depth of root penetration)
40	root_fract	Calculated from root_depth	Fraction of root in the current root zone
41	LAI	Copernicus LAI at 1km (Smets et al. 2019) https://land.copernicus.eu/global/products/lai	Leaf Area Index, one per month
42	overstory	MODIS landcover at 0.05°(Friedl and Sulla-Menashe 2015) and VIC vegetation library. https://lpdaac.usgs.gov/products/mcd12c1v006/	Lag to indicate whether or not the current vegetation type has an overstory TRUE for overstory present [e.g. trees], FALSE for overstory not present [e.g. grass])
43	rarc	MODIS landcover at 0.05°(Friedl and Sulla-Menashe 2015) and VIC vegetation library. https://lpdaac.usgs.gov/products/mcd12c1v006/	Architectural resistance of vegetation type (~2 s/m) Not sure about this!! #use the values from the veglib
44	rmin	MODIS landcover at 0.05°(Friedl and Sulla-Menashe 2015) and VIC vegetation library. https://lpdaac.usgs.gov/products/mcd12c1v006/	Minimum stomatal resistance of vegetation type (~100 s/m) use the values from the veglib
45	wind_h	MODIS landcover at 0.05°(Friedl and Sulla-Menashe 2015) and VIC vegetation library. https://lpdaac.usgs.gov/products/mcd12c1v006/	Height at which wind speed is measured
46	RGL	MODIS landcover at 0.05°(Friedl and Sulla-Menashe 2015) and VIC vegetation library and VIC global parameter file. https://lpdaac.usgs.gov/products/mcd12c1v006/	Minimum incoming shortwave radiation at which there will be transpiration. For trees this is about 30 W/m2, for crops about 100 W/m2.
47	rad_atten	default 0.5	Radiation attenuation factor. Normally set to 0.5, though may need to be adjusted for high latitudes.
48	wind_atten	default 0.5	Wind speed attenuation through the overstory. The default value has been 0.5.

49	trunk_ratio	default 0.2	Ratio of total tree height that is trunk (no branches). The default value has been 0.2.
50	albedo	Copernicus surface albedo at 1km (Smets and Sánchez-Zapero 2018). https://land.copernicus.eu/global/products/sa	Shortwave albedo for vegetation type
51	veg_rough	Vegetation roughness length is typically 0.123 * vegetation height. Vegetation height is obtained from Healey et al. (2015). https://webmap.ornl.gov/wcsdown/dataset.jsp?ds_id=10023	Vegetation roughness length (typically 0.123 * vegetation height) one value per month
52	displacement	Vegetation displacement height is typically 0.67 * vegetation height. Vegetation height is obtained from Healey et al. (2015). https://webmap.ornl.gov/wcsdown/dataset.jsp?ds_id=10023	Vegetation displacement height (typically 0.67 * vegetation height) one value per month

Table 9. Parameters and sources for the Groundwater model coupled to VIC.

Variable number	Variable name	Units	Description	Data source
1	Sy	[-]	Specific_yield	Gleeson et al. (2014) and calibration factor
2	Trans	[m2/day]	Transmissivity – a value must be given, even if K is specified	dummy
3	K	[m/day]	hydraulic_conductivity – a value must be given, even if T is spcified	Gleeson et al. (2014) and calibration factor
4	mask	[-]	mask: active cells of the model domain are set to 1	-
5	dem	[m]	digital elevation model	SRTM dtm (Jarvis et al. 2008)
6	zbase	[m]	Base of the aquifer in m above datum	100 m
7	zriver	[m]	elevation of the river elevation, e.g DEM or DEM - 5	Dem -5
8	driver	[m]	Thickness of the river bed	1
9	C_eff	[1/day]	Conductance for leakage cells of effluent_river	calibration
10	C_in	[1/day]	Conductance for leakage cells of influent_river	
11	C_leak_eff	[1/day]	Conductance for leakage cells effluent	0
12	C_leak_in	[1/day]	Conductance for leakage cells influent	0
13	headBC	[m]	Head[m] of specific head boundary cells, or -999 for non-specified head boundary nodes	0 at the coast
14	river_area	[m2]	River area or cells where a river is present	Grid cell area

15	aquifer map	[-]	Zones of 1 are unconfined aquifer, and zones of 0 are confined aquifer	1
16	c_n	[m]	distance of the cell centre to the cell centre of the cell to the north [m]	Calculated distance
17	c_e	[m]	distance of the cell centre to the cell centre of the cell to the east [m]	Calculated distance
18	e_n	[m]	length of the northern edge of the cell [m]	Calculated distance
19	e_e	[m]	length of the eatern edge of the cell [m]	Calculated distance
20	cell_area	[m2]	cell area of each cell in [m2]	Calculated distance
21	z_soil	[m]	total soil depth used in the VIC model	2
22	Sy_soil	[m]	specific yield of the soil as used in the VIC model	Phi_s from Zhang and Marcel (2018)

References

ASIAN DEVELOPMENT BANK 2016. Asian Development Outlook 2016, Strengthening water security in Asia and the Pacific.

BEYER, R, KRAPP, M AND MANICA, A 2020. An empirical evaluation of bias correction methods for palaeoclimate simulations. *Clim. Past* 16(4), 1493-1508.

COPERNICUS CLIMATE CHANGE SERVICE 2021. What is bias correction? . *https://climate.copernicus.eu/sites/default/files/2021-01/infosheet7.pdf.*

DEPARTMENT OF PUBLIC WORKS AND HIGHWAYS 2016. National Hydrologic Data Collection Program (NHDCP).

FAN, Y, MIGUEZ-MACHO, G, JOBBÁGY, E G, JACKSON, R B AND OTERO-CASAL, C 2017a. Hydrologic regulation of plant rooting depth. *Proceedings of the National Academy of Sciences* 114(40), 10572.

FAN, Y, MIGUEZ-MACHO, G, JOBBÁGY, E G, JACKSON, R B AND OTERO-CASAL, C 2017b. Hydrologic regulation of plant rooting depth, https://wci.earth2observe.eu/thredds/catalog/usc/root-depth/catalog.html.

FICK, S E AND HIJMANS, R J 2017. WorldClim 2: new 1-km spatial resolution climate surfaces for global land areas. *International Journal of Climatology* 37(12), 4302-4315.

FRANCHINI, M AND PACCIANI, M 1991. Comparative analysis of several conceptual rainfall-runoff models. *Journal of Hydrology* 122(1-4), 161-219.

FRIEDL, M AND SULLA-MENASHE, D 2015. MCD12C1 MODIS/Terra+Aqua Land Cover Type Yearly L3 Global 0.05Deg CMG V006. 2015, distributed by NASA EOSDIS Land Processes DAAC.

GAO, H, TANG, Q, SHI, X, ZHU, C, BOHN, T J, SU, F, SHEFFIELD, J, PAN, M, LETTENMAIER, D P AND WOOD, E F 2010. Water Budget Record from Variable Infiltration Capacity (VIC) Model. *Algorithm Theoretical Basis Document for Terrestrial Water Cycle Data Records* (in review).

GLEESON, T, MOOSDORF, N, HARTMANN, J AND VAN BEEK, L P H 2014. A glimpse beneath earth's surface: GLobal HYdrogeology MaPS (GLHYMPS) of permeability and porosity. *Geophysical Research Letters* 41(11), 3891-3898.

GLOBAL ADMINISTRATIVE AREAS 2012. GADM database of Global Administrative Areas, version 2.0., www.gadm.org.

HAMMAN, J J, NIJSSEN, B, BOHN, T J, GERGEL, D R AND MAO, Y X 2018. The Variable Infiltration Capacity model version 5 (VIC-5): infrastructure improvements for new applications and reproducibility. *Geoscientific Model Development* 11(8), 3481-3496.

HEALEY, S P, M.W. HERNANDEZ, D.P. EDWARDS, M.A. LEFSKY, E. FREEMAN, P.L. PATTERSON, E.J. LINDQUIST AND LISTER., A J 2015. CMS: GLAS LiDAR-derived Global Estimates of Forest Canopy Height, 2004-2008, https://daac.ornl.gov/cgi-bin/dsviewer.pl?ds_id=1271, ORNL DAAC, Oak Ridge, Tennessee, USA

HENGL, T, DE JESUS, J M, MACMILLAN, R A, BATJES, N H, HEUVELINK, G B, RIBEIRO, E, SAMUEL-ROSA, A, KEMPEN, B, LEENAARS, J G, WALSH, M G AND GONZALEZ, M R 2014. SoilGrids1km--global soil information based on automated mapping. *PLOS ONE* 9(8), e105992.

HERSBACH, H, BELL, B, BERRISFORD, P, BIAVATI, G, HORÁNYI, A, MUÑOZ SABATER, J, NICOLAS, J, PEUBEY, C, RADU, R, ROZUM, I, SCHEPERS, D, SIMMONS, A, SOCI, C, DEE, D AND THÉPAUT, J-N 2018. ERA5 hourly data on single levels from 1979 to present, Copernicus Climate Change Service (C3S) Climate Data Store (CDS), https://cds.climate.copernicus.eu/cdsapp#!/dataset/reanalysis-era5-single-levels?tab=overview.

JARVIS, A, H.I. REUTER, A. NELSON AND E. GUEVARA 2008. Hole-filled SRTM for the globe Version 4, CGIAR-CSI SRTM 90m Database.

LOHMANN, D, NOLTE-HOLUBE, R AND RASCHKE, E 1996. A large-scale horizontal routing model to be coupled to land surface parametrization schemes. *Tellus, Series A: Dynamic Meteorology and Oceanography* 48(5), 708-721.

MACKAY, J D, BARKWITH, A AND GUZMAN, M A L G 2022. PhiGO Seasonal Groundwater Forecasting System. *British Geological Survey,* OR/21/066.

MAJOR, J J, JANDA, R J AND DAAG, A S 1996. Watershed disturbance and lahars on the east side of Mount Pinatubo during the mid-June 1991 eruptions. *Fire and Mud: Eruptions and Lahars of Mount Pinatubo*, 895-919.

MET OFFICE HADLEY CENTRE 2018. UKCP18 Global Climate Model Projections for the entire globe. ANALYSIS, C F E D (ed), http://catalogue.ceda.ac.uk/uuid/f1a2fc3c120f400396a92f5de84d596a.

MORENO, A AND HASENAUER, H 2016. Spatial downscaling of European climate data. *International Journal of Climatology* 36(3), 1444-1458.

NATIONAL MAPPING AND RESOURCE INFORMATION AUTHORITY (NAMRIA) 2015. Philippines - Water Courses (Rivers), OCHA Philippines, https://data.humdata.org/dataset/philippines-water-courses.

NIU, G Y, YANG, Z L, DICKINSON, R E, GULDEN, L E AND SU, H 2007. Development of a simple groundwater model for use in climate models and evaluation with Gravity Recovery and Climate Experiment data. *Journal of Geophysical Research Atmospheres* 112(7).

SCHEIDEGGER, J M, JACKSON, C R, MUDDU, S, TOMER, S K AND FILGUEIRA, R 2021. Integration of 2D Lateral Groundwater Flow into the Variable Infiltration Capacity (VIC) Model and Effects on Simulated Fluxes for Different Grid Resolutions and Aquifer Diffusivities. *Water* 13(5), 663.

SMETS, B AND SÁNCHEZ-ZAPERO, J 2018. Copernicus Global Land Operations "Vegetation and Energy" "CGLOPS-1", Copernicus, https://land.copernicus.eu/global/products/sa.

SMETS, B, VERGER, A, CAMACHO, F, VAN DER GOTEN, R AND JACOBS, T 2019. Copernicus Global Land Operations "Vegetation and Energy", Copernicus, https://land.copernicus.eu/global/products/lai.

UNIVERSITY OF WASHINGTON COMPUTATIONAL HYDROLOGY GROUP 2021. Variable Infiltration Capacity (VIC) Macroscale Hydrologic Model. *https://vic.readthedocs.io/en/master/Documentation/Drivers/Image/ImageDriver/*.

WOOD, E F, LETTENMAIER, D P AND ZARTARIAN, V G 1992. A land-surface hydrology parameterization with subgrid variability for general circulation models. *Journal of Geophysical Research* 97(D3), 2717-2728.

ZHANG, Y AND MARCEL, G S 2018. A High-Resolution Global Map of Soil Hydraulic Properties Produced by a Hierarchical Parameterization of a Physically-Based Water Retention Model. YONGGEN, Z AND MARCEL, G S (eds), Harvard Dataverse.